UiT
THE ARCTIC
UNIVERSITY
OF NORWAY

FACULTY OF SCIENCE AND TECHNOLOGY

Department of Geology

Reservoir structure and geological setting of the shallow PEON gas reservoir

—

Håkon Mikalsen

EOM-3901 Master's Thesis in Energy, Climate and Environment

June 2014

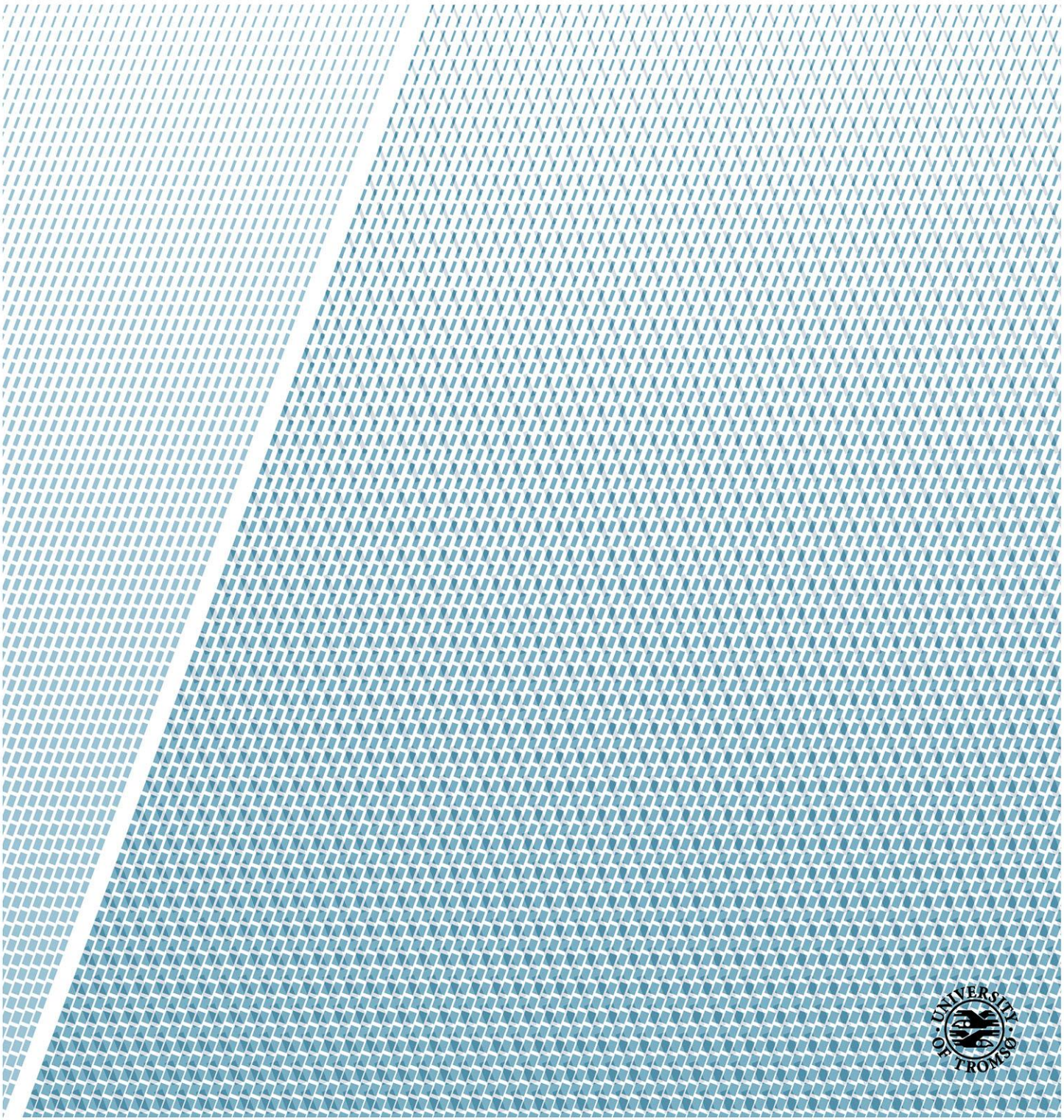

Abstract

In recent years, the petroleum industry started to look for new, unconventional energy resources. Peon, a shallow gas discovery in the northern North Sea, are being assessed as a possible energy resource. However, there are challenges related to reservoir pressure, sealing mechanism, and fluid migration. In this regard, geophysical and well log analyses is figured out to get a better understanding of the depositional regime and stratigraphy in the Peon area, as well as the structure of Peon and the dipping nature of the gas-water contact.

During the last 1.1 million years, the Norwegian Channel Ice Stream have fed the Norwegian Continental Shelf with enormous amounts of sediments. Peon is located at the base of a regional unconformity in the outer part of Norwegian Channel. The overburden and the reservoir reveal several prominent surfaces, distinguishing sub-horizontal bedded units. The presence of iceberg plough marks and mega-scale glacial lineations on these surfaces and several till units interbedded, testifies what great actor the ice streams had during deposition. Peon reservoir deposited likely during a glacial retreat. Orientation of reservoir, erosional truncations and structures in the top reservoir indicate a glacial advance has remobilized and cut the reservoir, forming a lensoid-shaped reservoir.

Acknowledgement

Tiden for innlevering av oppgave er kommet. Det føles godt, men også litt vemodig. Ønsker å takke alle som har støttet meg gjennom disse årene.

Takk til min veileder Stefan og biveileder Sunil for kyndig veiledning. Takk til Iver som stadig vekk kom innom kontoret for å hjelpe, flere ganger uten at jeg trengte å spørre. Og takk til Jessica for at du tok deg tid til å lese gjennom oppgaven og rette. Det settes stor pris på!

Familie, venner, og medstudenter har bidratt til at studietiden har vært en fantastisk fin tid. Takk til mamma, pappa og mine søsken for deres støtte – det betyr mye. En spesiell takk til bror for tålmodighet og hjelp med matematikk- og fysikkoppgaver.

Føler meg privilegert og takknemlig som har fått muligheten til å kombinere skolegang og toppidrett. Takk til Universitet i Tromsø for tilrettelegging av studiet.

Endelig er graden fullført, og jeg ser fram til nye utfordringer!

Håkon, juni 2015

Contents

1 Introduction

1.1 Objectives

The primary objectives of the project are to identify and map the Peon reservoir, delineate its trap consisting of glacigenic sediments, potentially identify individual reservoir compartments and their contacts, and better understand the geological setting and development of this shallow reservoir. Secondary objectives include to better understand the dipping nature of the gas-water contact.

1.2 Motivation

Petroleum exploration has taken place on the Norwegian continental shelf for almost 50 years. Conventional oil and gas fields have supplied the world with huge amounts of fossil energy. The amounts of hydrocarbon resources is limited and the production of oil and gas in Norway has decreased the last 10-15 years (NPD). In recent years, the industry change mindset and has been looking for new, unconventional energy sources.

In 2005 Statoil made the very shallow gas discovery of Peon in the northern North Sea. Such a shallow gas accumulation has never before been considered as a resource. This discovery was assessed as a valuable resource, and Peon became a pioneer in hydrocarbon industry. Peon is an example on how the petroleum industry have changed their mind in response to shallow gas accumulations. A "problem" has become a potential and viable resource (Carstens, 2005). In recent years, they have been looking for opportunities for exploiting these shallow energy resources. There are some challenges and limitations according to reservoir pressure, recoverable volumes, sealing mechanism and presence of unconsolidated sand. New technology will probably provide solutions for making these reserves economical to extract.

There is a certain of interest to extract so much information as possible from the Peon area, with respect to depositional history, reservoir properties, trapping mechanism, sealing rock and other geological information. The continental margin has been covered by glaciers several times the last hundreds years, and the understanding of these processes are important.

The tools that have been used in this thesis are seismic interpretation and well log data to extract information of the Peon stratigraphy, reservoir and sealing rocks, fluid migration pathways and

gas accumulations in reservoir and the overburden to get an understanding of the petroleum system and the depositional processes.

1.3 Shallow gas

Shallow gas is accumulations of gas trapped in the uppermost part of the stratigraphy. The upward migration of gas could stop due to barriers and impermeable layers close to the surface, and there can occur a potential accumulation of shallow gas. Shallow gas refer to gas pockets at less than 1000 m below seafloor (Davis, 1992). The Petroleum Safety Authority (PSA) of Norway define shallow gas as pockets of gas in the zone drilled before the blow-out preventer (BOP) is installed (PSA, 2007). There is no general, accepted term classifying shallow gas, but it is certainly accumulations of gas closer to surface than typically where reservoirs occur. As the Peon gas is covered by only 164 meter of overburden, this gas definitely falls under the category of shallow gas.

Where seals are well developed, extreme overpressures can build up in shallow reservoirs. Shallow gas accumulations are therefore risky to drill into due the relatively high pressure within the gas pockets, and the flows could be very hard to control. During a drilling operation, the uppermost 600-800 meters is drilled without BOP. Low fracture gradients make it problematic to inject dense enough formation fluids into the wellbore to stop the flow when blow-out occurs. According to PSA's definition, shallow gas will always considered as risky zones and prospects for drilling.

There have been major risks in association with drilling into shallow gas accumulations, and the petroleum industry has always tried to avoid them. Such gas accumulations are common in offshore areas and occur rapidly in petroleum provinces as the North Sea and Gulf of Mexico. The 6th of October 1985 the rig West Vanguard drilled into a shallow gas pocket in the Haltenbanken area. Uncontrolled flammable gas occurred and the rig was set to fire due to the blowout from the gas accumulation. The crew, with exception of one, managed to evacuate in lifeboats and saved their lifes. Shallow gas blowouts are the most common cause for drilling rigs to be lost. Reports from the Petroleum Safety Authority Norway testify that 44 of all wells drilled on the Norwegian continental shelf in the period 1984-2006 was implicated to shallow gas events (PSA, 2007).

The pressure within a shallow reservoir will often be much lower than a typical gas reservoir, and therefore it will be difficult to produce the shallow gas. By assuming a hydrostatic pressure within the young Peon reservoir, reservoirs buried to a couple of thousand meters will have up to ten times more gas in place, given the same reservoir volume. This requires the shallow gas accumulations to be much larger in extent and volume than deeper reservoirs to be commercial. The pressure at Peon is measured to 59.7 bar, while temperature of the Peon reservoir is 13 ^{o}C, inferring poorly compacted and consolidated sediments (NPD). Difficulties related to sand production will likely arise. The formation of hydrates is another issue to consider, especially at the production start-up when there is low temperature and relatively high pressure.

On the coast of Norway, shallow gas accumulations are thought to have been deposited in a glacial environment. They have developed in sorted glacial-derived sediments with a certain content of sand. The Peon consists of unconsolidated sands most likely deposited during deglaciation of the Norwegian Channel Ice Stream (Ottesen, et al., 2012).

1.3.1 Generation

Shallow gas has the same origin and composition as other natural gas. Natural gas in marine sediments originates in three ways – biogenic, thermogenic and abiogenic. Common for the first two are their naturally origins: living plants, animals and microbes. The distance of upward migration indicates the origin of the gas. Biogenic natural gas tends to generate in the top hundreds meters below the seabed. Low temperature and pressure conditions are favored, and the temperature does not exceed 60 °C. The gas generates as a consequence of bacterial activity and biological processes in sediments with high organic content.

Thermogenic natural gas, on the other hand, expels due to extensive burial and heating of organic matter. Microorganisms are not present in the generation of thermogenic gas. The temperature has to exceed about 120 ^{o}C to generate large amounts of gas, which occurs at burial depths at least 1000 meter below sealevel (Floodgate & Judd, 1992), depending on the geothermal gradient. High pressure and temperature is required to crack the organically derived kerogen into gas – a chemical, biological and physical process called maturation. A mature source rock experience the right conditions for alternation of kerogen. The third way of generating gas is abiogenic, where gas generates deep in the subsurface and high temperatures occur. In an abiogenic process, gas is formed from non-organic content. Figure 1 provides an

overview of petroleum generation. As the figure illustrates, biogenic gas expels without the presence of overburden, while other hydrocarbons require burial depths to generate. Oil generates before thermogenic gas, meaning thermogenic gas requires sufficient burial depth to generate. Time, temperature and kerogen type are the main factors in hydrocarbon generation.

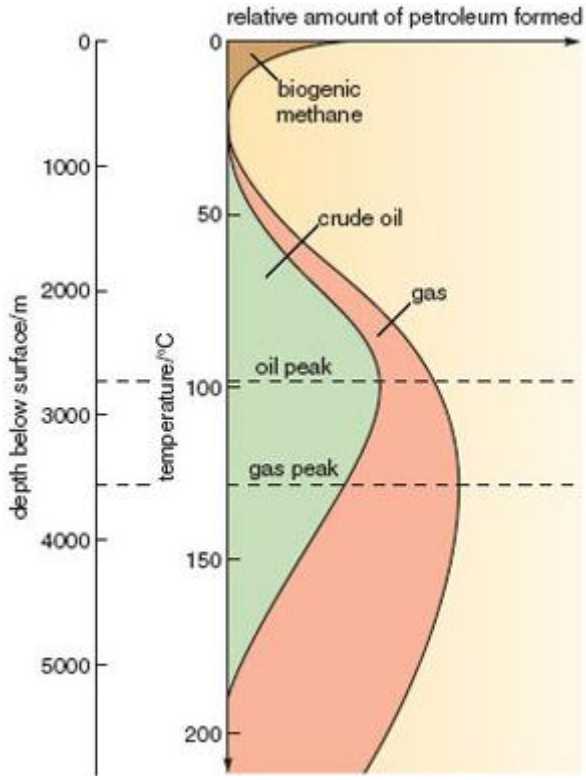

Figure 1: The relationship between burial depth, temperature and the relative amount and type of hydrocarbons formed. (From Open.edu)

If the origin of the gas is thermogenic, there has to be a source deeper in the formation. Shallow gas is therefore considered as a good indicator for deeper hydrocarbon resources. The composition of biogenic gas is almost pure (>99%) methane while thermogenic gas is composed of higher percentages non-methane hydrocarbons. The Peon field contains very dry gas with 99.54 % methane (NPD). There is an overview of the total composition of the Peon gas in Table 1.

Methane	0,9954
Ethane	0,001
Propane	0,001
i-Butane	0,0005

n-Butane	0,0005
i- Pentane	0,0005
n-Pentane	0,0005
n-Hexan	0,0004

Table 1: Composition of Peon gas measured at well 35/2-1 (NPD)

1.3.2 Migration

The generation and accumulation of petroleum occurs generally at different places in the subsurface. Hence, the oil and gas has to be transported from a source to a reservoir, a process called primary migration. Generation and migration is long-term processes and occurs at the same time. Secondary migration is internal migration within the reservoir. The fluids migrate through porous and permeable beds into traps and accumulates by a sealing mechanism. Figure 2 provides a conceptual overview of primary and secondary migration.

Compaction and deposition of overburden creates a pressure difference in the subsurface, making fluids to escape to adjacent areas of lower pressure. Darcy's Law gives a picture of the fluid flow in rock, and is given by

$$F = k\frac{\Delta P}{\mu} \quad (I)$$

The fluid flow (F) is thus dependent on, and proportional with, the permeability (k) to the rock, the pore pressure difference (ΔP) between the places where the flow is supposed to be, and inversely proportional to the viscosity (μ) of the fluid. Since gas has low viscosity, it flows smoother and faster than oil e.g.

Fluids can migrate laterally and vertically. Hydrocarbons have lower densities than other fluids in the subsurface, and due to the law of gravity, they tend to migrate upwards. If there are no barriers on their path, they will reach the surface. Vertical migration is upwards seepage of hydrocarbons trough stratified sediments. Lateral migration occurs along the stratigraphy where impermeable or more compacted layers act as barriers for vertical migration. Impermeable layers in the subsurface are necessary for accumulations of oil and gas. In fact, most of the hydrocarbons originated migrate to the surface. The lateral migration could extent for more than hundreds of kilometers in the most extreme cases.

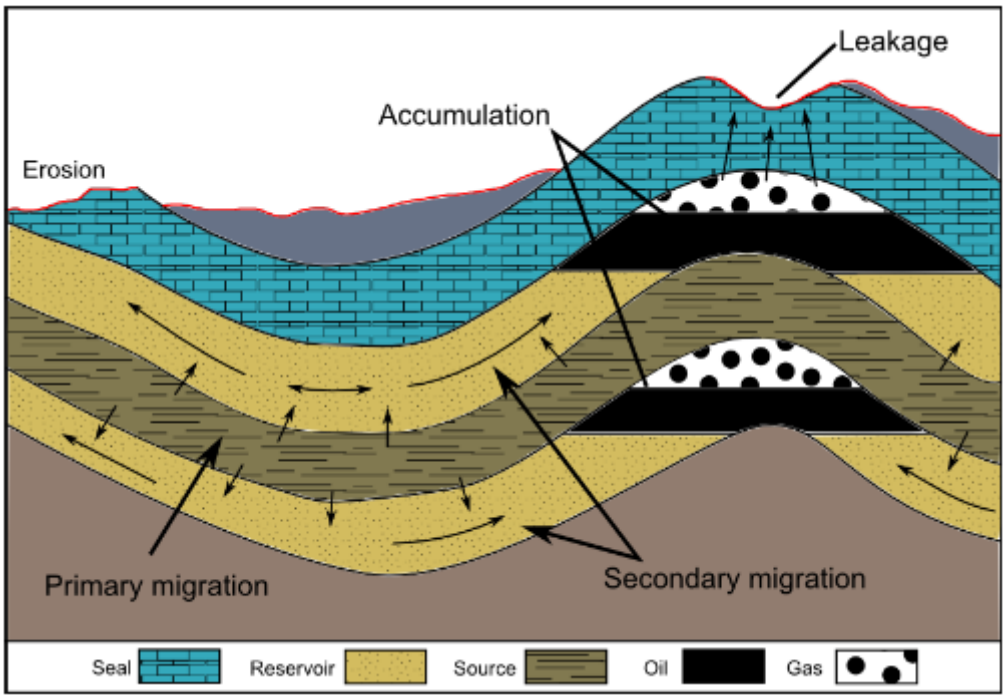

Figure 2: Petroleum migration and accumulation. Migration from source rock to reservoir is considered as primary migration, while secondary migration occurs within the reservoir. From (Kjerkreit, 2014).

Vertical migration or fluid flow through stratified marine sediments is a common process occurring on both passive and active continental margins worldwide (Vadakkepuliyambatta, et al., 2013). As mentioned, migration occurs due to pressure differences in the subsurface according to Darcy's law. Fluids tend to migrate when an excess pore-fluid pressure builds up. Several mechanisms and processes could trigger fluid migration. Vadakkepuliyambatta et. al. (2013) mention rapid sediment loading, uplift and erosion, dissociation of gas hydrate, polygonal faulting, as well as the general migration from source and reservoir rocks as such processes.

Networks of polygonal faults deform the initial sealing integrity when fracturing the rock. Cartwright et. al. (2007) infer that sealing sequences of Eocene age in the North Sea is deformed by extensive polygonal fault systems. Due to that, many underlying Paleocene reservoirs may have a defect seal, and hence no or little hydrocarbon is present in the reservoir.

Vertical fluid flow features could be interpreted in three ways in the seismic picture; leakage along faults, as acoustic pipes/gas chimneys and all other features that is not included in the first two categories (Vadakkepuliyambatta, et al., 2013). Figure 3 illustrate the first two

occurrences. The acoustic transparent zone in a) is interpreted as gas chimney where vertical fluid flow have occurred. The closely related high amplitude anomalies (HAA) is good indications of local gas accumulations. Leakage along faults is illustrated in b). Also here the HHAs is observed close to the migration pathway. Chaotic and low-amplitude reflections is common close to the root of major faults, indicating fluid migration from a deeper source (Vadakkepuliyambatta, et al., 2013). HAA along fault planes do often occur, and are observed in Figure 3b. This testify the presence and local accumulations of gas (Løseth, et al., 2009). The lateral extent of the migration is commonly smaller along faults than through gas chimneys (Figure 3b).

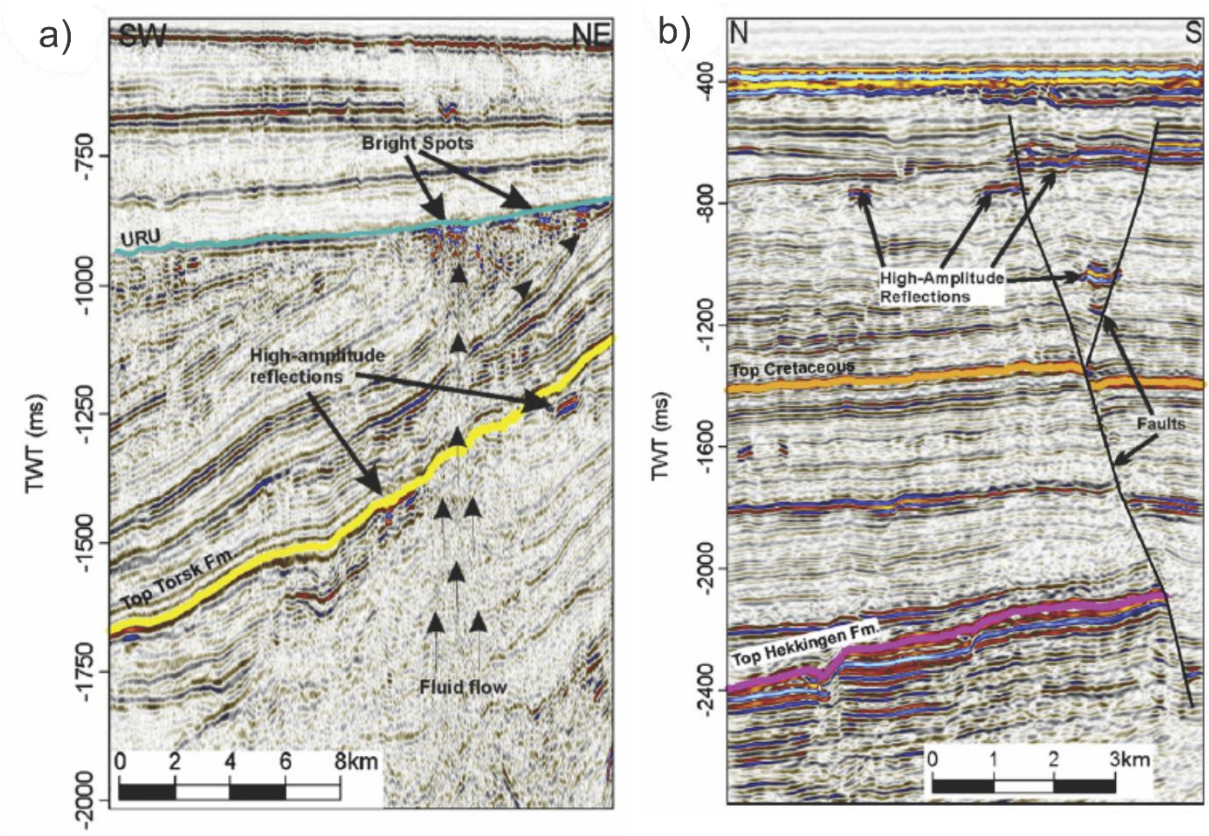

Figure 3: a) Showing interpreted fluid flow pathways connected to high-amplitude reflections and bright spots. The shallow bright spots reveal reverse polarity with respect to seafloor, indicating gas-filled sediments. The seismic profile is from Sørvestnaget basin close to Veslemøy High in the Barents Sea. However, there are similarities to Peon area with respect to stratigraphy and trapping mechanism. Stratified, conform, parallel units overlie dipping beds, separated by upper regional unconformity (URU). The Peon gas is accumulated right above the URU, like the gas here (represented by bright spots). b) Showing faulting and associated fluid leakage and high-amplitude reflections in the Hammerfest basin in the Barents Sea. Figure modified from (Vadakkepuliyambatta, et al., 2013).

1.3.3 Accumulation

Accumulation of shallow gas requires a barrier or a sealing mechanism to hold back for the upwards acting buoyancy forces. Both a consistent trap and an impermeable layer on top should act together. An effective seal must overlie a trap to accumulate amounts of hydrocarbon. If there are more than one fluid present within an accumulation, they will separate due to density variations. Gas floats on top of oil and water, respectively, as Figure 4 illustrates. If the source rock generates only gas, or the oil migration is absent, gas overlies water, and there will be a gas-water contact (GWC). The different parts of the reservoir are filled with different fluids, and are labeled gas cap, oil zone or oil leg, and water zone (Figure 4).

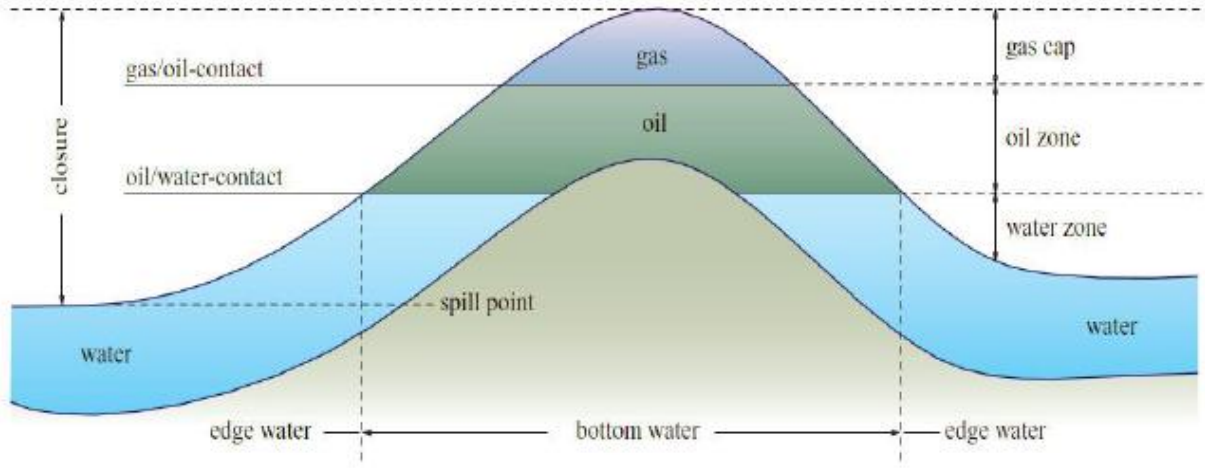

Figure 4: Anticlinal trap structure illustrating the fluid distribution within a reservoir containing gas, oil and water. Spill point is the lowermost point of the trapping structure. The structure is completely filled by hydrovarbons when gas or oil is filled to this point.

Sealing rocks should be impermeable, and shales are an example of that. The fine grain sizes prevent fluid flow through the layer, even though they are porous. A trap is a closure or entrapment for upwards migrating hydrocarbons. There are two major types of traps, structural and stratigraphic. In addition, diapiric, hydrodynamic and combination traps occur. Tectonic, post-depositional processes form structural traps. Forces as compression, compaction and extraction in the earth originate folding structures and faults, which are common structural traps. Stratigraphic traps are formed due to lithological changes either during (e.g. channels) or after deposition (e.g. truncations) (Selley, 1998).

A good reservoir has high porosity and permeability where the pore space is the most important factor. High porosity, meaning high percentage of pore space, makes it possible for hydrocarbons to accumulate. The pore spaces are generally filled with connate water, but is replaced by hydrocarbons within a field or a petroleum accumulation. The little burial depth of

a shallow accumulations means that diagenetic effects as compaction and cementation had has less impact on the reservoir. Very good porosities and permeabilities could occur, while very low degree of cementation could give rise to sand production. A small amount of cementation is therefore beneficial (Selley, 1998).

1.3.4 Seismic indications of gas

The presence of gas is best provided and detected by seismic data. There are several seismic attributes in reflection seismology that indicates the presence of hydrocarbons, and are known as direct hydrocarbon indicators (DHIs) (Wikipedia, Hydrocarbon indicator). Amplitude anomalies, including bright spot, flat spot and dim spot, polarity reversal, wipe-out zone, velocity effects and loss of frequency are common DHIs.

Contrasts in acoustic impedance subsurface gives rise to seismic reflections. The product of compressional p-wave velocity and density defines acoustic impedance (AI) (Andreassen, et al., 2007). Differences in acoustic properties between two sedimentary layers give rise to the reflection coefficient (RC), thus the strength of the reflections:

$$RC = \frac{AI_{layer\,2} - AI_{layer\,1}}{AI_{layer\,1} + AI_{layer\,2}} \quad (II)$$

The high density and velocity contrast between gas-filled and water-filled sediments gives rise to a large negative reflection coefficient, resulting in high amplitude anomalies in the seismic image. Gas in sediment pore space causes a dramatic reduction of compressional p-wave velocity. Hence, top-reservoir reflections are phase-reversed compared to strong, positive seafloor reflections.

In Figure 5, the seismic appearance of gas overlying water is shown by the seismic wavelet (b) and amplitude map (c). Due to AI contrasts between gas and water, the seismic wavelet appears as a trough when the signal penetrates the gas accumulation. This amplitude anomaly is called bright spot. In addition to top reservoirs, bright spots may indicate minor amounts of gas present in sediments. The amplitude map in Figure 5c shows strong negative amplitudes within the gas-filled body due this reduction in AI.

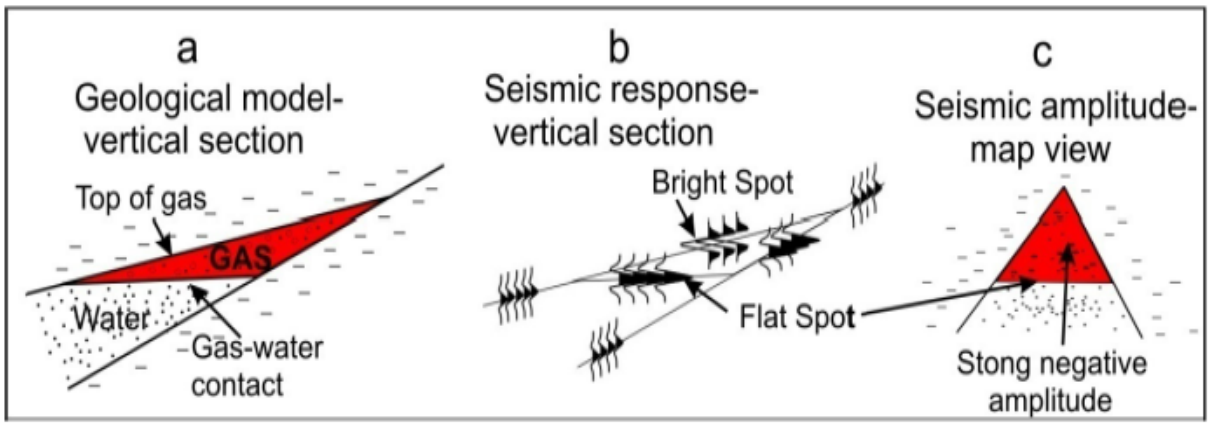

Figure 5: Sketch showing a) a gas accumulation in a vertical section, b) seismic response and c) seismic amplitude map. From (Andreassen et al, 2007)

The gas-water contact at the base of a gas accumulation is often represented by a flat spot, given that the accumulation is thick enough (Andreassen et al 2009). Figure 5b illustrate that flat spots appear as peaks on seismic traces, and thus represent positive reflection coefficients. This relates to the fluids density differences. In addition, the lower p-wave velocity in gas contributes to higher AI contrasts. There will always be an increase in acoustic properties at the interface between gas and water. Flat spots are among the best indications of gas and represent the base of a gas-filled reservoir. Oil-water contacts (OWC) could give rise to flat spots, as well. The impedance contrast is generally lower for OWC than GWC.

As mentioned above, gas-filled sediments have lower p-wave velocities than water-filled sediments. This infers that the seismic signal "delays" due to longer travel times, and a pull-down of the reflections could occur below gas accumulations in the two-way time sections. This velocity effect is a DHI and occur when there are thick enough gas accumulations. "Pull-downs" do often occur in combination with acoustic blanking. This is a "wipeout zone" in the seismic section where patches of the reflections are faint or absent. This effect is attributed to absorption and scattering of acoustic energy by an overlying body of gas-charged sediment (Davis, 1992), and hence falls under the category of direct hydrocarbon indicators. Wipeout zones may be interpreted as gas chimneys.

Loss of high frequencies occur in connection with bright spots caused by gas accumulations. Gas concentrations attenuate more high frequencies than water-bearing sediments. Zones below gas reservoirs could therefore occur as "low-frequency shadows". There might be more than 10

reasons for these shadow zones, thus intrinsic attenuation is among them. Also thinner gas reservoirs may give rise to these shadow zones (Castagna, et al., 2003).

Acoustic pipes are narrow, vertically stretched zones of acoustic masking.

1.4 Pockmarks

Pockmarks are depressions on the seabed caused by fluids escaping from the subsurface. They appear as craters due to the subsidence and collapse of sediments when gases and liquids migrate through them (Judd & Hovland, 2007). The shape could be circular or elliptical, depending on the slope of the seabed and current patterns, among others. From an environmental perspective, such seabed features give indications of natural pollution by gas seeping into the sea and surface. Enormous amounts of petroleum for a long period releases to the marine environment. On the other hand, pockmarks testify the presence of petroleum in the region, and presence of pockmarks will be considered when exploring for petroleum resources. They are treated as recorders and indicators of past and present hydraulic seabed activity (Hovland, et al., 2002). Pockmarks which are located straight above leaking faults and vertically disturbed seismic signals may indicate fluid migration pathways to the seabed. Also paleo-pockmarks can be identified on buried surfaces on seismic data and are clear indicators for fluid flow in the past, as well as the presence of deeper located hydrocarbons ((Ligtenberg, 2005) (Heggland, 1998)).

Pockmarks in the northern North Sea are observed back to the 1970s. Gas seepage related to the structures were quite rapidly indicated, and finally proofed in 1983 (Judd & Hovland, 2007). Especially, pockmarks are widely distributed in the Norwegian Channel. The density varies between 0 and 60 per km^2, and they appear most frequently close to the Troll gas field (Judd & Hovland, 2007), south of Peon. Due to that fact, this area has been very interesting in a petroleum exploration point of view. Troll, Veslefrikk and Snorre are fields located in the Norwegian Trench surrounded by many pockmarks.

Due to the shallow location, echo sounder and side-scan sonar records visualize pockmarks in a good manner. These kind of data are not available for this study. High resolution seismic visualize this seabed feature.

2 Geological setting and glaciation history

2.1 The North Sea

The North Sea is a major province according to petroleum activity and resources. This has led to acquisition of huge of amounts of geophysical, geological and geotechnical data from the area. The bedrock of the shelf comprises sedimentary units ranging in age from Triassic to Pleistocene.

The generation and break-up of the Pangaean supercontinent were the two major tectonic phases of the Phanerozoic eon, which covers the last 541 million years. In association with the break-up, tensional forces acted in the North Sea region from Permian, during Triassic and Jurassic, and ended during the Tertiary. This lithospheric extension formed sedimentary basins, where the sea level was the main factor controlling the depositional processes. Detrital sedimentation in a subsiding rift system was typical for the Triassic, while rifting, block faulting and erosion occurred in the Jurassic (Isaksen & Tonstad, 1989).

Cenozoic occurred from 66 ma until present and is subdivided into three periods; Paleogene, Neogene and Quarternary, and seven epochs: The Paleocene, Eeocene, Oligocene, Miocene, Pliocene, Pleistocene and Holocene. Sediments considered in the study area are relatively young sediments. Deposition took place during late Pliocene and Pleistocene. In the early Tertiary, several events of rifting occurred due to the opening of the North Atlantic Ocean. The earth movements stabilized during that period and uplift of the mainland occurred. This resulted in subsidence and formation of a sedimentary depocenters in the North Sea basin. Glennie (1990) stated that the Tertiary sediments constitute post-rift subsidence fill from previous periods (Jordt, et al., 2000). Later on the basins filled in with sediments.

According to Norwegian Petroleum Institute's factpages (NPD.no), four plays are present in the northern North Sea region; Paleocene, Cretaceous, Upper Jurassic and Upper Triassic to Middle Jurassic. The Peon is located in the very upper part of the stratigraphy and is of Pleistocene and Pliocene age. In that manner, Peon is an unconventional energy source whereas it differs from the typical play models in the region.

2.2 The Naust formation

The Nordland Group is the youngest group in the stratigraphic column and overlies the Hordaland Group. Nordland Group is extensively distributed on the Norwegian continental shelf (NCS) and consists of four formations; Kai, Molo, Naust and Utsira formation. They vary in extend over the shelf. Kai, Molo and Utsira formation are older than Naust formation. Thus, the stratigraphic column of interest in this study is the upper formation of the upper group.

The Naust formation comprises sediments from the Late Pliocene and Pleistocene. Prograding sedimentary wedges that underlies a column of flat-lying sheet-like units characterize the Naust formation (Ottesen, et al., 2009). Glacial-interglacial cycles resulted in deposition of huge amounts of hemipelagic, glaciomarine and contouritic sediments controlled bv the Fennoscandian ice sheet (Sejrup, et al., 2004). During ice-free periods or less extensive ice sheets, the Norwegian Atlantic Current played a major role controlling the depositional regime. Hemipelagic and contouritic, fine-grained sediments deposited on the slope. Figure 6a illustrates the current pattern present during interglacials. Peon is landward (SE) of the Norwegian Atlantic Current.

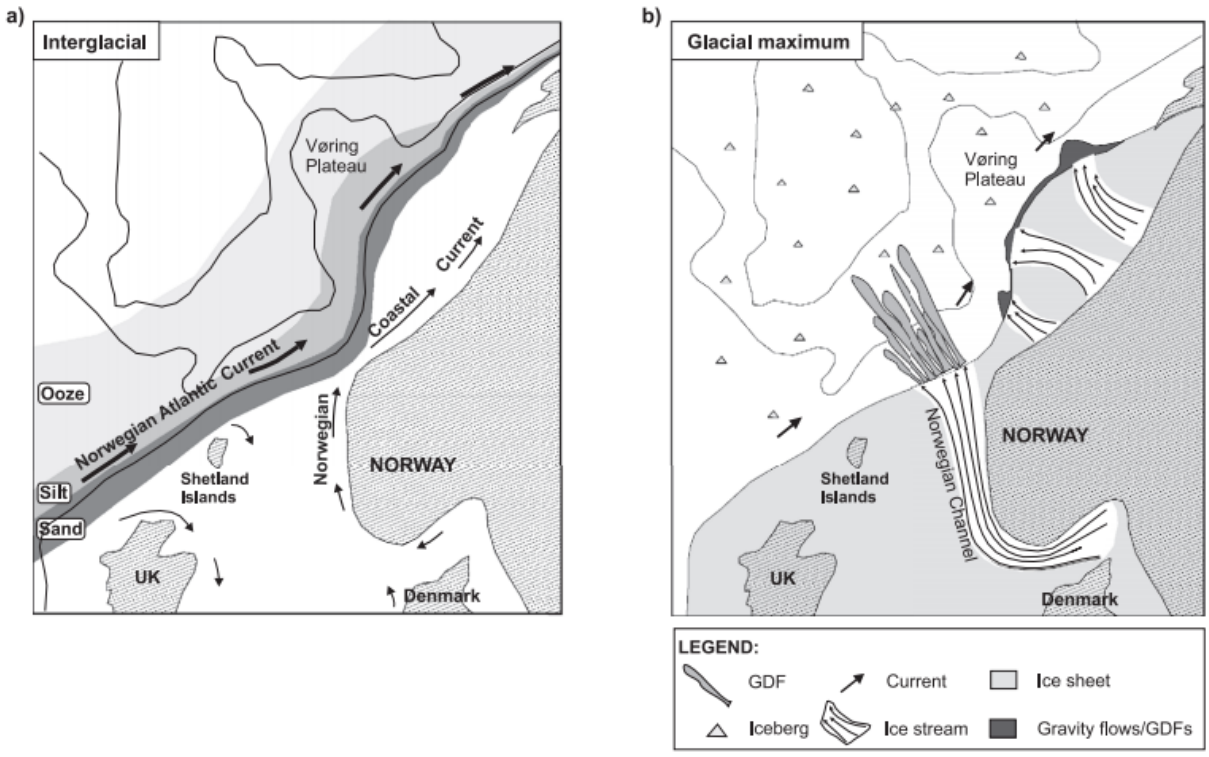

Figure 6: Setting of the North and Norwegian Sea during interglacial (a) and glacial maximum conditions (b). a) The Norwegian Atlantic Current played a major role during interglacial cycles. Hemipelagic and contouritic dominated on the slope. b) The NCIS fed the NCS with huge amounts of sediments during glaciations. Ice sheets deposited on the

inner shelf while glacigenic debris flow deposits dominate on the slope. The entire NCS reveal signs of iceberg deposits/ice-rafted debris, from the inner shelf to the outer slope. From (Sejrup, et al., 2004).

Several repeated glaciations controlled the depositional environment and sediment supply to the continental shelf during the last 2.7 million years (M.a.). Glacial ice streams, and hence ice sheets and icebergs, have fed the Norwegian continental shelf with huge amounts of sediments, as Figure 6 display. Naust formation represents sediments deposited the last 2.7 M.a., during the Pleistocene and late Pliocene period. The formation is laterally continuous across the Mid-Norwegian Shelf and is subdivided into five sequences, from oldest to youngest; N, A, U, S and T. The sequences N, A and U comprise sediments from the first glacial and interglacial periods. The start of the deposition of Naust formation correlates with the large increase in ice-rafted sediment supply, tentative dated to 2.7 Ma (Ottesen et. al., 2012). Deltaic units from the Molo formation are at the base and east of Naust.

Moderate glacial conditions and rather small ice caps were present over the Scandinavian mainland during the time period 2.7 - 1.1 Ma (Henrich & Baumann, 1994). However, a dramatic increase in the IRD flux is noticed at 2.7 M.a. This most likely represent the significant increase of ice sheets and volumes in connection with the startup of glaciations on the Northern Hemisphere ((Hjelstuen, et al., 2005), (Jansen, et al., 2000)). Naust N assumes to be deposited ca 2.8-1.5 M.a, while sequence A is tentatively dated to 1.5-0.6 M.a (Rise, et al., 2006). These deposits reveal a seismic signature of prograding wedges with a massive acoustic signature. Some of the units in Naust A probably represent glacigenic debris flow (GDF) deposits deposited during glacial maximums (Ottesen, et al., 2009).

About 1.1 Ma there occurred a climatic change. Deep-sea cores infer a significant increase of ice-rafted sediment deposits on the slope after 1.1 Ma.. This correlates with the growth of the Fennoscandian Ice Sheet (Henrich & Baumann, 1994). At that time, ice sheets originated on the NCS in the North Sea. Henrich et. al. (1994) documented increased environmental contrasts between glacials and interglacials in the period 1.0-0.6 Ma, and stated that more intense glaciations occurred at that time. Westwards transport of erosional products from the Norwegian mainland and inner shelf accumulated in basins offshore Norway, mainly as prograding sediment wedges (Rise, et al., 2005). Ice sheets reached the continental shelf break at glacial maximums, which led to large amounts of sediment supply to the shelf. Due to rapid loading, a lot of mass wasting activity occurred on the slope. High sedimentation rates were

followed by normal marine sedimentation during interglacials, where the ice only covered fiords and the inner part of the shelf (Hjelstuen, et al., 2005). Sediment delivery to the shelf was absent and slow hemipelagic sedimentation occurred (Ottesen, et al., 2012).

The period from 0.6 to 0.4 M.a is represented by sequence U (Rise, et al., 2006). Again, there was a glacier advance by the Fennoscandian Ice Sheet at 0.5 M.a. Several episodes have occurred the last 0.5 M.a. (Hjelstuen, et al., 2005), especially high sedimentation rates the last 400 k.a. (Ottesen et. al., 2012). Naust S was deposited during the period 0.4-0.2 M.a. Sequences S and T were deposited by the NCIS and are dated by records that are more reliable than the older sequences N, A and U. Sequence S comprises sediments from the third last major glaciation reaching the Mid-Norwegian and northern North Sea continental shelf, Elsterian. During this period enormous amounts of sediments were brought out in to the trough mouth fan, distributed as glacigenic debris flow lenses west of the shelf edge. Units from this sequence occurred locally on the shelf, and reveals an acoustic transparent character (Rise, et al., 2005).

Sequence Naust T comprises sediments from the last two glacial-interglacial periods, the Saalian and Weichselian (Ottesen et. al., 2012, (Rise, et al., 2006)). These glaciations occurred 0.2-0.125 M.a. and 0.125 M.a. - 15 ka (Fjellaksel, 2011), respectively. During the Saalian Ice Sheet, deposition of laterally stacked “till tongues” (TT) occurred. TT are wedge-shaped deposits of sediment interbedded with stratified glaciomarine sediment, and they constitute discrete stratigraphic units laid down near the margins of marine-ending ice sheets (King, et al., 1991). King propose that the formation of till tongue occurs from subglacial meltout beneath neutrally buoyant ice in contact with the seabed as it advances and retreats across the continental shelf. Poorly sorting and varying composition of gravel, sand, silt and clay (diamicton) characterizes these deposits. The seismic signature of tills reveals characteristic acoustically incoherent and blanken reflections, in contrast to the bordering coherent reflections, interpreted as ice-proximal, glaciomarine sediments (King et. al., 1991).

Weichselian is kind of twofold; Early and Middle Weichselian, and the Late Weichselian. The NCIS got few signs of ice sheets reaching the outer part during the early and middle period. Borehole readings and seismic interpretation suggests that normal marine sedimentation occurred during that time. The ice sheets expanded during the late stage of Weichselian and reached the mouth of the NC several times. Glacial and interglacial periods interacted and

changes between glacial maximums to normal marine sedimentation occurred in only a few hundred years (Hjelstuen, et al., 2005). Calculations by Nygård et. al. (2004) estimates that the NCIS brought up to 6300 km^3 of sediments during the Late Weichselian.

The Naust formation has little to no degree of sorting, which support a sedimentary environment dominated by glacial activity and processes. However, there are some sand layers of limited thickness interbedded, especially in the northern North Sea. Well data reveal that up to 40 meter of sand and gravel has been deposited in the period 12500-10800 ^{14}C years BP (Rokoengen & Rønningsland, 1982). This infers development of reservoirs within the depositional period of Naust formation.

2.3 The Norwegian Channel

The Norwegian Channel is by far the most prominent seabed feature in the North Sea, located adjacent to southern and southwestern Norway, terminating at the continental margin of the northern North Sea. The formation of the channel has been debated for long time, but in 1983 Rokoengen and Rønningsland stated that buried erosional features indicated ice movement within the channel (Ottesen, 2006). Todays common understanding is that the Norwegian Channel results from processes related to repeated ice stream activity through the last 1.1 M.a. (Sejrup & Larsen, 2003). Ice streams are parts of an ice sheet that has higher speed than the surrounding ice, and they can move more than 1000 meters a year. They are fast-flowing curvilinear elements within ice sheets that have sharp velocity gradients to slower flowing (10 m/yr) ice beyond their margin (Dowdeswell, et al., 2005). Water at the base of the ice sheet acts as a lubricating mechanism, making the flow faster (Ottesen, 2006). Ice streams expanded to the shelf edge within the channel and acted as a transport mechanism for glacial sediments. Norwegian Channel Ice Stream (NCIS) refers to the ice streams that acted in the Norwegian Channel.

Figure 7 visualize the direction of flow within the NCIS while Figure 9 display the outline and depth of the channel. The channel follows the coast in a northward direction (Rise, et al., 2004), originating in the Oslofjord area in southeast via Skagerak and reaches the depocenter at Stad. The trench is 50 to 100 km across in general before it widens northwards - up to 160 km at the shelf break, close to the study area. Average depth is 100 m in the North Sea but up to 700 m

off the coast of Arendal (Sejrup & Larsen, 2003). The NCIS is formed like a trough, which reveals an asymmetric shape, where the western slope is gentle and the landward is steep.

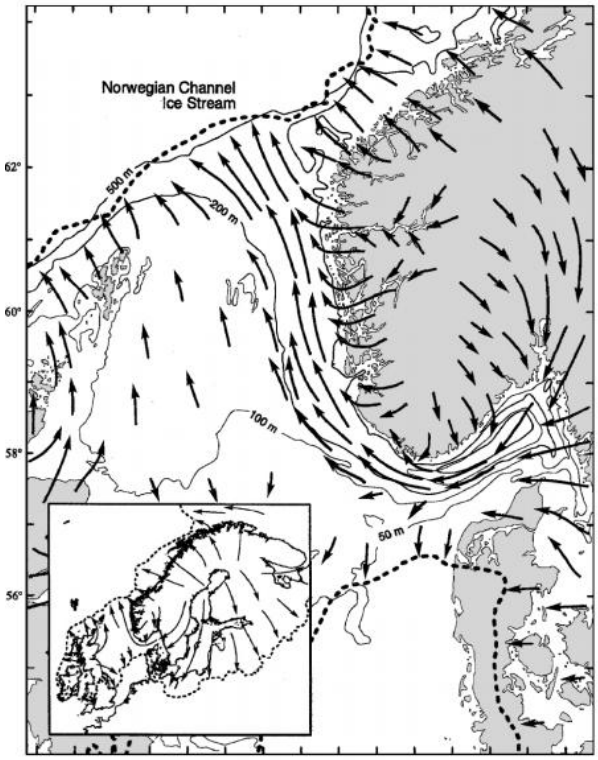

Figure 7: Tentativ outline of the Norwegian Channel Ice Stream. Relative length of arrows depicts ice velocity (from Sejrup et. al., 2008).

The indications for the lowermost, and hence oldest, till unit overlying marine sediments is dated to 1.1 million years by paleomagnetism, amino acids and strontium isotopes. This infers the presence of the NCIS at that time ((Hjelstuen, et al., 2005), (Sejrup & Aarseth, 1995)). Sejrup et al 1994 concluded that the last deglaciation period within the Norwegian Trench terminated close to 15.1 ka BP. The entire trough area is dominated by several till units on top of a regional unconformity. Typical till units are channel-like units of 30-40 meters thick till deposits. They are surrounded by marine/glaciomarine sediments and separated by extensive glacial eroded surfaces (Sejrup, et al., 2004). GDF deposits on the North Sea Fan connect these till deposits in the downslope direction (King et al, 1998). This suggests that during glacial maximum, when ice sheet were grounded at the shelf edge, the NCIS delivered basal till to the edge and were distributed further downslope as GDFs ((Sejrup, et al., 2004) (Ottesen, et al., 2009)).

The North Sea Fan testify that huge accumulations of sediments accumulated at the mouth and outer limit of the NCIS. The North Sea Fan is considered as a trough mouth fan, which Laberg & Vorren (1996) describe as a terrigenous, cone- or fan-shaped deposit located seaward of a glacially formed submarine or subaerial trough. The large North Sea fan at the mouth of the NC consists of up to 1800 m thick Late Pliocene-Pleistocene succession of sediments (Sejrup, et al., 2004). The ice stream pattern and direction of ice streams has some variation from different glaciations, and appears to be the main reason for the changing location of depocenters within the fan (Ottesen et. al., 2012).

Peon is located at the border to the North Sea Fan, at the outer limit of the Norwegian Channel Ice Stream (Figure 8, Figure 9). The Måløy plateau is located east of the channel, as we see in the zoomed in map in Figure 8.

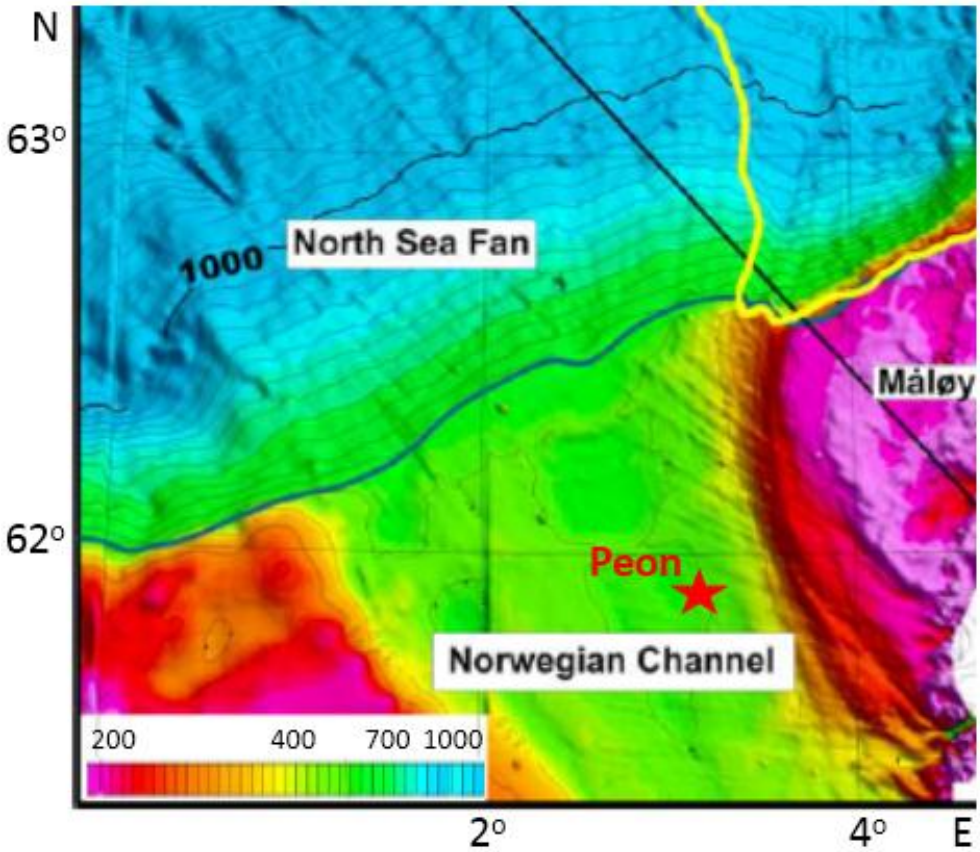

Figure 8: Zoom in of Norwegian channel and position of Peon. Peon is located towards the eastern border of the NC, close to the Måløy Slope. Overview location of Peon is illustrated in Figure 9. Modified from (Rise, et al., 2005).

Ice sheets and glaciers have two primary sources of sediments; sediments fed onto the glacier surfaces, and erosion and transport of sediments at the base of the glacier. The latter is the major transport mechanism for large ice sheets. Erosion and deposition are two processes interacting

within an ice stream system. The ice streams differ from onshore glacial activity in at least two ways; the ice is grounded in seawater and the glaciers are eroding into soft sediments on the seabed. In general, an ice stream can be divided into minor systems or stages. The inner part of the ice stream is where ice is acting and covering the seafloor on the continental shelf. Erosional processes dominate; rapid ice flow deforms the seabed, where drumlins typically form. Depositional processes do also occur in the inner part of an ice stream system. Remobilization of sediments and deposition of tills are examples of such subglacial depositional processes. Closer to the ice contact and the shelf break, the depositional system is becoming glaciomarine rather than subglacial. Huge amounts of sediments is deposited as ice-rafted debris (IRD) and suspension fall out. These IRDs are typically unsorted and contain all types of sediments. However, we differ roughly between proximal gravel, sand and mud diamict and finer distal mud deposits. Finer material keep in suspension for longer periods and can therefore be transported further out from the source. On the shelf break and slope, mass transport agents as gravity flows occurred.

The North Sea Fan (NSF) is a depocenter for these sediments, a result of the ice stream processes in the Norwegian Channel and is located north/northwest of the NC. The location of the NSF infers that the NCIS has been very important for the sediment supply to the continental margin. Especially during the last glaciation, the Late Weichselian, the Norwegian Channel Ice Stream transported large volumes of sediments to the shelf. This contributed to extensive debris flow activity and 400 m thick GDF deposits accumulated as prograding wedges on the continental slope (Rise et. al., 2004, Ottesen et. al., 2012). Stacks of mounded GDF deposits and major slide debrites are the two main characterizing depositional facies for the proximal province in the North Sea Fan. They occur as continuous elongated lobes, lensoid in cross-section, 2-40 km wide and up to 60 m thick (Sejrup, et al., 2004). In addition, contorted to transparent facies and laminated facies characterize the proximal part of the NSF (Nygård, et al., 2005).

The deposited sediments have imprints like drumlins, mega-scale glacial lineations (MSGL), and stone orientations in tills and striations, which are possible related features to the Norwegian Channel Ice Stream (Sejrup et. al., 2003). The presence of MSGL (streamlined lineations) bedforms indicate the location of the past ice streams. The lineations are formed at

the base of fast-flowing ice streams by deformation processes affecting the upper few meters of the sediments (Dowdeswell et. al., 2005).

2.4 Study area

Peon gas accumulation is located in the outer part of the Norwegian Channel in the northern North Sea, on the border to the Norwegian Sea. Figure 9 shows a bathymetry map of the NCS,

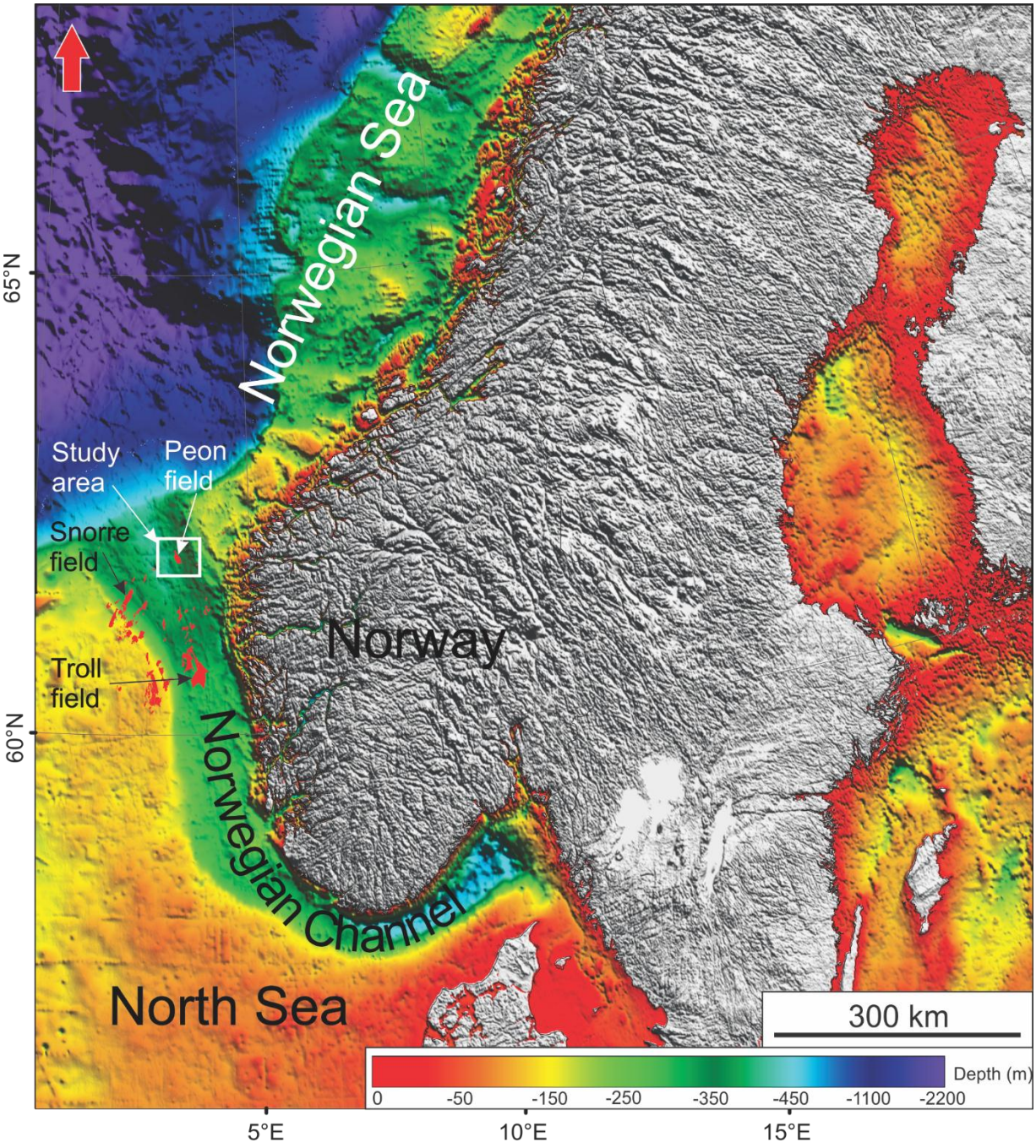

Figure 9: Bathymetry map of North Sea and Norwegian Sea showing location of the Norwegian Channel, Snorre and Troll field and the Peon discovery (study area). Modified from Vadakkepuliyambatta et. al. 2014.

indicating the deeper Norwegian Channel and the Peon discovery located within, as well as the Troll and Snorre field.

Peon was discovered in 2005 by exploration well 35/2-1 and appraised by 35/2-2 in 2009. The discovery is located between 61.8 and 62.0 °N and 3.3 and 3.5 °E, north of the Troll field, west of the city Florø and approximately 75 km northeast of Snorre field (Figure 9). Recoverable resources are estimated to be 19.5 billion Sm^3 of gas (NPD). Peon was planned to be developed by three oil companies, but the operator Statoil announced early 2014 that the field will not be economical beneficial today due to lack of infrastructure and low reservoir pressure. Technology and experiences from other fields on Norwegian continental shelf will be used in a future evaluation.

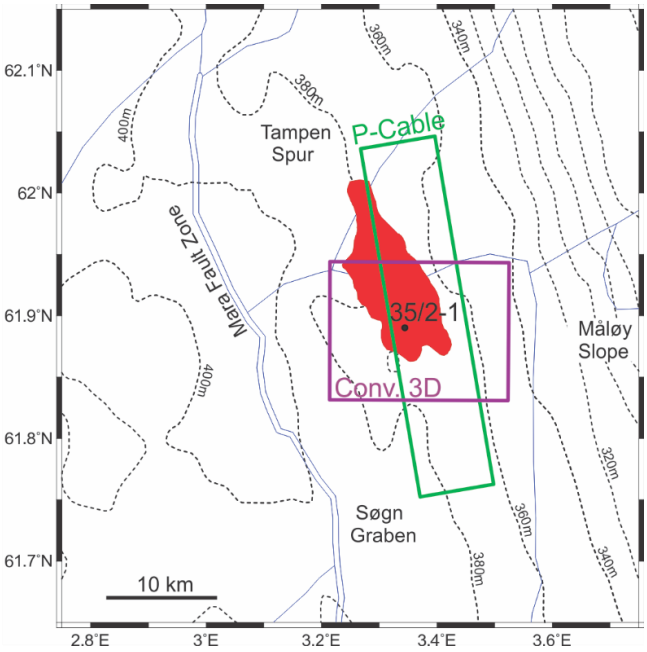

Figure 10: Outline and location of the Peon reservoir (red body), p-cable dataset (green rectangle) and conventional 3D dataset (purple rectangle) relative to the major structural elements and latitude and longitude. Numbers and black dotted lines indicate height of water column. Mara fault zone to the west and Måløy Slope to the east of Peon. Modified from (Vadakkepuliyambatta, et al., 2013).

Figure 10 provides a more exact position of Peon with latidude and longitude on the axes. The structural elements Tampen Spur is north, Søgn Graben south, and the Mara fault zone west of the discovery. The Mara fault zone strethes NNW-SSE and is parallel to the elongate shaped Peon. The discovery is mainly located in block 35/1 and 35/2, but touches upon block 6203/10 in north and 35/4 and 35/5 in south. The discovery consists of dry gas in the Pleistocene Peon sandstone with a lateral extent of ca 120 km^2.

Water depth is 384 meter and the reservoir is located at 548 mbsl, inferring overburden of only 164 m. A conceptual overview of the Peon sand body is shown in Figure 11. The 164 m thick stratigraphy will be evaluated in detail. Data from NPD measured the net to gross ratio to 0.99, which means very high content of sand within the reservoir. Peon reservoir has a temperature of 13 ^{o}C and a pressure of 59.7 bar. Permeability measurements up to 4 Darcy infer good drainage properties within the reservoir (NPD).

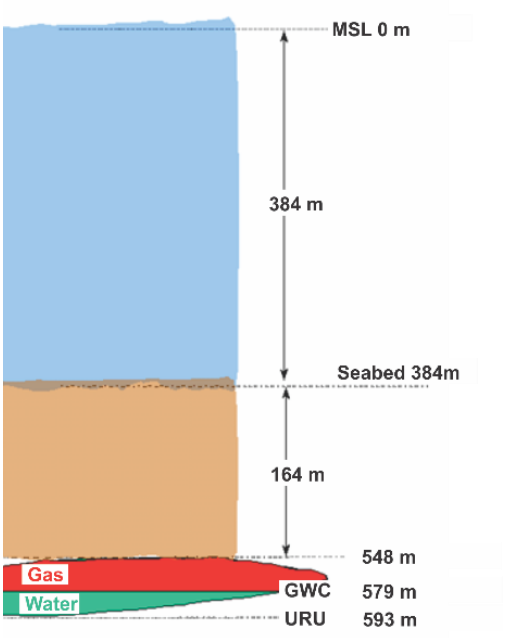

Figure 11: Conceptual overview of the Peon sand. Depth data are subsea true vertical depth (SSTVD) at well 35/2-1. Overburden consists of 164 m while the 45 m thick reservoir zone is between 548 and 593 mbsl. The upper regional unconformity (URU) represents the lower boundary for the reservoir. Gas-water contact is located at 579 mbsl. Figure modified from (Internal report, u.d.).

2.5 Upper Regional Unconformity

The base of Peon is located right on top of a regional angular unconformity, the Upper Regional Unconformity (URU). The URU separate underlying steeply dipping layers from sub-horizontal layers of lying on top. The sediment package on top is glacial in origin, and is about 200 meter thick in the study area. The package comprises mainly flat-lying tills and layered marine/glaciomarine deposits (Sejrup et. al., 1995). The Upper Regional Unconformity is present in many areas of the shelf, and it is marking an abrupt change in the layer architecture. The unconformity represents the base of several erosional events produced by the third last glaciation, Elsterian, and is located on the base of sequence T in the Naust formation (Ottesen et. al. 2009). The amounts of sediments eroded at the URU is debated, as well as the age of the unconformity.

3 Data and methods

3.1 Seismic data

3.1.1 P-cable data

High resolution P-cable 3D seismic data, conventional 3D seismic data and well log data is applied in this study. The P-cable data provide high-resolution seismic images up to one second two-way travel time. It is the primary data in this study, used to characterize the reservoir and the upper part of the stratigraphy. Small amounts of the acoustic energy from high-frequency data penetrates to the deeper formations. P-cable technology allows a number of seismic profiles to be acquired simultaneously in a cost-effective way.

The P-cable dataset of Peon was acquired in 2009 to extract more information and to get a better understanding of the overburden and the reservoir. Fluid migration pathways and shallow gas accumulations visualize in a better manner. Figure 12 display the acquisition method of the p-cable dataset. 24 streamers run parallel to the ship direction with a spacing between 6-12 m. The 25 m long streamers are hooked to a cross-cable towed behind the vessel. Each of them contains 8 groups of 4 hydrophones (Vadakkepuliyambatta, et al., 2014). The sample interval is 0.5 milliseconds.

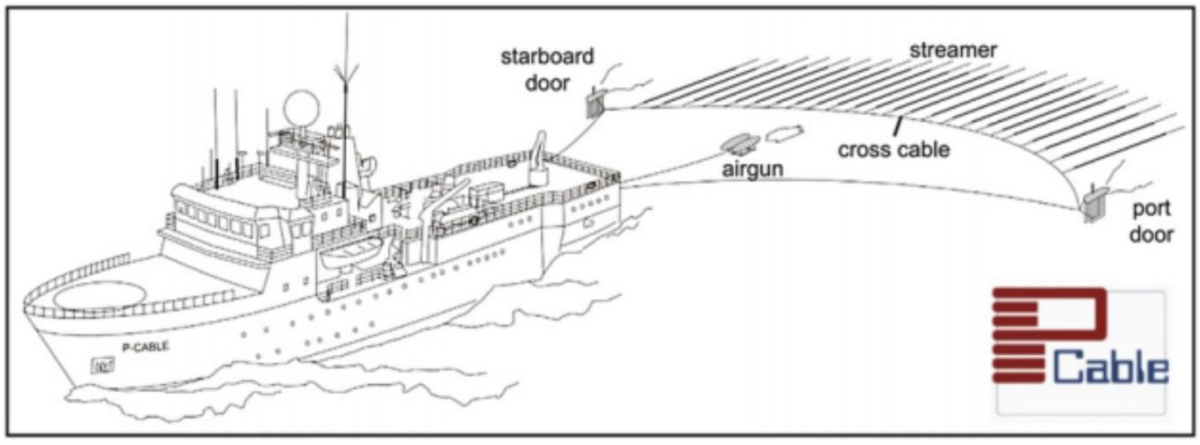

Figure 12: Schematic illustration of p-cable 3D seismic system. The vessel in front of 24 streamers oriented parallel to the direction of acquisition. The airgun is towed directly behind the boat, in front of the crosscable that hooks the streamers. Figure from (Petersen et al., 2010).

In contrast to conventional three-dimensional seismic technology, P-cable system is lightweight and can be deployed quickly from small vessels. The system is particularly useful for acquisition of small three-dimensional cubes of 10-50 km^2 in focus area, rather than extensive mapping of large regions (Planke, et al., 2009). Acquisition done over the Peon area has focused

on the eastern part of the discovery. There occur two parallel stripes of no data on all interpreted horizons and maps from the p-cable 3D dataset. They are oriented in the inline direction, which indicates problems due to acquisition and/or processing of the data. The inline direction is NNW-SSE, meaning the boat travelled back and forth in that direction during acquisition. The processed seismic data covers areas of about 150 km^2, 30 km in the inline direction and 5 km across. Peaks in the seismic data represent a negative impedance contrast. This infers that the seafloor reflection reveals negative amplitude values, even though it represent a positive reflection. It is worth to notice when we consider the interpreted horizons.

The seismic energy is provided by four Sleeve guns which are shooting with an interval of 6.25 m and a pressure of 2000 psi. Bin spacing is 6.25 x 6.25m and the dominant frequency is about 100 Hz (Vadakkepuliyambatta et. al., 2014). The average p-wave velocity is 1700 m/s. According to formula 1, the seismic resolution of this dataset is 17 m. Hence, the vertical resolution is about 4 m (one quarter of the dominant wavelength). Horizontal resolution depends on bin spacing, thus 6.25 m is a good indication for the horizontal resolution for the P-cable dataset.

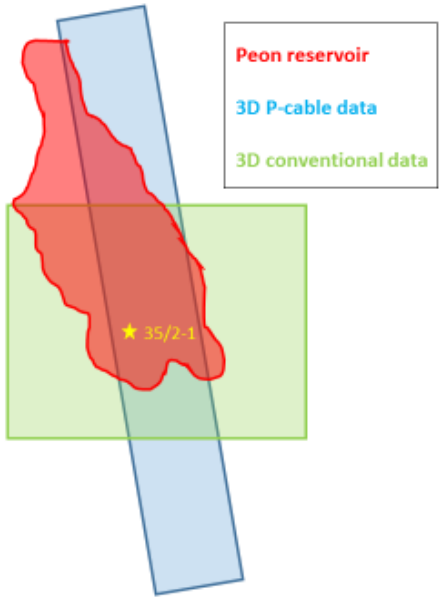

Figure 13: a) Relative location of Peon reservoir, 3D datasets and well 35/2-1. The outline of Peon is indicated by the elliptical, red-filled body. Blue and green rectangles gives location of 3D p-cable and 3D conventional datasets, respectively. b)

In Figure 13, the outline of the Peon reservoir and the available data is illustrated. This figure is used as a reference map when showing location of interpreted horizons and seismic sections in this thesis.

3.1.2 Conventional 3D data

The acquisition of conventional 3D seismic data is done in a more central and quadratic area than the P-cable seismic data, and it covers the southern areas of the Peon reservoir (Figure 13). The inline direction for this dataset, as well as the direction of acquisition, is W-E. 16 km (inline direction) times 12 km (x-line direction) gives a total area of about 190 km^2. The two types of seismic datasets complement each other. The conventional 3D seismic data has poorer resolution in the overburden and reservoir than the p-cable data, and therefore the latter data are most commonly used. Dominant frequencies between 18 and 40 Hz makes these signal penetrate deeper in the subsurface. Assuming the p-wave velocity for the uppermost stratigraphy to 1700 m/s, the seismic wavelength is between 42 and 94 m, and a vertical resolution between 10 and 24 m.

3.1.3 Seismic resolution

Resolution is the ability to separate two features that are close to each other, and could be defined as the minimum distance between them that makes it possible to distinguish them. Features are seismic resolvable if they are identified individually rather than as one feature. The velocity (v)/frequency (f) relation determines seismic resolution, and is expressed in terms of seismic wavelength (λ);

$$\lambda = {}^{v}/_{f} \quad (III)$$

High seismic frequencies relate to low wavelengths, which implies a good resolution. Attenuation of seismic energy is the reduction of amplitude or loss of seismic energy with depth. The high frequencies attenuate faster than lower frequencies. Sediments and rocks are more compacted deeper in the formation. In general, the seismic p-wave velocity increase with depth. According to the formula (III) and Figure 14, the dominant wavelength of the seismic pulse will increase rapidly as the wave travels through the earth. Both the frequency decrease and the velocity increase trigger an increasing wavelength. Thus, there is a quite large increase in wavelength with depth.

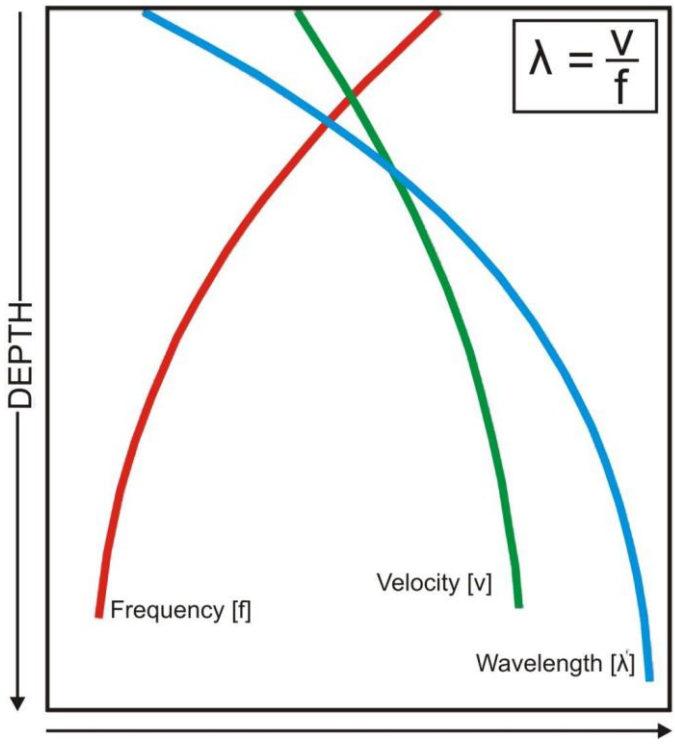

Figure 14: Relationship between frequency, velocity and wavelength with increasing depth (from Vevik 2011).

3.1.3.1 Vertical resolution

Seismic resolution comprises two aspects – the vertical and horizontal resolution. Vertical resolution is defined as one quarter of the dominant wavelength. Below that wavelength, two wavelets interfere to form a single wavelet of high amplitude, and we could not distinguish them. This is the minimum distance between two objects to both be visualized in seismic data, and is known as the tuning thickness (Andreassen, 2009).

3.1.3.2 Horizontal resolution

The wave front of seismic signals spread out spherically when traveling into the earth. The Fresnel Zone characterizes horizontal resolution, known as the lateral extent/area a wave front is covering by one quarter of a wavelength. This means that two features within the Fresnel Zone will not be separated on the seismic data. Fresnel Zone radius (rf), and hence horizontal resolution, is dependent on depth (given in two-way-travel time, t), velocity (v) and frequency (f), given by the formula

$$rf = \frac{v}{2}\, x \left(\frac{t}{f}\right)^{1/2} \quad (IV)$$

The horizontal resolution improved a lot when the 3D seismic method complemented and almost replaced the 2D seismic method. The grid spacing was reduced from about a kilometer to 25 m or less. The bin spacing is often considered as the ultimate limit of the horizontal

resolution in 3D seismic data. It allows complex geological structures to be accurately imaged in three dimensions (Cartwright & Huuse, 2005), and the new technology was a breakthrough for the hydrocarbon exploration and production. Reservoir structures, salt domes and thrust fault systems have previously been problematic to map out, but 3D seismic data has solved many of the interpretation challenges with such complex structures. This also applies to architectural elements in depositional systems, such as submarine channels and glacial footprints. Geomorphologic mapping of surfaces has become a valuable tool to investigate in paleo-environmental regimes.

3.1.4 Seismic attributes

Seismic attributes is very useful to complement the detailed mapping of the subsurface, and may help an interpreter to see features, relationships and patterns that otherwise might not be detectable. Seismic signals provide a lot of lithological, structural and stratigraphic information about the subsurface. These patterns and features are visualized in a good manner by seismic attributes

A seismic attribute is defined in several ways. Chopra & Marfurt (2005) mentioned them as a quantitative measure of a seismic characteristic of interest, while (Nauriyal, et al., 2010) defined a seismic attribute as a mathematical transform of the seismic trace to predict physical properties of the rock. Attributes can be applied on seismic sections, a constant time interval (time-slices), random intersections, surfaces and as volume renders (Vevik, 2011). Brown (1996) classified time, amplitude, frequency and attenuation as the main seismic attributes. Their derivatives, which means the rate of change, are also important attributes. Time attributes provide information on structure, whereas amplitude attributes provide information on stratigraphy and reservoir (Chopra & Marfurt, 2005).

The attributes are often a function of the characteristics of the reflected seismic wavelet (Taner, 2001). The seismic wavelet can be expressed in terms of a time-dependent amplitude A(t) and a time-dependent phase θ(t) (Taner, et al., 1979);

$$f(t) = A(t) \cos \theta(t) \quad (V)$$

The reflection strength attribute is given by A(t) while θ(t) defines the instantaneous phase attribute. High reflection strength often represent lithological boundaries in the geological record and fluid contacts, and could therefore be a hydrocarbon indicator. An abrupt change in depositional environment or another discontinuity may cause such a lithological contrast, and hence high reflection strength. There are also a large number of seismic attributes available for characterizing different sedimentary environments (Andreassen, et al., 2007).

3.1.4.1 Instantaneous frequency

Instantaneous frequency is given by the time-derivative of the phase: $\omega(t) = \frac{d\,\theta(t)}{dt}$, in other words the rate of change of the phase. Frequencies vary due to both wave propagation effects and geological events, and hence used to identify geological events. Hydrocarbon indicator, fracture zone indicator and bed thickness indicator are some of the uses for instantaneous frequency attribute (Taner, 2001). There is often observed lower frequencies below reflectors representing hydrocarbon-filled sediments, and is referred to as a "low-frequency shadow". This is a result of scattering and absorption of seismic energy from the hydrocarbon-filled sediments (Andreassen, 2009). This is also an important tool for structural analysis, and lower frequencies could occur in connection with fractures in the seismic. Sharply interfaces with thinner beds, such as laminated shales, give rise to higher frequencies than thick packages, for example massive beds of sandstone.

3.1.4.2 Root Mean Square (RMS)

Another frequent used attribute in this study is the root mean square (RMS) amplitude attribute. This attribute is averaging the amplitudes over a picked interval. It is defined as the square root of the sum of the squared amplitudes divided by the number of samples within the chosen interval. Commonly used to study areas of high-anomaly amplitudes in more detail. Since it is squaring both positive and negative amplitudes, this attribute is effectively highlighting areas of large acoustic impedance contrast. The RMS amplitude attribute is smoothening the reflection strength for the area of interest. By doing a volume attribute, we can smoothen the complete 3D cube and get a new cube based on RMS amplitudes. This provides a good overview of the concentration of high amplitude anomalies over the 3D cube.

3.1.4.3 Variance

The variance attribute is calculating the trace-to-trace variability in the seismic data. Large changes in acoustic impedance from one trace to another gives a high variance value, and opposite for similar traces next to each other. The variance attribute map effectively discontinuous features as faults and lithological changes. Those features reveal high variance coefficients. Small local variances, or low trace-to-trace variability, display transparent/weak reflections on a variance attribute map. The variance attribute is helpful for gas chimney mapping and for discrimination between high and low continuity of seismic reflections (Schlumberger, 2010). The Edge method refers to the variance attribute in Petrel, and is useful in detecting edges. Edge means discontinuities in the horizontal continuity of amplitude (Eidsnes & Sonnonberg, 2013).

3.1.5 Software and interpretation

The interpretation of seismic data is done in Petrel 2014.1, a software provided by Schlumberger. Different interpretation techniques and methods are applied to interpret horizons. Combined use of guided autotracking and seeded 2D and 3D autotracking has been useful. Manual interpretation perform a linear interpolation between the chosen points along a horizon and is applied in challenging areas. Guided autotracking is an automatically tracking of the horizon where it chooses the best route between two picked points. Seeded autotracking tracks points along a reflection until it comes to a discontinuity or the signal is too weak according to the specified parameters. The strong seabed reflector was interpreted by 3D seeded autotracking. Seeded and guided 2D autotracking were useful for deeper and more discontinuous horizons. Thus, the interpretation method depends on the lateral continuity and reflection strength. Manual interpretation together with guided autotracking is preferred for interpretation of intra-reservoir reflections.

The seismic interpretation and observations presented is a result of the identification and mapping of the Peon reservoir and horizons in the stratigraphic column above. Interpretations on the p-cable 3D seismic data provides information of the Peon reservoir, structure, seal and overburden, while conventional 3D seismic data was applied for complimenting interpretations on reservoir structure, as well as deeper horizons and structures. The focus on this project has been on reservoir and shallower horizons.

3.2 Well data

Exploration well 35/2-1 was drilled in 2005. The well penetrated into the reservoir at 548 mbsl close to the apex of a mound structure of the reservoir and continued down to 713 mbsl. Well log data is correlated with seismic data to get a better understanding of the reservoir, the fluid contacts and lithological boundaries. These data provides information about reservoir properties. Gamma ray, density and p-wave velocity/sonic measurements are used to characterize the stratigraphy, reservoir and intra-reservoir reflections. The well is also used to identify stratigraphic units.

Density and sonic measurements have been carried out for the reservoir zone at well 35/2-1. Gamma ray values is measured from well top to TD. Synthetic seismic is based upon density and sonic measurements and is therefore available for the reservoir zone only. These well log data provides good and exact information from at the well location. By correlating well data and seismic data, we can strive to get a regional picture and see if the lithology, fluid content and stratigraphy is lateral extending and continuous.

3.2.1 Gamma ray

The gamma ray is one of three common logs measuring radioactivity to formations. This log measure the natural radioactivity using a scintillation sensor. Different lithology and mineral composition implies varying radioactivity content and gamma ray values. Potassium is the major radioactive element in rocks, commonly found in illitic clays and to some extent in feldspars, mica, and glauconite (Selley, 1998). In addition, uranium and thorium are contributors to high radioactivity levels. Shale consists of clays and small particles rich on minerals with high natural radioactivity. Thus, shale has high gamma ray values and the gamma ray log is a good shale indicator. It is the main log used to identify the lithology, and to differ between sands and shales, for example. Commonly, sandstones consists of coarser and "cleaner" grains, meaning lower levels of radioactive minerals. They contain a lot of nonradioactive quartz. However, sands could consist of radioactive rich minerals, and those contain higher gamma ray values. Gamma ray values may give indications of grain size distribution and trends. For example if the reservoir consists of clean sand or there is a coarsening upwards sequence.

3.2.2 Sonic log

The sonic log measure the P-wave velocity in the subsurface, and its primary objective is to evaluate the porosity in rocks. Interval transit times are recorded by using a sonde downhole. A transmitter sends signals through the formation to the receiver at the other end of the sonde. This is a measure of rocks' properties to transmit seismic waves. In general, increasing travel times indicate increasing porosity. Low fluid content and a high degree of compaction characterizes a layer of high sonic velocity. Gas in the formation decrease the acoustic velocity. This measure is important in combination with seismic evaluation determining interval velocities and relate seismic reflectors to actual sediments packages, according to the definition of acoustic impedance. It's valuable for converting seismic time to depth and to generate velocity models in seismic analyses.

3.2.3 Density log

The density log measure the concentration of electrons in the formation. Gamma rays are transmitted into the formation and detectors measure varying amounts of gamma rays returning. Density is one of the main controlling components determine the p-wave velocity to the formation, and is thereby strongly related to the sonic log. This log is important for seismic evaluation, as density is one of two factors the acoustic impedance depends on. The formations density vary due to lithology, fluid type and saturation, degree of compaction and other rock properties. Gas lowers the density of a rock while oil has little effect.

4 Results

4.1 Stratigraphical framework of overburden

The overburden consists of sediment for about 200 ms in seismic sections, and is accurate measured by well data (well 35/2-1) to 164 m close to the top of the structure. The water column at the well is 384 m, while the Peon sandstone was penetrated at 548 mbsl. The thickness of the Pleistocene succession above Peon reservoir varies between 160 to 190 m. Seismic data reveals a stratigraphy characterized by several prominent, continuous, sub-parallel horizons. They are separated by zones of weaker to absent seismic reflections. The next sections provides an interpretation of the horizons in a chronological order.

The study of overburden is of great importance and may provide information about depositional environment and regime, sealing mechanism and potential fluid migration. Stratigraphy deals with age, formation type and deposition of sediments and sedimentary rock in the geological record. By studying different layers and horizons in the overburden, it can be possible to correlate the layers to time periods. The stratigraphy will provide useful information about the depositional history for the Peon reservoir and sealing mechanism. In the following chapters, stratigraphic units are mapped out and described with respect to seismic characteristics. The changing seismic character in the layers occur due to lithological changes and fluid content. Individual packages with distinct, characteristic seismic facies, separated by strong, laterally continuous reflectors defines units in this master.

4.1.1 Interpreted horizons

In total, seven seismic markers are mapped out and interpreted above the reservoir; the seafloor, H0, H1, H2, H3, H4 and H5. Colored lines on inline 2570 in Figure 15 provides an overview of their position and seismic character. High continuity and strong amplitudes characterize the reflectors. The outer limits of the dataset delineate these key seismic markers. Hence, the interpreted horizons, as well as the units within, are laterally continuous for the p-cable 3D dataset of Peon. This means they are regional extending for about 30 km in the N-S direction and about 5 km wide in the W-E direction. The next sections consider the stratigraphy by describing and evaluating the horizon and unit characteristics. The seismic section in Figure 15 gives a stratigraphic overview of the Peon area. Interpreted surfaces visualize morphology and interesting features on the horizons.

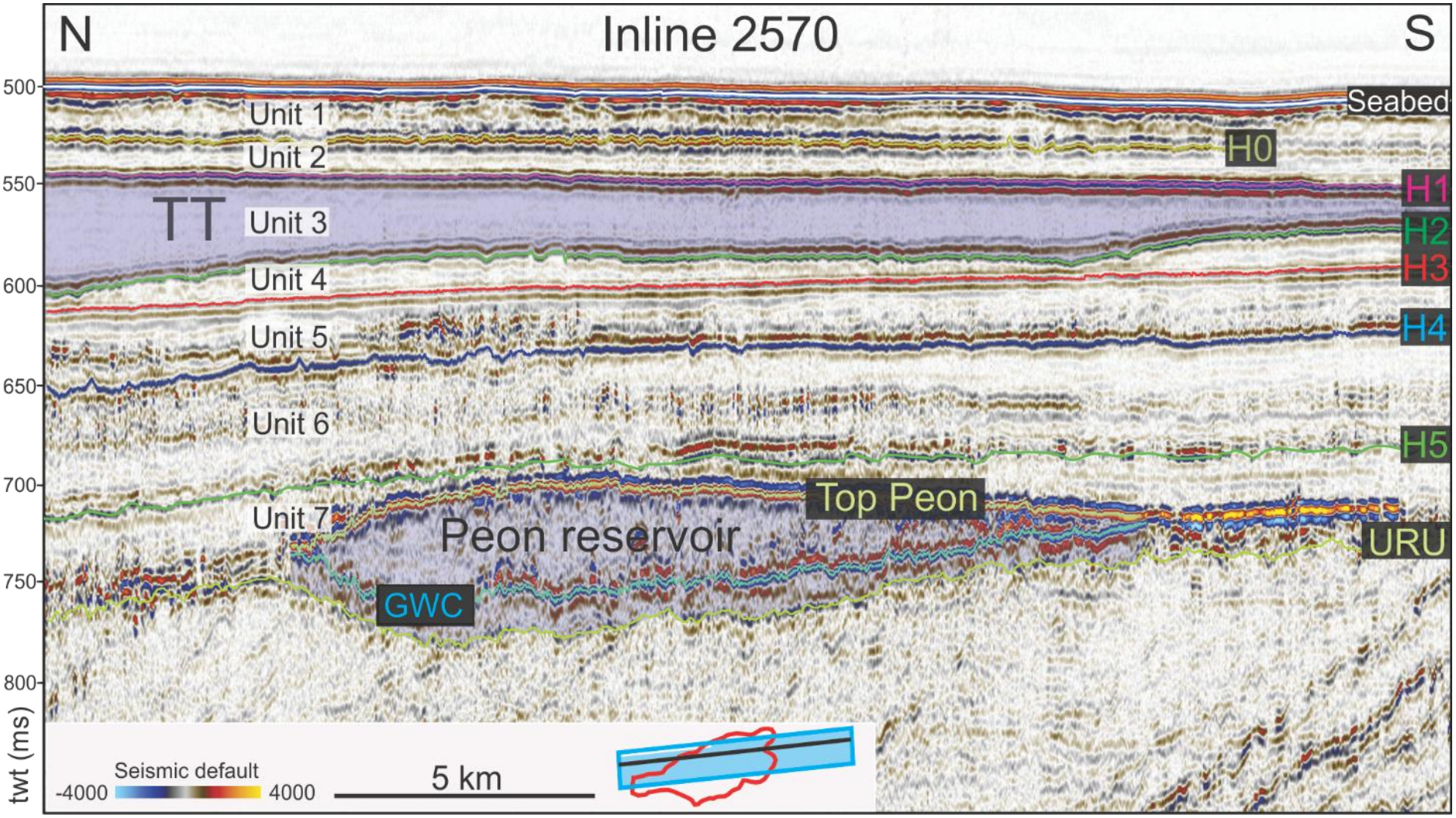

Figure 15: Stratigraphic overview map with interpreted horizons, units and reservoir indicated. TT is the interpreted till tongue unit. GWC is the gas-water contact while URU is the upper-regional unconformity. The seismic section is the inline 2570 from the p-cable dataset.

The stratigraphic column above (Figure 15) shows seven sedimentary units, which makes up the overburden of Peon. Unit 1 is the youngest while unit 7 is the oldest and deepest package. Most of the overburden reflectors are parallel to each other which suggest uniform sedimentation regime for an infill or sequence (Veeken & Moerkerken, 2013). The seismic signature in between some of the markers are characterized by reflection free and transparent areas, whereas some bedding planes are more irregular, discontinuous and wavy in particular areas.

Most of the high amplitude reflectors are normal sedimentary reflections representing boundaries for the packages on top of Peon. A few reflectors represent unconformities and time gaps in the geological record. Large differences in acoustic properties among the sedimentary layers give rise to these high reflection amplitudes. Since the packages are deposited in a chronological order, they represent time intervals in the geological record. The sedimentary reflections represent smaller periods of similar depositional conditions (Veeken, 2007).

Due to its high resolution, the p-cable dataset is the primary data to investigate and extract information of the overburden, correlated with well log data from 35/2-1.

4.1.2 Seabed

4.1.2.1 P-cable

Seafloor reflections are generally represented by peaks in the seismic data, indicating an increase in acoustic impedance from water to solid ground. In Figure 15, the seafloor reflector is interpreted on troughs (blue reflector), which infers that positive amplitudes are represented by troughs in this dataset.

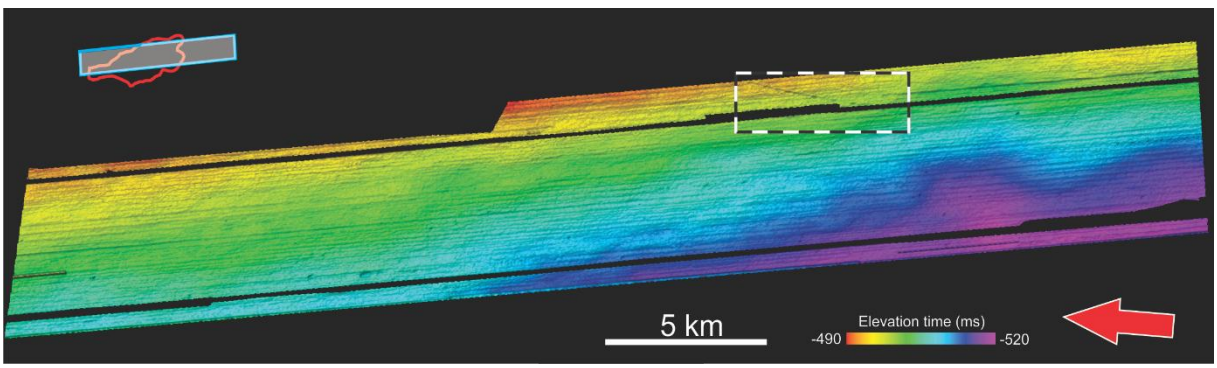

Figure 16: Time surface map of Seabed. Position of elongated feature indicated by black-white dotted square visualized in Figure 17.

The visualized seafloor from the P-cable dataset in Figure 16 reveals a smooth surface with few irregularities, except for two features. Parallel stripes are observed over the whole surface throughout the whole dataset. This is due to the data acquisition and is difficult to remove completely when processing the data. The seafloor contains a general and constant dip towards southwest.

The time surface map and variance map in Figure 17 display a single elongated NNE-SSW trending depression in the seabed. It stretches into the datasets from NNE and terminates towards SSW. The feature follows the small black arrows in the conventional dataset (Figure 18) and exceeds the data coverage. The depression is up to 200 m wide, up to 2 ms deep and more than 10 km long. A seismic section across several places shows a pattern of high amplitudes at the seabed and deeper in the formation in connection with the depression. The reflectors seem to be displaced a bit. The high amplitudes in the vertical sections indicate this to be an artefact. In addition, the orientation of the feature is uncommon and it crosscuts the general direction of the striations described on the conventional dataset. This is deeper and seems to cut through the other striations.

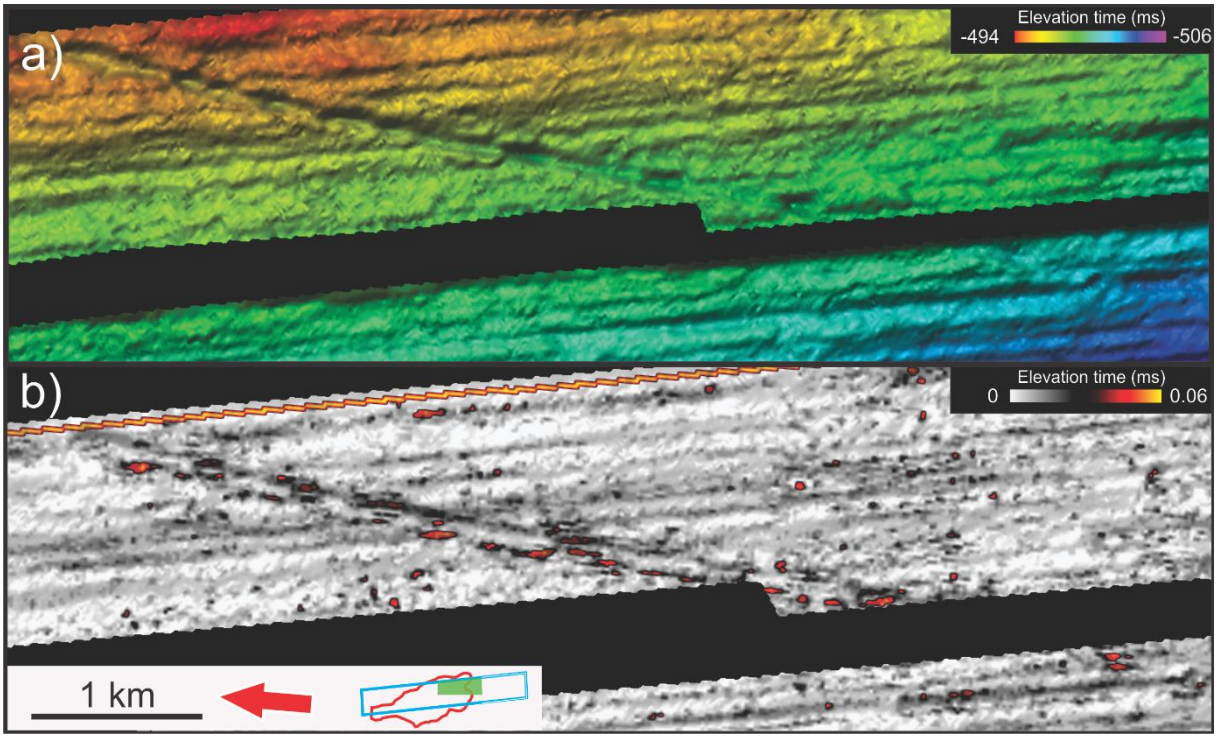

Figure 17: Elongated NNE-SSW oriented feature at seabed displayed by a) time surface map and b) variance map.

4.1.2.2 Conventional dataset

The time surface map in Figure 18 visualize the interpreted seabed from the conventional dataset. In the dipping direction NNE-SSW, there is a drop of 75 ms from the NE corner to SW corner. The horizontal distance is 20 km across. Assuming a p-wave velocity of 1450 m/s, the seafloor inclines 54 m, which is less than 0.25°. Eastern part of the dataset, also located east of the Peon outline, reveals many NNW-SSE trending, elongated, parallel striations. Blue arrows on the seabed appoint this feature. Some of them terminates within the dataset while other stretches across the surface, and hence is more than 10 km long. Similar features are extensively distributed in the Barents Sea and are interpreted as mega-scale glacial lineations (MSGLs) (Andreassen, 2007). These striations are present in the eastern part of the dataset, where the shallowest water depths occur.

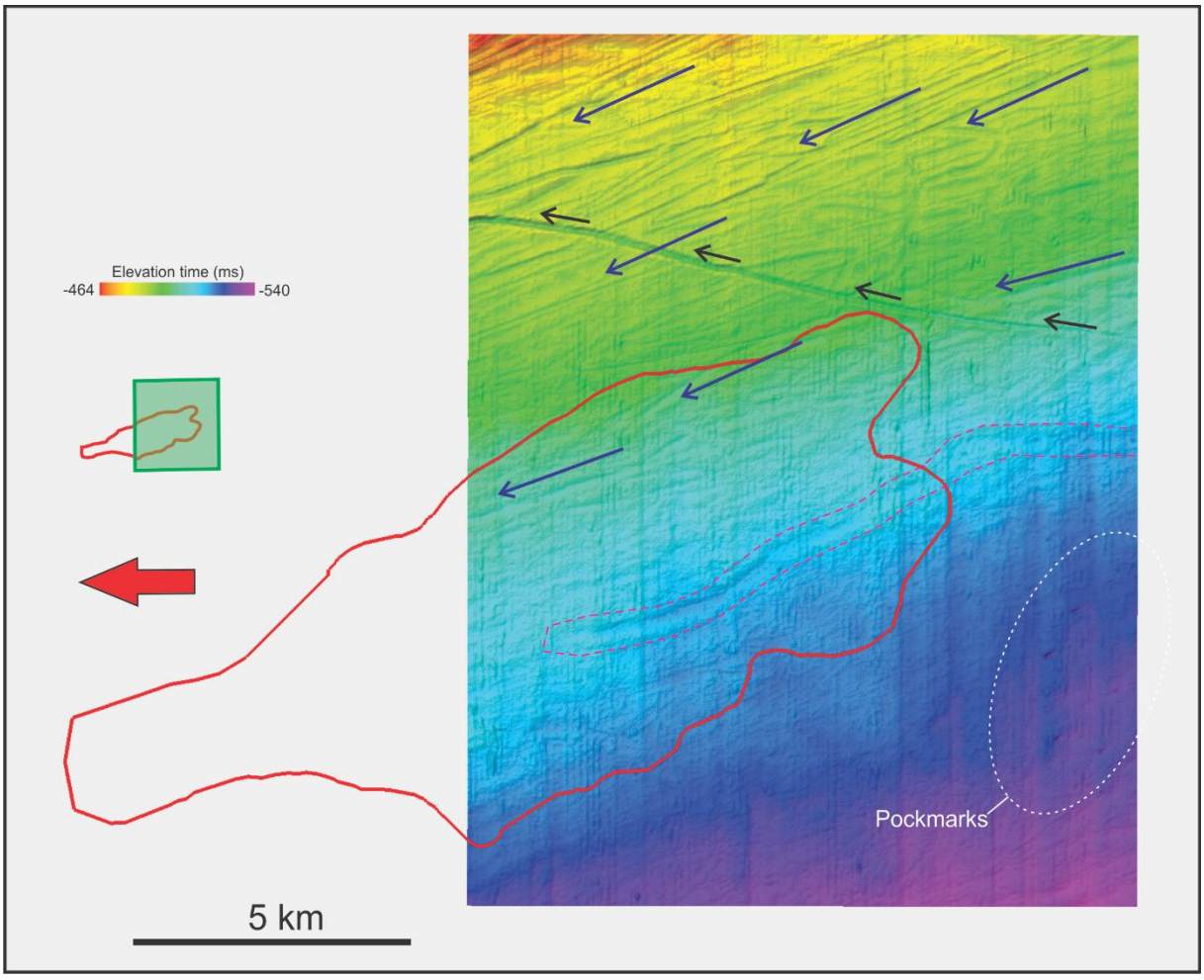

Figure 18: Visualization of seabed from conventional 3D dataset with indications of seabed features. Black arrows refer to feature visualized in Figure 17. Blue arrows indicate orientation of elongated, parallel striations, interpreted as mega-scale glacial lineations.

The white ellipsoid in the southwestern area of the seabed (Figure 18) indicate the position of big concentrations of circular, depressional features. The diameter vary from 50 up to 300 meter. In connection with the circular hollows, high amplitudes occur in the vertical zone below the features. These can be described as pipe structures. Thus, the features at the seabed relates to processes deeper in the formation and not to external influences on the surface. The hollows at the seabed reveals the same characteristics and connected fluid flow structures as (Judd & Hovland, 2007) describes as pockmarks.

4.1.2.3 Unit 1

Unit 1 is the uppermost layer of the subsurface and contains the youngest sediments. The seafloor reflector and the H0 reflector make up its upper and lower boundary. This layer comprises many seismic reflections, even though it is a thin layer. The time thickness map in Figure 19 visualize this gradually thinning from 30 ms in the northwestern part to 20 ms in southeast. This coincides with the pinch out of horizon H0 in south, which is mentioned in the next section. The upper unit contains seismic facies characterized by parallel, laminated reflections. The reflectors are thick, implying lower frequencies in this unit, while the degree of continuity is low to medium. The seabed reflectors and the nearest reflectors below are very continuous. Lower part of the unit contains more transparent and none-reflective facies.

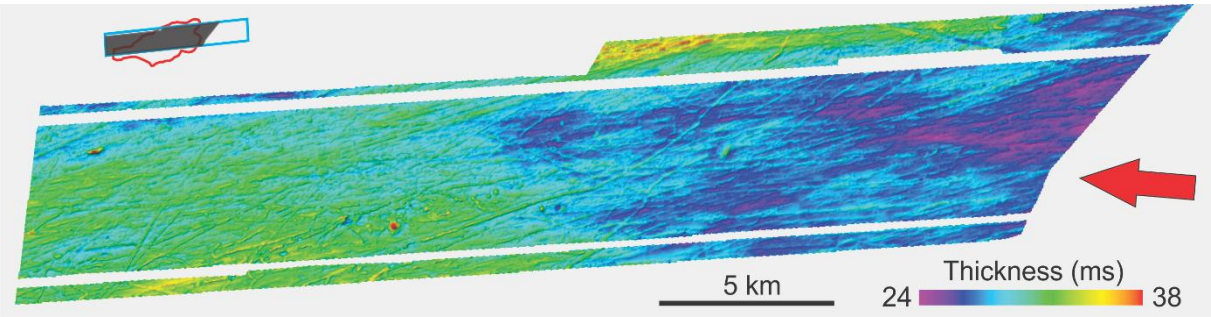

Figure 19: Thickness map of Unit 1

4.1.3 Horizon H0

Strong negative amplitudes characterizes the H0 reflector (Figure 15). Hence, it is phase-reversed compared to the seafloor reflector, indicating decreasing acoustic properties for the layer below H0. Towards the southern border of the dataset the surface is pinching out. The pinch out is making a southern border for the surface which is oriented NW-SE. Due to that the surface H0 is not represented over the whole dataset, unlike most of the other surfaces.

The interpreted surface of H0 is displayed in Figure 20 and reveals a lot of stripes, hollows and furrows. The variance map extracted from the surface, visualized in Figure 21, confirms these observations. Furrows, structures and stripes stands out with high variance values. The characteristics of the striations varies a lot, where some are parallel and elongated with a direction SSE-NNW. They stretches over the complete surface where the red lines in Figure 20 show the orientation of them. These striations are similar to those observed on the eastern part of the seabed and are interpreted as MSGLs. They represent erosional imprints by fast flowing ice streams, and we notice they holds the common orientation (SSE-NNW) of the NCIS.

In addition, a more curved, irregular and randomly oriented and shaped striation-like feature occur, indicated by blue arrows on the time surface map (Figure 20). However, these curvilinear furrows with changing directions do also have a generally orientation, stretching SE-NW. The depth vary between 2 and 5 ms. Some of the stripes make up interesting and nicely developed patterns. In the middle of the map there is a N-S trending stripe turning left and right every other time (Figure 21). The length vary between a few hundred meters to more than 15 km. They are typical features formed by icebergs and got the same characteristics as Ottesen et al (2012) interpreted as iceberg plough marks. They may have formed by icebergs dragged by wind and currents, making up these more random characteristics. Observed in Figure 20 that this randomly oriented striations crosscuts the straight, elongated striations. Thus, the iceberg plough marks are interpreted a younger erosional feature.

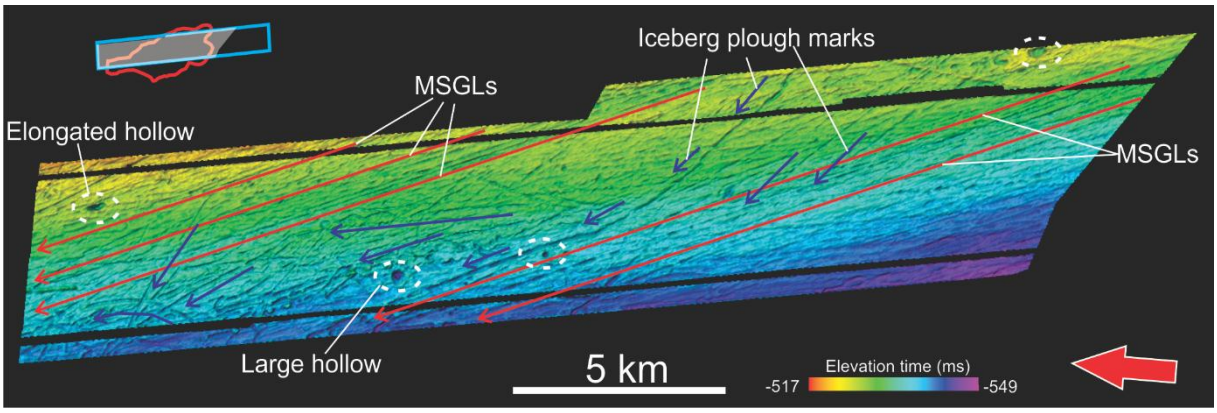

Figure 20: Time surface map of horizon H0 with interpreted morphological features indicated. White dotted circles indicate hollows.

A few hollows is visible on the surface in the western part, as well as one southeast (Figure 20). These are marked out by white dotted circles. Their shape is conical. Especially one of them is prominent and large with diameter about 360 meter and depth up to 10 ms. The smaller hollows

are about 150-200 meter in diameter and up to 5 ms in depth. The seismic signal underneath these hollows is disturbed and reveal small signs of pipe structures. This may be indications of fluid migration and paleo-pockmarks. In the northeastern corner an elongated hollow occur, and it reveals the same direction as the above-mentioned stripes and furrows (NNW-SSE) (Figure 20). It is 370 meter long, 130 meter wide and up to 10 ms deep. This may be due to eroding iceberg scaring into the surface.

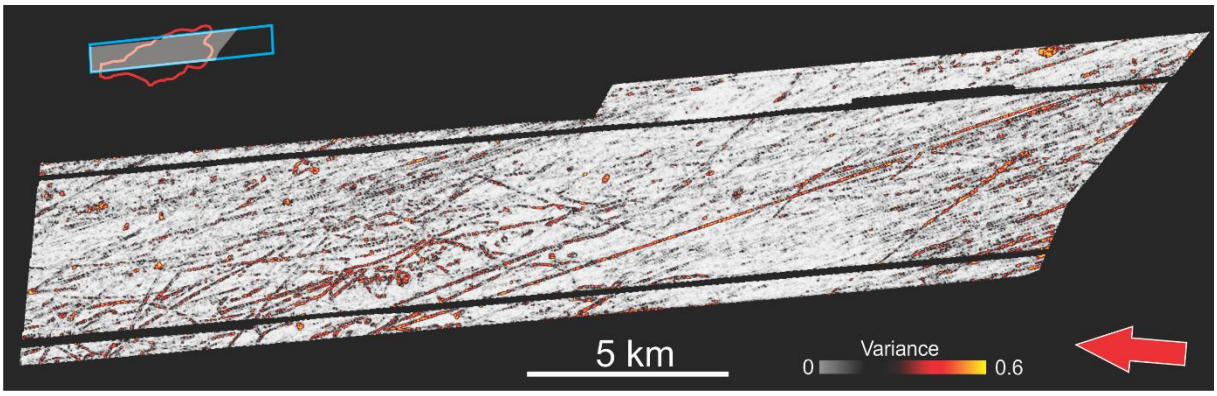

Figure 21: Variance map extracted from horizon H0. Elongated and curved features, as well as hollows, reveals strong amplitude values.

4.1.3.1 Unit 2

Seismic reflectors with low amplitudes, high continuity and relatively flat-lying parallel configuration characterizes the layer between H0 and H1, unit 2. It seems to be a conform package with low degree of internal variation. The thickness of unit 2 is constant close to 20 ms (Figure 22). Especially in the NNW-SSE direction, the thickness map reveals constant values of the unit. The imprints from MSGLs on surface H0 are prominent on the time surface map. This is due to the homogeneous layer and constant thickness, and therefore this feature could be prominent. In addition, the above-mentioned hollows stand out on the thickness map in Figure 22.

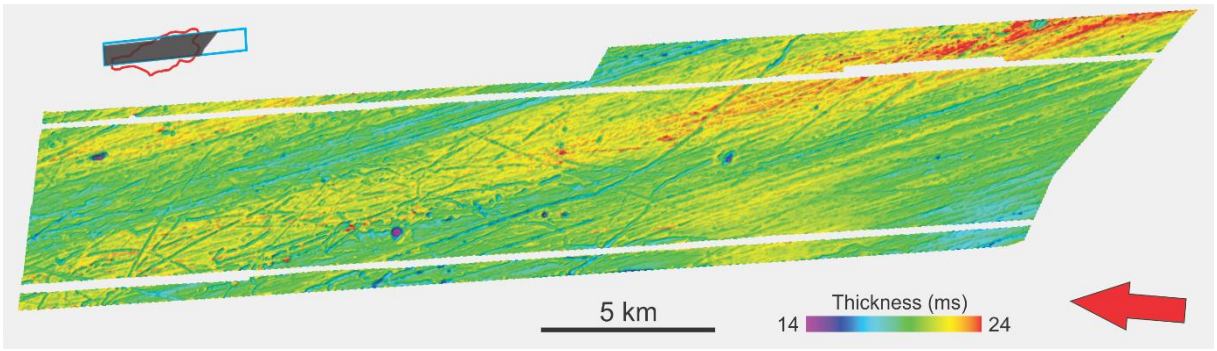

Figure 22: Thickness map of unit 2

4.1.4 Horizon H1

A prominent reflector in the seismic appear strong and continuous for the whole surface. This nicely developed reflector, displayed by pink line in Figure 15, makes up the H1 horizon. The reflector is more or less parallel to the seafloor. Time surface map displayed in Figure 23 infers an inclination towards SW. H1 is located between 40 and 45 ms below the seafloor and has the same polarity as the seafloor, indicating an increase in acoustic impedance when going from the overlying to the underlying layer.

The surface of the horizon reveals a more flatten and smoothen signature than H0, and is displayed by the time surface map in Figure 23. Low variance values, as we see in Figure 24, manifest these observations. However, several features are present on the surface. There are some small "dots" or hollows of high variance values (Figure 24) and is marked out by white dotted lines in the time surface map (Figure 23). Several curvilinear striations in the southern part is present, stretching in a NNW-SSE direction. Three of them are large and stretches trough the dataset, indicated by blue arrows in Figure 23. One of them crosscuts the other two. These are interpreted to be iceberg plough marks. In the NNW-SSE direction there occur elongated, parallel striations throughout the complete dataset. Those striations are indicated by red lines on the time surface map (Figure 23) and are similar to them as interpreted as MGSLs. In addition, parallel striations in the inline direction occur. These are artefacts and related to acquisition noise. The NNE-SSW stretching artefact is the same as we observed on the seabed.

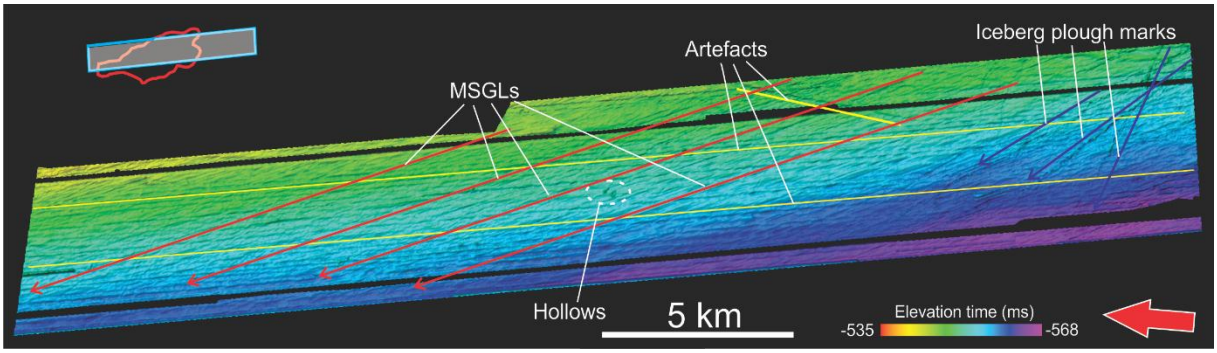

Figure 23: Time surface map of horizon H1 with interpretation of morphological features and artefacts.

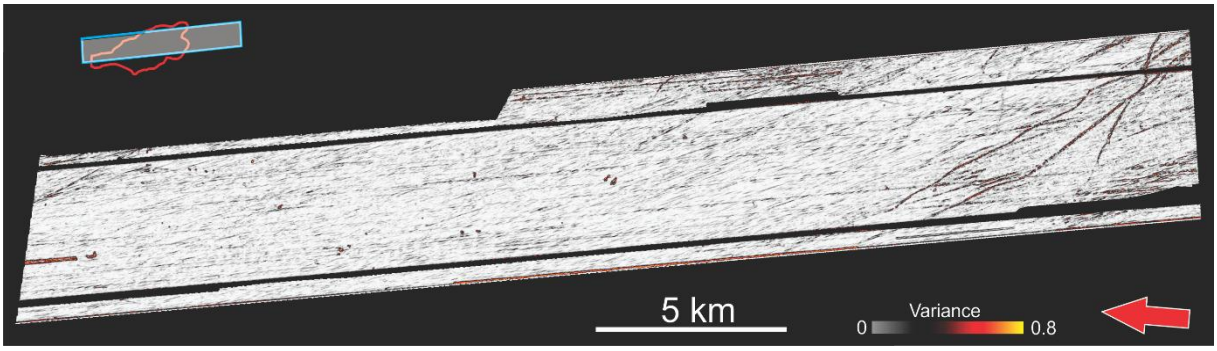

Figure 24: Variance map extracted from horizon H1

4.1.4.1 Unit 3

A characteristic layer occurs beneath the H1 reflector. Among all units, this layer got the highest variation in thickness, observed from the thickness map in Figure 25. Time thicknesses of 70 ms in NE decrease linearly towards south, where it pinches out. As observed from the seismic data (Figure 15), this layer appears as an acoustically transparent zone, comprising very low amplitudes. Such a transparent and non-reflective layer represents a homogenous package with little internal changes in acoustic properties. The reflection free zones indicate a layer where the acoustic impedance contrast is close to zero, implying a homogenous lithology. This could be sands, shales or a mix of them like a diamicton. Layers containing similar seismic characteristics has been interpreted as till tongues (Ottesen, et al., 2012).

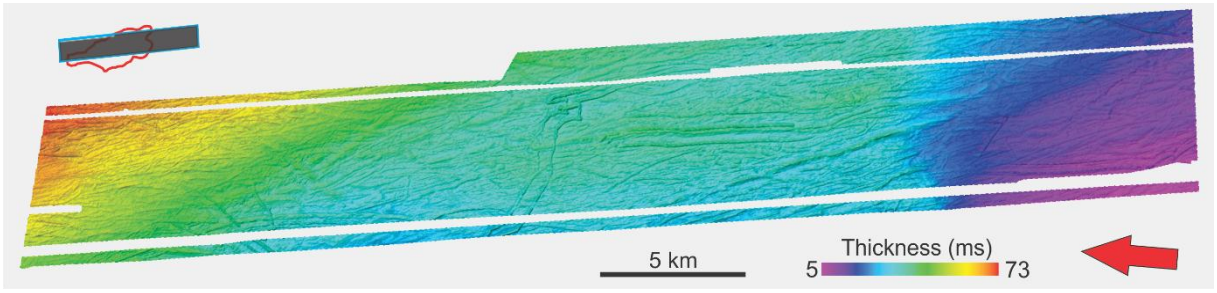

Figure 25: Thickness map of Unit 3

4.1.5 Horizon H2

H2 reflector is a strong and continuous reflector. There occurs a major change in the dipping nature of the horizons in the overburden at the H2 reflector. Opposite to the horizons above, H2 is dipping towards north. As the time surface map displays (Figure 26), the deepest parts in north is at 620 ms while the southern region is located at 570 ms. Meaning the surface is inclining by about 30-40 meter over a distance of 30 km. The northern and southern areas are most inclined, as we see on the seismic section (Figure 15) and time surface map (Figure 26). However, the areas of H2 in the middle of the dataset are quite parallel to the seafloor.

The H2 surface covered by the p-cable dataset is highly irregular and characterized by depression-like striations and furrows, even more than observed at H0. This is clearly visible in the time surface map (Figure 26) and variance map (Figure 27) of H2. Unlike striations described above, some of these are large, curvilinear features. They are up to 10 m deep, 300 m wide and more than 10 km long. Pink arrows indicate the position, size and direction of these depressions (Figure 26). This feature has a trending orientation SE-NW. They are interpreted as large iceberg plough marks. Smaller striations do also occur on this surface, similar to those interpreted as iceberg plough marks on other surfaces. Some of the striations occur parallel to each other, at least three places on the surface, and marked out by blue arrows in Figure 26. In the middle of the map, E-W trending parallel striations occur. This feature is also present on the western flank, both in south and north, oriented N-S. They all reveal characteristics of plough marks. Icebergs has reworked and extensively eroded this surface. These features forms by ice drifting in shallow water masses. Currents and wind drag the ice in the seabed and form randomly oriented striations.

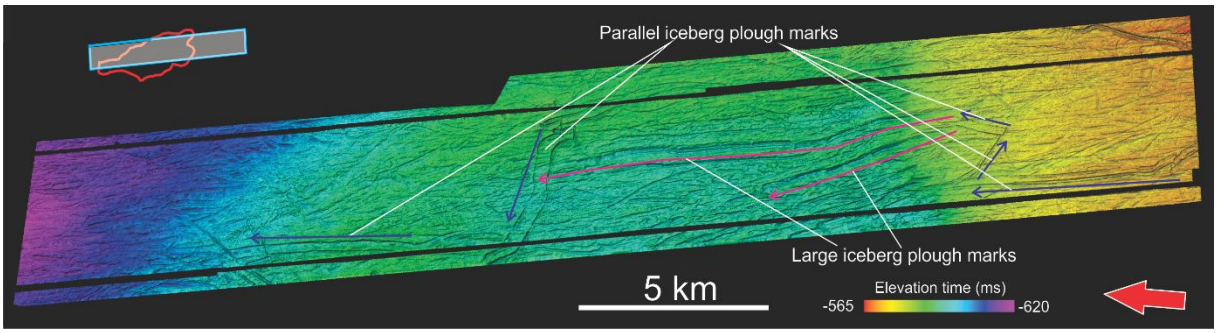

Figure 26: Time surface map of horizon H2 with interpretation of morphological features.

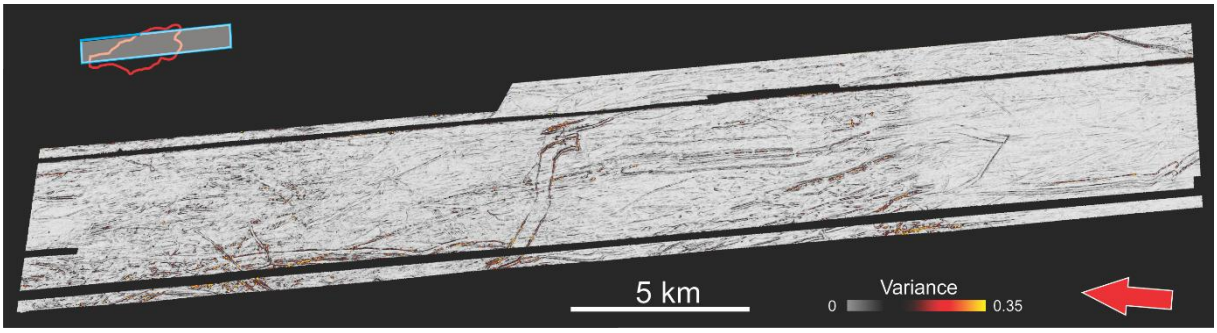

Figure 27: Variance map extracted from horizon H2

4.1.5.1 Unit 4

A thin package of sediments is located in between H2 and H3. The package is thinning towards north, and in the N-S seismic section in Figure 15 there are two mounded like packages observed in the middle and in south. This is due to the shape of the H2. Transparent seismic signature, similar to unit 2 and 3, characterize the reflections within unit 4.

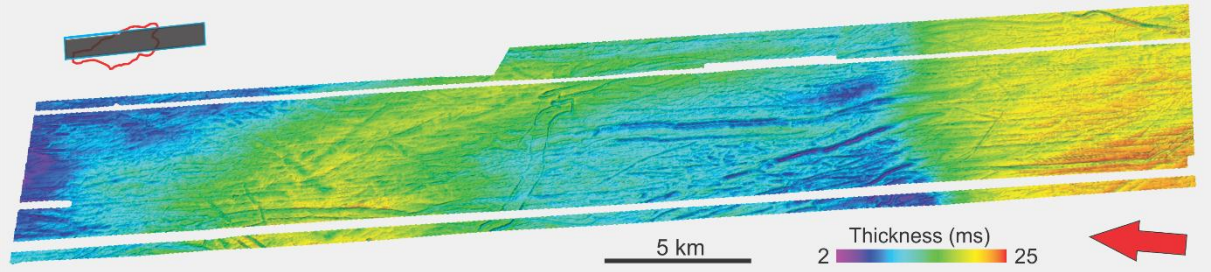

Figure 28: Thickness map of Unit 4

4.1.6 Horizon H3

The time surface map of Horizon H3 (Figure 29) display a smooth surface with a gentle and constant dip towards north. The horizon is dipping from 590 ms to 623 ms, a height difference of about 25 meters. Except from acquisition noise in the inline direction, only a few stripes and elongated features occur on this sedimentary boundary. The striations are concentrated in the center of the dataset, indicated by black ellipsoid in the variance map (Figure 30). They seem to follow the inline direction, but have a gentle deviation towards west when going south-north (direction indicated by blue arrows on variance map). The variance map of the horizon visualize them better than the surface map. The features are depression-like stripes, as also observed and described as iceberg plough marks. Except for those, the variance map reveals a smoothen character.

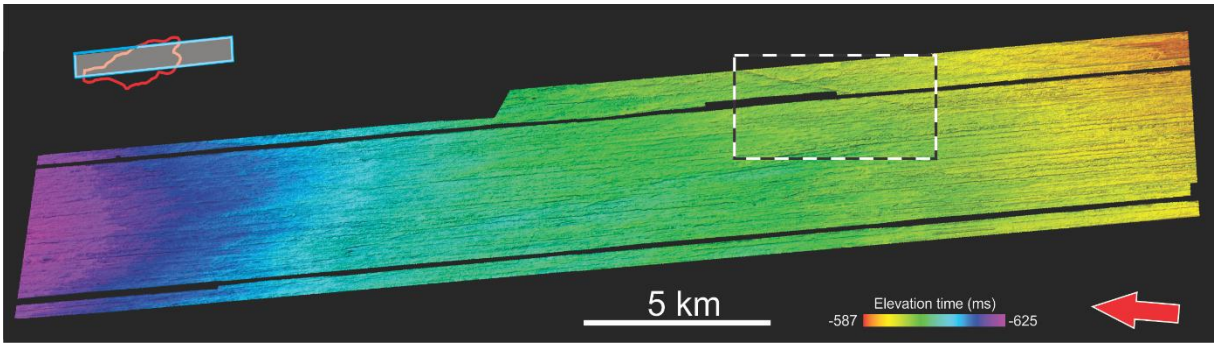

Figure 29: Time surface map of horizon H3

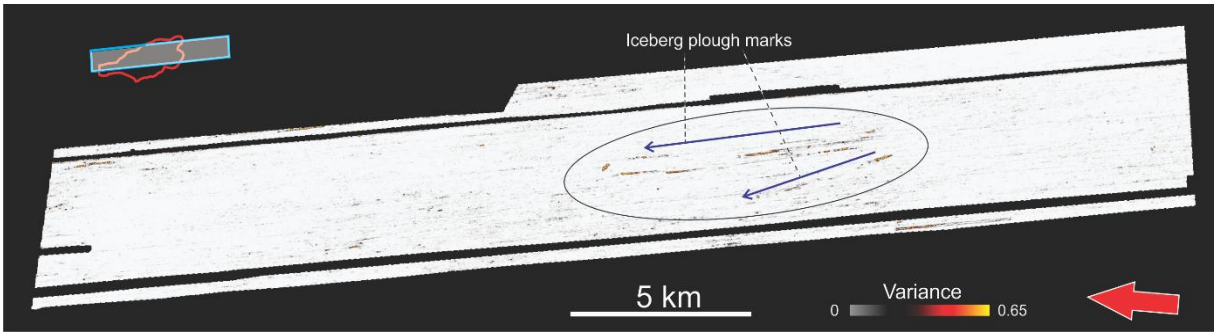

Figure 30: Variance map extracted from horizon H3. Feature of interest within black ellipsoid.

One of the stripes stand out with regard to shape and direction. As shown within the black-white dotted square on the surface map of H3 (Figure 29), a straight feature about 5 km occur in the southeast with orientation SSE-NNW. It contains both a depression and a high. This feature is crosscutting the acquisition noise in the inline direction. This feature is also described and observed on the seabed, and has the same orientation and extent. The same feature occur on all the other horizons as well. This features is most likely not a geological feature, but may be due to acquisition or processing.

4.1.6.1 Unit 5

Unit 5 reveals a quite constant thickness, but there is a general trend of thickening towards NW. There is an area in northwest that differ from the other areas, which can be seen on the thickness map (Figure 31). The general thickness of the surface is about 30-35 ms, while this area is more than 40 ms thick. This is probably due to the high-amplitude anomalies observed, and the real thickness of the unit in the mentioned area is most likely similar to other areas. These anomalies are considered in section 4.3.1.1.1. A bit stronger reflectors seems to be present, related to the three units above. The seismic reflectors are more conform and parallel in the upper unit and chaotic, irregular and discontinuous closer to the base (H4).

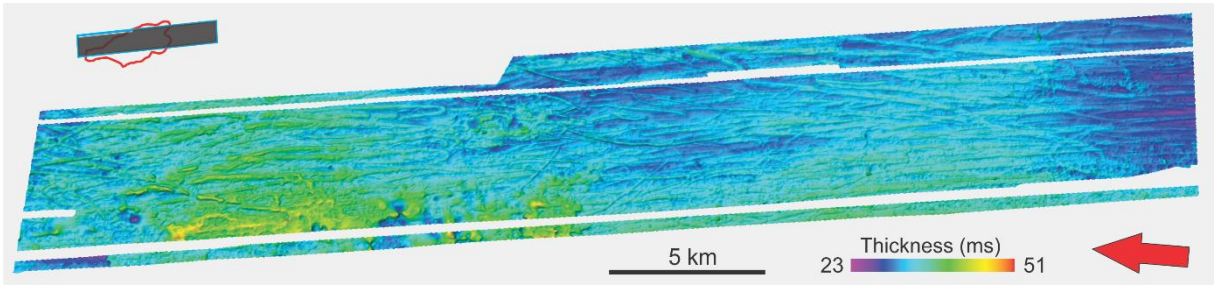

Figure 31: Thickness map of Unit 5.

4.1.7 Horizon H4

H4 is strong reflector with same polarity as the seafloor, indicating an increase in acoustic properties for the layer below. Most of the southern parts of the dataset contains undisturbed data, and the reflector appears strong and continuous. The confidence for the interpretation is good, opposite to the northern areas. Due to high amplitude anomalies, the chaotic and disturbed seismic signature makes it difficult to interpret the H4 horizon in the middle and western areas. Those areas reveals very high variance values as we observe from the variance maps (Figure 33 and Figure 35b). In the western part, there are very high variance values, indicating a big trace-to-trace variability and hence low degree of internal organization. The seismic signals seems to be disturbed. This area coincides with the HAA described in section 4.3.1.1.1.

The surface is, as the other surfaces below H1, inclined from south to north. Unlike H1, H2 and H3, this surface is also a bit tilted towards west. The height difference is about 45 ms; the surface inclines from 615 ms in southeast to 660 ms in northwest.

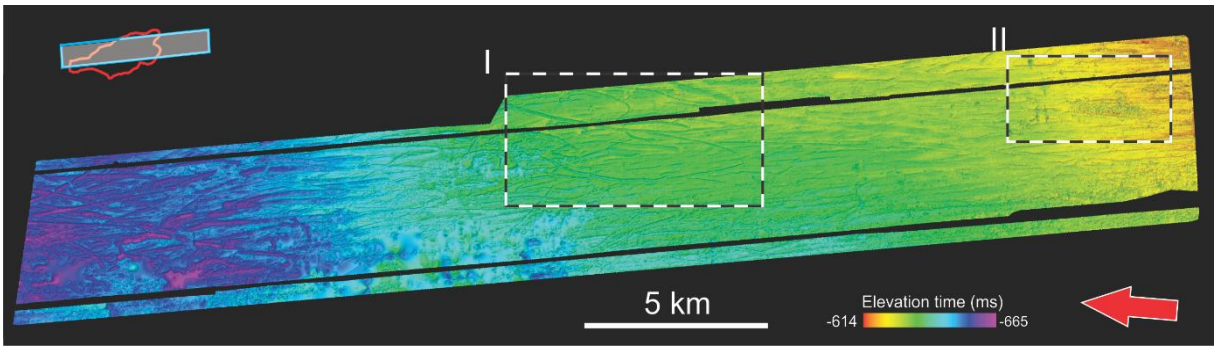

Figure 32: Time surface map of horizon H4. Area I and II indicated by black and white dotted squares.

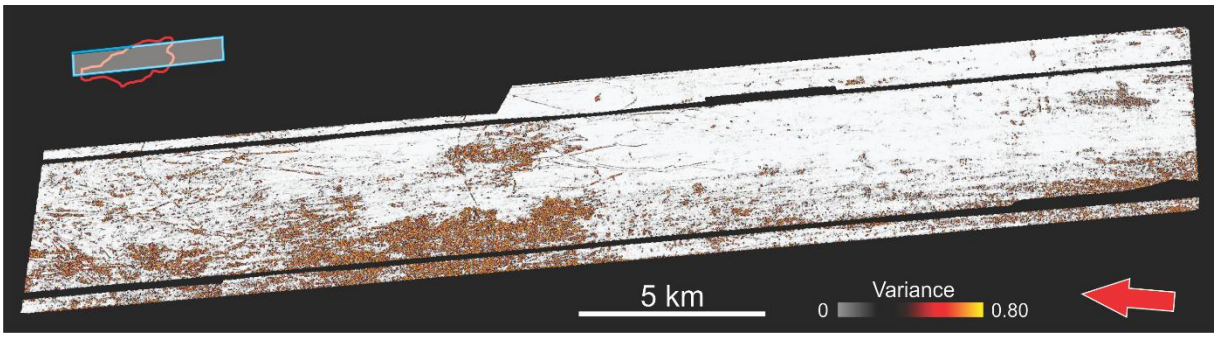

Figure 33: Variance map extracted from H4.

The topography of the surface is characterized by two sets of curvilinear and depression-like features (Figure 32). North-south trending elongated depressions is characterizing this highly influenced surface. They are long, wide and continuous, stretching over large parts of the

surface. They are up to 10 km long and several hundred meters wide. Some of the elongated depressions deviate from the general pattern and crosscut the scours with NW-SE and NE-SW directions. Especially in the north, several stripes have a NE-SW orientation. This feature is similar to the one described and interpreted as MSGLs on surface H0.

In area I marked out on the time surface map of H3 (Figure 32), there are observed prominent striations. The striations is more curved and randomly oriented than the MSGLs. As shown in the time surface map and variance of the zoomed in area I (Figure 34 and Figure 35), this feature has no general pattern or organization. The variance map gives a clear picture of the depressions shape and extent. The feature vary in shape, extent, orientation and concentration all over the surface. However, there is general trend that the most curved and randomly shaped depression occur in the middle of the dataset. In the northern and southern areas the stripes are more elongated, but still randomly oriented. They are smaller in length and consistently narrower than the feature described above. This is most likely plough marks created when icebergs were dragged around in the sediments by currents and wind.

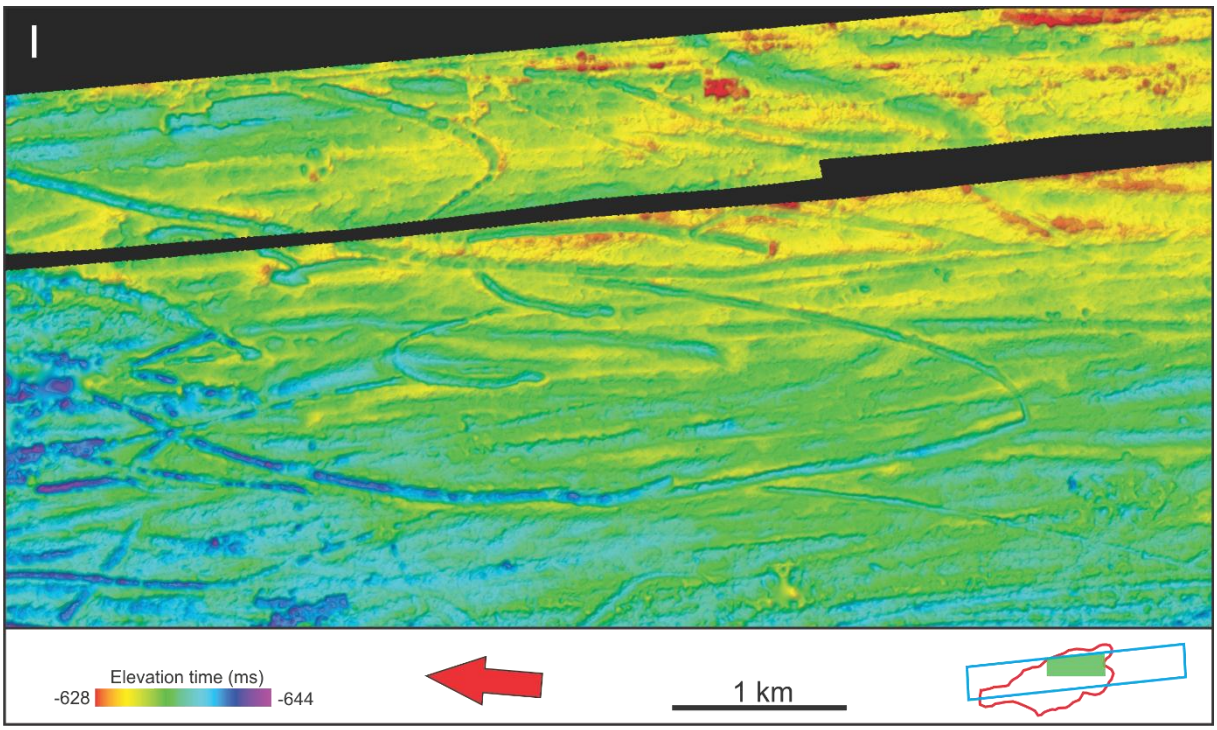

Figure 34: Time surface map of zoomed in area I at H4. Indicating orientation, shape and extent of iceberg plough marks.

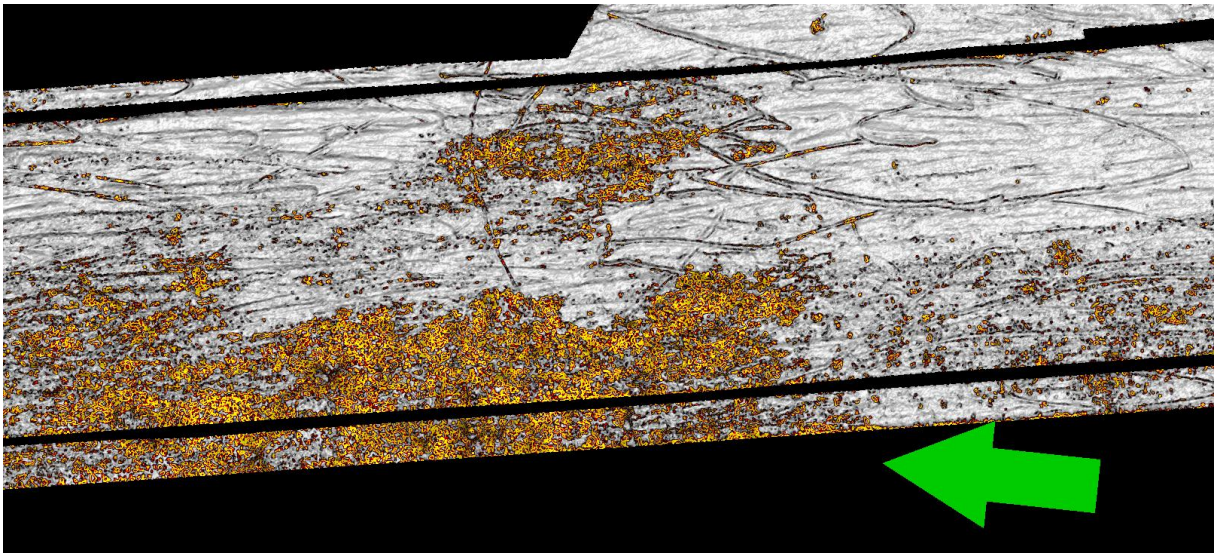

Figure 35: H4 variance map of zoomed in area I.

In the southeastern corner of the p-cable dataset, there are several interesting features observed, among them the two depressional features described above (Figure 32). We observe a highly disturbed and interrupted area. This is a rectangular shaped area with a north-south extent over 2 km and about 500 meter across. It seems to be a zone with several small hollows and there is very high internal variability, as noticed from the variance map (Figure 36). The large depression-like features is surrounding the concentrated hollows. The elongated features do not cut through this area, indicating the process or mechanism forming this most likely occurred after the process forming the striations. There are some bigger, single conical shaped depressions located directly north of the other. Some of them are more elliptical in shape. The same time perspective is valid for these hollows as for the concentrated ones.

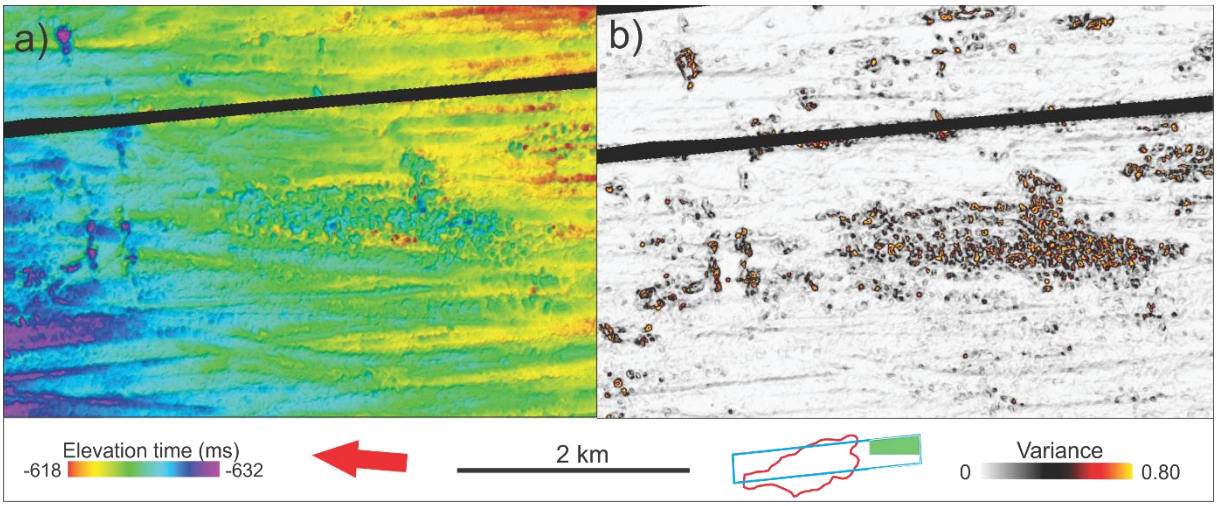

Figure 36: a) Time surface map and b) variance map of horizon H4 illustrating feature in south. Interesting feature in the middle of the map. The time-surface map reveals a lower relief (depression) at the feature.

4.1.7.1 Unit 6

The package between H4 and H5, unit 6, contains a constant thickness of about 35-40 ms. In a N-S seismic profile there are different facies within this unit. There are wedge shaped packages with very low amplitudes, both at the top and the bottom of this unit. This is visible in the stratigraphic column (Figure 15). The uppermost package is pinching out towards north while the lower wedge-shaped body is thinning southwards. Thereby the total thickness for unit 6 remains constant. The reflectors geometry is wavy and mounded, while the continuity of the reflectors is low, especially in the lowermost package. The signals is highly disordered. This signature got many of the same characteristics as unit 3.

In between these two wedge-shaped facies, a package containing higher amplitudes occur. The reflectors are discontinuous and are vertically displaced, making up a quite chaotic seismic signature. This facies reveals a constant thickness, except in north where it gradually increases.

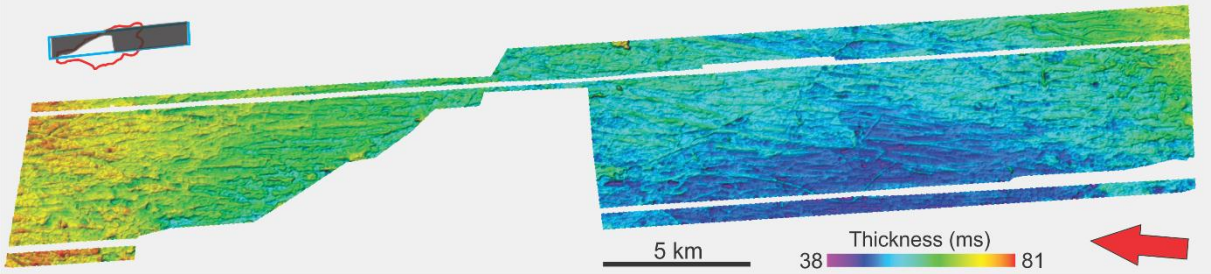

Figure 37: Thickness map of unit 6.

4.1.8 Horizon H5

The H5 reflector is located right above the Peon reservoir, and areas in the middle and western part of the p-cable dataset is even cut by the top reservoir. Due to that, the surface H5 and the package between H5 and top Peon is absent in the central region (Figure 38). Horizon H5 reveals the least continuous reflector of the interpreted horizons in the overburden and is interpreted with lowest degree of confidence. Especially the southern part of the reflector is discontinuous. The reflector is quite continuous in north. All over, it has a medium high amplitude.

The surface inclines from 670 ms in south to 730 ms in north. By comparison, the shallowest part of the reservoir is located at ca 700 ms. The topography of surface H5 is quite irregular and there are many depression-like features visible on the surface. Both the large and small depression-like features described on H4, occur on H5 as well. In Figure 38, red and blue

arrows, respectively, indicate their extent and orientation. The general orientation of the large, elongated striations is S-N, the same as the inclination of the surface. Figure 39 reveals large variance values located at the feature. The smaller depression-like feature, interpreted as iceberg plough marks and indicated blue arrows on the time-surface map, seems to be more elongated on this surface than are not that curved as observed on H4, and there is two trending directions for these narrow striations; NNE-SSW and NNW-SSE. Probably two generations of striations occur, where they crosscut each other.

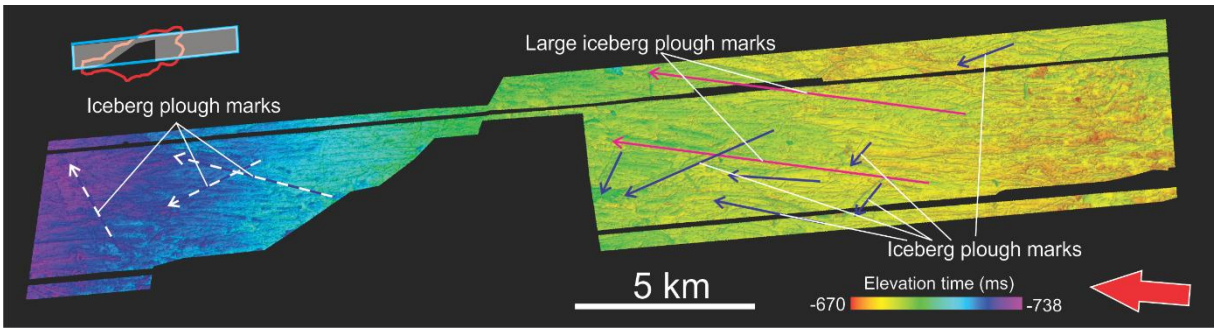

Figure 38: Time surface map horizon H5, including interpretation of morphological features.

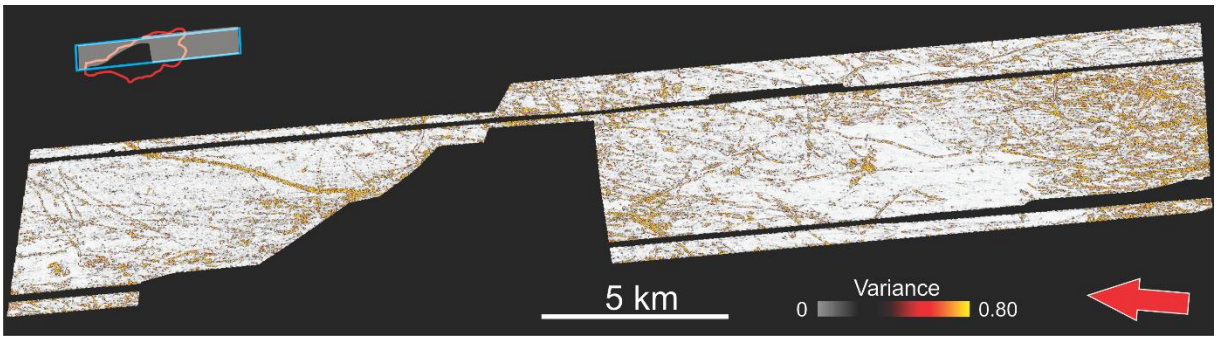

Figure 39: Variance map extracted from H5. Elongated features described above reveals high variance values.

4.1.8.1 Unit 7

Unit 7 is the sediment package between H5 and Top Reservoir in the reservoir zone and between H5 and URU in north and south. Top Reservoir and URU merge in the outer limits of the reservoir. This package gets thicker towards north (40 ms) and south (30 ms), while the reservoir even cuts through H5 in the middle, as mentioned. This is clearly indicated in the thickness map (Figure 40), with very low values close to the Top Reservoir and up to 52 ms in south.

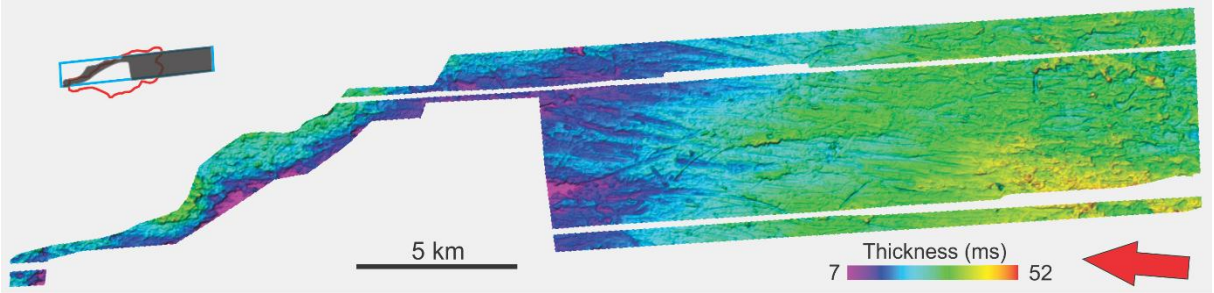

Figure 40: Thickness map of Unit 7

The seismic reflection configuration is characterized by parallel bedding interrupted by areas of dipping and chaotic reflections as well. On the flanks of the reservoir, reflectors in unit 7 is onlapping the mounded shaped Top Reservoir reflector. The onlapping reflections are sub-parallel to H5.

4.1.9 Upper Regional Unconformity

Considering the stratigraphy, there is a major change in layering architecture and dip of layers just below Peon reservoir, interpreted as the upper regional unconformity. The URU is by well data logged to be at 593 mbsl, distinguishing younger Pleistocene from Pliocene sediments (Carstens, 2005). As indicated in Figure 42, the URU is interpreted on a weak reflector, representing the base of the reservoir and also the unconformity (section 2.5). The weak reflector appointed in Figure 42 represents this boundary in the stratigraphic column, and it is, in contrast to the strong reflector, extending outside the lateral limits of the Peon reservoir. Dipping layers characterize the column below the reflector, while the layers on top are subparallel to the seafloor. This abrupt change in seismic character indicates a time gap and probably changing sedimentary environment. There seems to be a regional change in lithology, and that reflector is therefore interpreted to be the URU (Figure 42).

Biostratigraphic investigations from well 35/2-1 indicate the age of the URU to be 1.8 M.a. A report from foraminiferal analysis state that "*the occurrence of N. pachyderma (dextral) indicate a Late Pliocene age as young as approximately 1.8 Ma at 621 m (RKB)*" . The URU is at 621 m below rotary kelly bushing, meaning at 595 mbsl (SSTVD).

Regionally, and especially below the Peon field, the URU reflector is quite weak and difficult to interpret. The strong reflectors above absorbs a lot of acoustic energy and the seismic signal is hence weaker, in particular below the reservoir. However, the main reason for the low

amplitudes is most likely the small changes in acoustic properties between the sedimentary layers. This is reasonable when both is interpreted to consist of water-filled sediments.

4.1.10 Well data

Gamma ray measurements is the only well log applied considering the stratigraphic column above the Peon reservoir. However, this well log is common used as a lithology indicator. There is a general trend of increasing gamma ray values with increasing depth. Unit 1 and Unit 5, the layer in between H3 and H4, differs from the other with very variable values. Also a spike in lower part of unit 3 occur. Except for that, the gamma values increase almost proportionally with depth as observed from the well log display (Figure 41). A zoomed-in section included for Unit 5.

Unit 1 contains the uppermost sediments from the Seabed at 384mbsl to H0 at 403mbsl. The gamma ray acquired for the lower part of the unit. The values fluctuates and there is a spike down to 25 gAPI. At the H0, there is an increase in gamma values from 57 above to 67 right below. As already mentioned, the H0 reflector is negative and represent decreasing acoustic properties. Unit 2 is measured from H0 (403mbsl) to H1 (419mbsl) and shows gamma values between 54 and 70 gAPI. Higher values when entering the unit (Figure 41).

Unit 3 is the 29 m thick deposit from H1 (419mbsl) to H2 (448mbsl) and contains gamma values between 60 and 75 gAPI. The seismic p-cable signature in unit 3 reveals an acoustic transparent zone (right column in Figure 41), there is a spike in the log and it represent the second lowest gamma value for the stratigraphy, 33.2 gAPI. This is a 2 meter thick zone at 441 to 443 mbls. The low value could indicate that a clean sand is present. A high-energy sedimentation regime could have deposited coarser sediments. This could be a channel deposit or another event. However, the spikes in gamma logs are not necessary due to lithological changes. Reading error and other errors regarding acquisition may lead to such deviations. Even if a sand actually occur in the well, it can be a local accumulation. In “worst” case, a narrow channel with little lateral extent that can cause such measurements. With only the gamma ray log available, it is difficult to make a distinct interpretation on the spike. There could be presence of a cleaner sand.

Unit 4 is distinguished with seismic reflector H2 at 448mbsl and H3 at 458mbsl in well 35/2-1. Seems to be more clay-rich sediments, gamma values 72-78 in upper part and about 85 gAPI

in the lower part. There is a spike (69 gAPI) at the H3 reflector, as we see in from the well log in Figure 41.

Unit 5 extends from H3 (458 mbsl) to H4 (492 mbsl) at the well location. When penetrating H3 there is an abrupt increase in gamma values, exceeding 100 gAPI, as the zoomed-in view of the well log shows (Figure 41). This testify that a package of fine-grained sediments is present. The combination of low and high gamma readings characterize this unit. There seems to be three clay-rich layers interrupted by three more sandy depositional events, as the zoomed-in view in Figure 41 shows. This alternation is characteristic and unique for this unit. All three clay-rich layers are more or less 8 m thick and occur at 459-467 mbsl, 469-477 mbsl and 483-491 mbsl. This infers that there is thinner sand deposits in between, 2, 6 and 2 m thick, respectively. The upper and lower deposit is similar in thickness (2 m) and gamma (55 gAPI). Again, the low gamma readings may be to errors and it is hard to interpret them only based on this single well log. Even it is a sand the lateral extent is unknown. However, the frequent occurrence of them in this package gives indications for minor channel fills or other high-energy sedimentation regime. Glaciofluvial channels in front of a glacier that retreated or advanced is a likely deposition sedimentation regime. H4 is strongly affected by glacial events and reveals countless numbers of iceberg plough marks.

Well log readings from Unit 6 (492 mbsl - 534 mbsl) and Unit 7 (534 mbsl - 548 mbsl) reveals constant gamma values between 80 and 100 gAPI, indicating relatively high degree of fine-grained sediments. Both the lower unit 6 and 7 got a spike in record that got gamma values about 60 gAPI. The gamma log in Figure 41 display these relative constant gamma values from the H4 horizon and down to the Top Peon. Some variability occur and the spikes located at the base of the units.

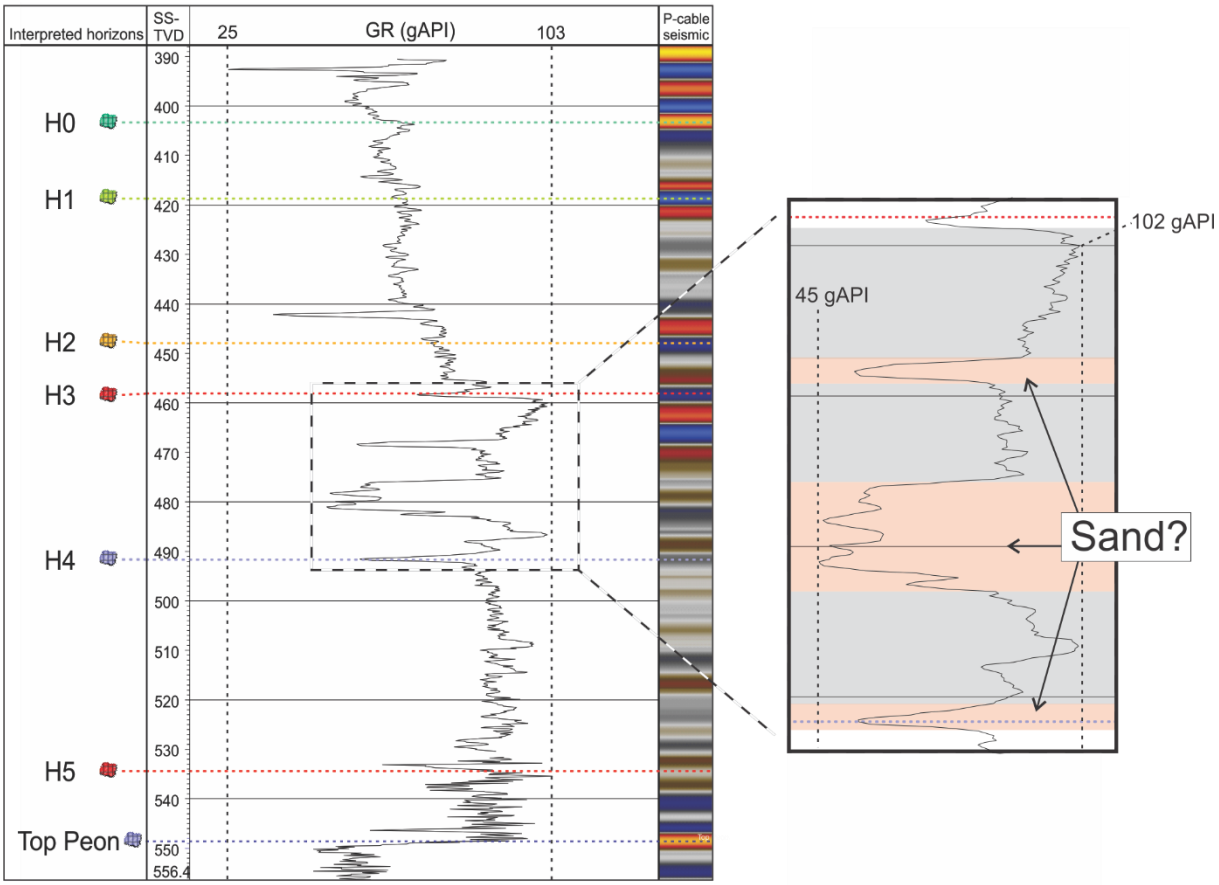

Figure 41: Gamma ray log of overburden from well 35/2-1. Possible interpretation of Unit 5 on right hand side. Depth is given in subsea true vertical depth (SSTVD). Values and type of log is indicated in the top row. Vertical, black dotted lines indicate minimum and maximum values measured in this section. Minimum value is measured in uppermost unit whereas the maximum value is located just below H3.

4.2 Interpretation of the Peon Reservoir

The Peon gas reservoir is located in a sand with a thickness of 45 m. Top Peon as the upper boundary and URU as the lower boundary delineate the reservoir in the stratigraphic column, which is displayed in Figure 42b. Top Peon occur at 548 mbsl and URU at 593 mbsl in well 35/2-1. The gas column is 30 m thick at well 35/2-1 (well log in Figure 48). The primary area of investigation in this thesis is the area covered by p-cable data.

4.2.1 Top reservoir

The Peon reservoir is distinguished in the seismic with a very strong reflector at top. This is interpreted and labeled Top Peon. The reflector is strong compared to other reflectors, included the horizons mentioned above. In a cross section oriented north-south (Figure 42), the Top Peon

appear as an asymmetrical shaped upper reservoir boundary. Top Peon reflector is characterized by strong amplitudes, phase-reversed compared to the seafloor reflection. These high amplitudes are referred to as bright spots, which are the best direct hydrocarbon indicator for gas. The big negative contrast in acoustic impedance is most likely due to the high primary velocity (v_p) contrast between water-filled mud-rich sediments on top of gas-filled sand. Primary velocity of these gas-filled sand deposits is approximately 700-800 m/s while the mud-rich sediments on top has velocities of more than 2000 m/s, as shown in the sonic measurement in well 35/2-1 (Figure 48). The amplitudes are even stronger in the southern areas, as the seismic section in Figure 42 and the amplitude map extracted from Top Peon in Figure 43a display. Areas delineated by white lines in Figure 43b are considered below.

The high amplitude characterizes the Top Peon reflector and hence the interpretation is done with high degree of confidence. There occur smaller, disrupted zones related to the Top Peon, probably due to vertical fluid migration and erosional features at the reflector. Except for those interrupted areas, the overall picture of the reflector appear continuous, according to Figure 43b.

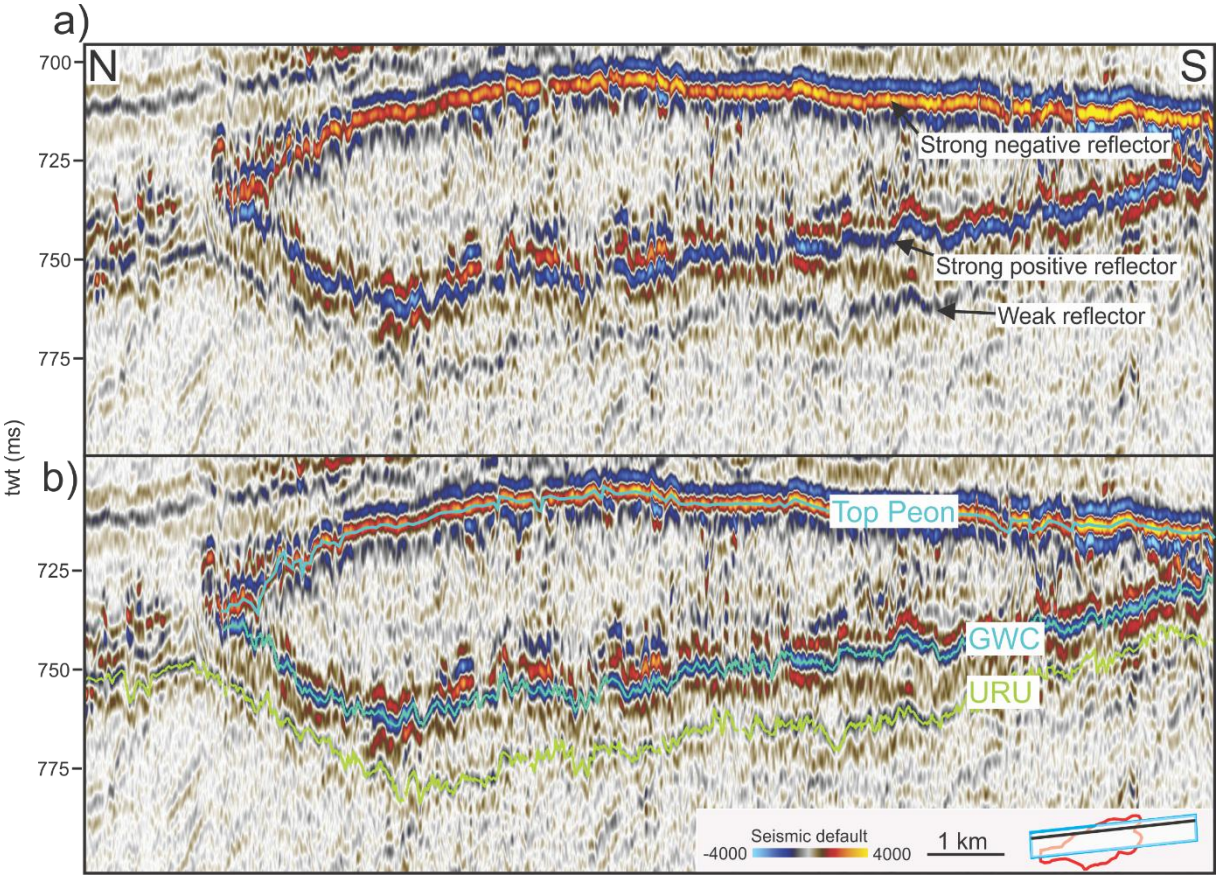

Figure 42: Seismic display of inline 2571 showing the reservoir in a N-S-profile where the interpretations are excluded (a) and included (b). In (a) arrows point to the reflectors of interest. Blue and green lines in (b) are the interpreted horizons of Top Peon, gas-waster contact (GWC) and the upper regional unconformity (URU).

Some areas of the Top Peon reflector reveal lower amplitudes, illustrated in the amplitude map in Figure 43b. Those areas are labeled "shadow zones". In opposite to the above-mentioned disrupted areas, the reflector within the shadow zones are continuous. High amplitude anomalies occur in the areas located vertically above these zones, as the seismic section in Figure 43b indicates. The absorption of acoustic energy from the HAA about 80 ms above the Top Peon reflector decreases the amplitudes of Top Peon. The visualized x-line (3350) in figure 43 extend across two areas of high-amplitude anomalies, and hence two zones of dimmed amplitudes appear at the location of x-line 3350 in the amplitude map. This dimming effect is due to attenuation of acoustic energy in overlying sediments (HAA). The areas with low amplitudes coincide with the presence of shallow gas located right above horizon H4, described in section 4.3.1.1.1.

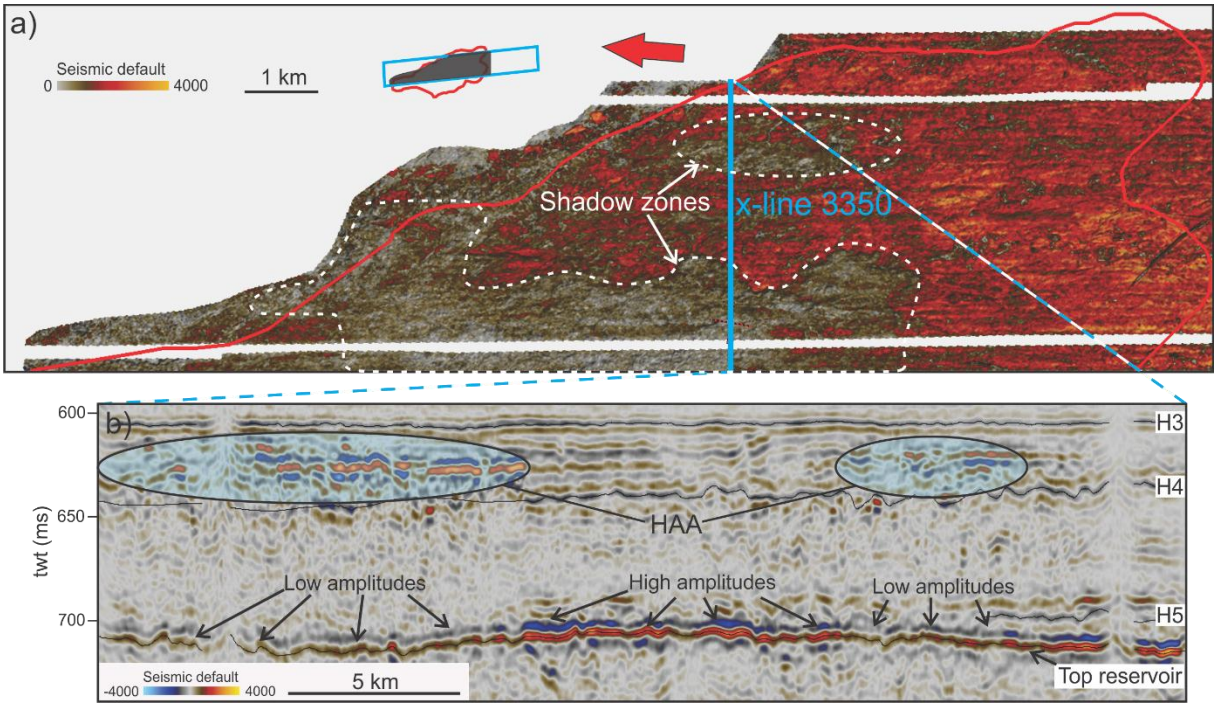

Figure 43: a) Amplitude map extracted from the interpreted Top Reservoir reflector. Shadow zones located directly below HHAs described and visualized in section 4.3.1.1.1. b) Seismic section x-line 3350 showing varieties in amplitude values in Top Peon reflector due to HAAs above.

4.2.1.1 Top Peon surface

The interpreted time surface of Top Peon reveals interesting morphological features. Figure 44 display the map with interpreted features indicated by arrows. Bigger concentrations of the features occur in the zoomed-in area in the figure. Elongated depressions and furrows are present on the irregular surface and resolvable by 3D p-cable seismic. Two major features are present on the surface that represent the upper boundary of the reservoir. Narrow, elongated depressions are widely distributed. White arrows infer their extent and orientation on the time surface map (Figure 44). The general direction of the striations is NNW-SSE, but some of them has a trending direction SSW-NNE. The furrows are between 1 and 5 km long and reveal elongated shape in general whereas some of them are curved. The elongated features are similar to that (Andreassen et. al., 2007) described in Barents Sea region, and are interpreted as iceberg plough marks. They are erosional features and infer the presence of icebergs after deposition of Peon reservoir. The trending SSE-NNW direction of the furrows is the same as similar features observed at younger horizons.

The other major feature on the Top Peon horizon is the wider, ridge-groove feature, concentrated in the southern and middle area of the p-cable dataset. Red, dotted lines in Figure 44 delineate some of those depressions. The largest depression is ca 7-8 km long, ca 200-300 m wide and up to 20 m deep. This is the most eastward of the delineated depressions on the surface map (Figure 44). The same feature occurs as a ridge on the time surface map of the interpreted GWC (Figure 45). From the time thickness map (Figure 46), the top and base (GWC) of the reservoir coincides at the mentioned area, and hence the thickness of the reservoir is close to zero at that particular area. These seems to be erosional scars formed by ice. Hence, there occur two sets of plough marks on the surface.

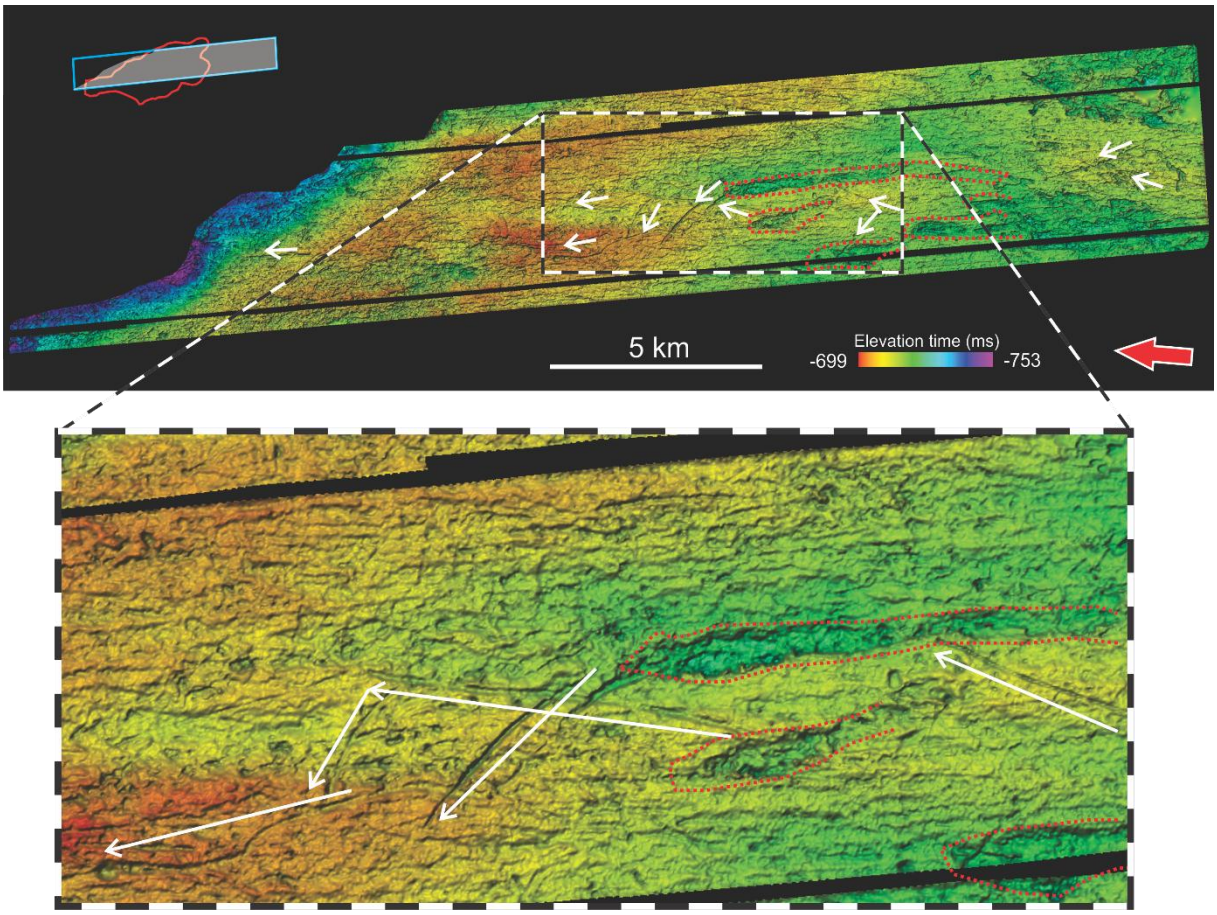

Figure 44: Time map of Top Peon including interpretation of features. Two depressional features are indicated by red dotted lines and white arrows and are interpreted as iceberg scour marks and plough marks, respectively. The easternmost scour mark indicated is referred to as the large one. The surface indicates the characteristic anticlinal shaped top reservoir, with steep dip on the northeastern flank (blue areas in north).

The two seismic 3D cubes available in this study do not cover the complete Peon reservoir, which makes it difficult to consider the overall shape and extent. However, the p-cable dataset covers the eastern part of the reservoir from north to south. The conventional dataset

complements towards west for the central and southern region, giving an indication of shape and extent of the reservoir in the west-east direction. Seismic data is available from both datasets at well 35/2-1 located in the southern part of the reservoir.

Time surface map of Top Peon reveals a convex lense-shaped structure, a kind of anticlinal shape. The deeper parts of the horizon is located in the outer limits in south and north. There is an abrupt change in reservoir structure in the northern part. A large drop in time values marks the limit for the northern boundary of the reservoir, which has a SE-NW orientation. As the red colors indicate on the time map (Figure 44), the shallowest parts of the reservoir is located along the northeastern "ridge" and a high in the middle of the reservoir. The southern parts of the top reflector is deeper, which coincides with N-S profiles from the seismic (Figure 42). It is worth noticing the southwards extend of the Top Peon reflector. High amplitudes are present south of the "outline" of Peon. The reservoir is so thin that is not considered at these areas. As the N-S profile from the p-cable dataset (Figure 42) and the W-E profile from the conventional dataset (Figure 47) reveals, the Top Peon reflector reveals an anticlinal structure. Anticlinal structures are among the most common hydrocarbon trapping mechanisms, where there is a structural trapping for the underlying petroleum. The questions of interest is if the seal is tight and the trap is closed towards the outer limits.

4.2.2 Gas-water contact

Estimation based on pressure evaluation and wire line logs gives the GWC to be located at 579 mbsl at well location 35/2-1. This makes difficulties when considering the GWC and URU in the seismic data, even though the vertical resolution is calculated to approximately 4 m (section 3.1.1). In the lower part of the reservoir, some reflectors that could coincide with the observations from the well data are observed. In Figure 42a, two reflectors are marked in the lower part of the reservoir, a weak and a strong reflector. With the high velocity contrast between gas-filled and water-filled sediments in mind, the gas-water contact is interpreted on the strong reflector pointed out in Figure 42b.

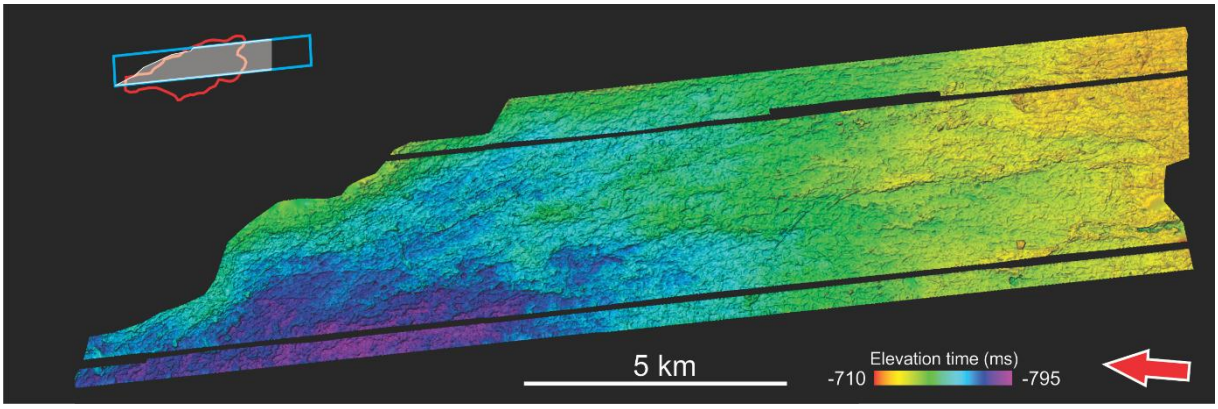

Figure 45: Time surface map of interpreted gas-water-contact (GWC). The fluid contact is inclined towards NNW.

Typically, flat spots mark the boundary between gas and water in the reservoir. The strong reflector is everything but flat, and the GWC in the Peon reservoir can be described as wavy, irregular and inclined. The irregularities, as well as the dipping nature, of the gas-water contact are not that common. From the time surface map of the GWC (Figure 45), there is an overall dipping towards NNW. The GWC is located at about 720 ms in southern part and at 780 ms in the northwestern part, inferring increasing depth towards NW. Those deeper areas are indicated by the blue color on the time surface map. The large ridge-groove feature observed on Top Peon is visible here as the yellow ridge in the southern area, in the middle of the dataset. Due to the small reservoir thickness in south, it is reasonable that these erosional features occur on this surface.

4.2.3 Base reservoir

The Peon reservoir is located right above the Upper Regional Unconformity. The underlying sediments are dipping sedimentary layers that are truncated by the URU. The base of the reservoir is the lowermost sediments that has the sub-horizontal layer architecture. The URU is described in more detail in section 4.1.9.

4.2.4 Peon reservoir

The outline of Peon reservoir is illustrated together with the outline of the two 3D seismic datasets (Figure 13). As we can see, the reservoir is not completely covered by seismic data. However, it is enough to extract information about shape, extent and intra-reservoir characteristics. The outline of Peon reservoir covers an area of approximately 120 km^2. It stretches 20 km from north to south and up to 8 km in the W-E direction. The outline has a kind of ellipsoidic shape, with the longest axis directed NNW-SSE.

The overall shape of the reservoir mounded or wedge-shaped in a cross-section view in the SSE-NNW direction. The N-S display of the seismic inline 2571 in Figure 42 indicate this characteristic shaped reservoir. Both the upper (Top Peon) and lower boundary (URU) of the reservoir contribute to this shape. An asymmetric anticlinal structure characterizes the Top Peon reflector, with steeper side towards north, as the time surface map of Top Peon reflector reveals (Figure 44). The URU reflector is weak or absent for the major part of areas covered by seismic data. This is due to the GWC lying above stealing acoustic energy, as Figure 42 displays. Visual observations infer that the GWC and URU reflectors are lying parallel throughout the Peon reservoir. Hence, it is reasonable to use the GWC as lower boundary to get a picture of the overall shape and thickness. Figure 46 shows the time map of GWC extracted from the Top Peon. There is a gradual thickening towards NNW, which coincides with the anticlinal shape of Top Peon, visualized in Figure 44, and the dipping nature of the GWC as we see in Figure 45. The northern area has a NE-directed boundary with an abrupt thinning. In the southern area of the thickness map (Figure 46) the top and base coincides, as the pink color indicates. This is why the outline of the reservoir is north of the southern boundary for Top Peon, according to Figure 13 and Figure 44.

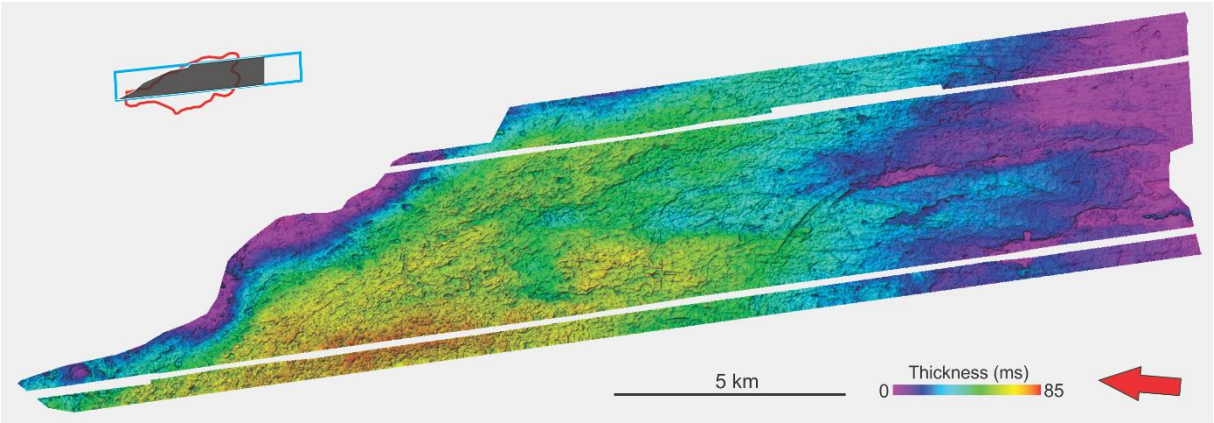

Figure 46: Thickness map of Peon reservoir calculated by extracting the GWC from the Top Peon. Thicker accumulations of sediments occur in the northwestern areas of the p-cable dataset. Pink areas in south indicate very low or zero thickness.

The reflectors reveal symmetrical shapes in southern parts of Peon, as the seismic section of inline 5322 from the conventional 3D dataset illustrate (Figure 47). The blue line shows interpretation of Top Peon whereas green line mark the interpreted gas-water contact. They reveal anticlinal and synclinal shapes, respectively, and both are gently tilted towards west. The seismic section reveals a depression on the top of the structure (Top Peon in Figure 47). This

coincides with observations done on the time surface map of Top Peon in Figure 44. This feature is interpreted as an iceberg scour mark.

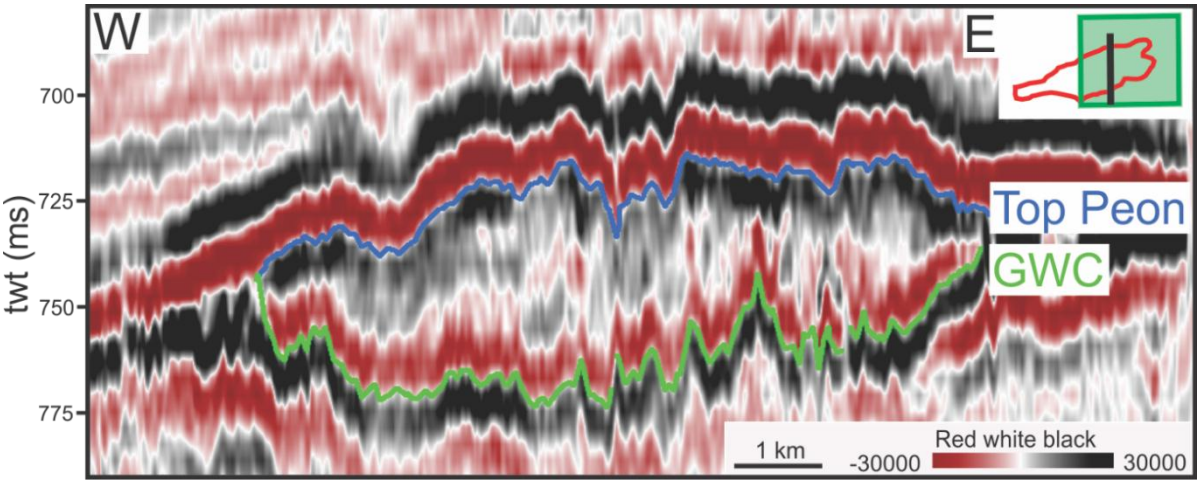

Figure 47: Seismic section of inline 5322 from the conventional 3D dataset. Interpreted horizons Top Peon and GWC marked out by blue and green lines, respectively. They coincide in east and west of the seismic section, indicating this lense-shaped Peon reservoir in the W-E direction.

The distance between the GWC and URU is estimated to 14 meter (579 -593 mbsl) at well 35/2-1 (Figure 49). With the irregular and dipping GWC in mind, we have to consider the seismic resolution together with this relatively short distance between the GWC and URU. The fluid contact and the regional boundary could in some areas be too close to each other to be seismic resolvable, and could be a contributory reason why there is a weak or absent reflector for the URU in the dataset. The package in between the GWC and the URU consist of two smaller packages. As we can see from the interpreted the well log in Figure 49, a clay-rich package of sediments occur just below the GWC (578-587mbsl). Underneath that package a sand layer occur from 587 to 592 mbsl. 5 meter thick deposition of sand in between layers consisting of clay may not be thick enough to resolve on the seismic data, and hence the URU reflection is weak or absent. As already mentioned the vertical resolution of the p-cable dataset is about 4 meter. The thin sand layer is most likely even thinner in areas where the URU reflector is absent. Gamma values for the sand layer is similar the values for the gas-filled part of the reservoir, about 45-60.

4.2.4.1 Well data

4.2.4.1.1 Gas-filled reservoir

Figure 48 visualize the well log data for the reservoir between the Top Peon and the gas-water contact. The green dotted line shows the interpreted top reservoir and coincides with the strong

negative reflector in the p-cable seismic, shown in the outer right column of Figure 48. The three logs decrease dramatically when penetrating the Top Peon. The synthetic seismic (second column from the right in the well log), which is calculated on sonic and density measurements in the well, match nicely with the interpretation of Top Peon reflector in the p-cable dataset. The density log reveals a quite constant value of about 2.25 g/cm^3 between H5 and Top Peon. In the upper reservoir, from 548 to 558 mbsl, the values alternate between 1.95-2.00 g/cm^3, before it gradual decrease to 1.87 g/cm^3 at 562 mbsl. There is also a sharp increase at 568 mbsl. From there it is a linear increase towards 2.16 g/cm^3 at the GWC (579 mbsl). The increases in density may indicate the presence of material higher density or it may be due to lower gas-saturation levels. It could be more and higher concentrations of gas in the upper part of the reservoir and that the saturation decreases with depth. This coincide with the nature of gas to migrate upwards.

The gas-filled part of the reservoir got seismic p-wave velocities between 820 and 900 m/s. The upper and lower boundary has 1-2 m transition zones where the values decreases and increases dramatically, respectively. The velocity right above Top Peon is 2000-2100 m/s. The presence of gas in the sediments is the major contributor for this drop in sonic values.

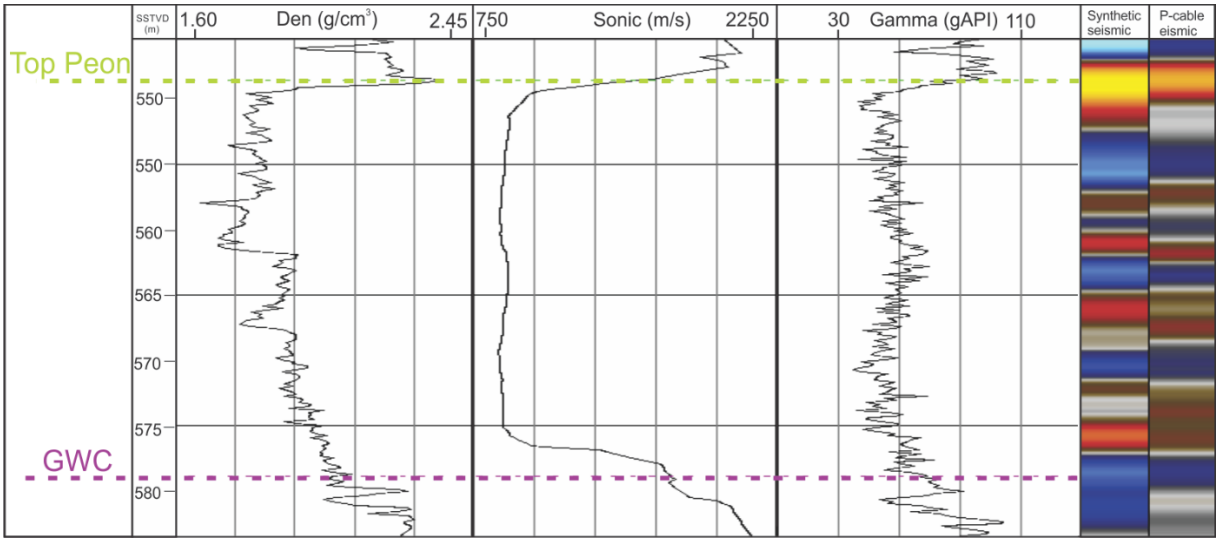

Figure 48: Density, sonic and gamma ray measurements within the gas-filled part of reservoir from well 35/2-1. Correlated with synthetic seismic and p-cable seismic data. The depth is the subsea true vertical depth (SSTVD). Values and type of log is indicated in the top row.

Minor and frequent changes of values in the span 40-70 gAPI characterize the gamma log within the gas zone, as the third column from right in Figure 48 shows. Such a variability could testify the presence of a silty sand, meaning some mixing of clay and smaller particles within the reservoir sand. A clean and homogeneous sand would often have lower and more constant

gamma values. The gamma ray values right on top of Peon is 80-90 gAPI, inferring more compacted and clay-rich sediments. However, there is some trends in the gamma log to notice. Splitting the gas-filled zone in three equal parts, there is a fining upwards sequence in the lower and a coarsening upwards sequence in the middle part. Together with the density log, they infer a sand with increasing clay content downhole.

4.2.4.1.2 Water-filled reservoir

The water-filled reservoir, meaning the zone between the GWC and URU, reveals three characteristic layers in the well data. They are visualized in the well log data acquired from the water-saturated part of the reservoir (Figure 49). As we can see, there is a dramatic increase in sonic velocity at the GWC, which is the main factor for the strong positive seismic reflector interpreted as the GWC. The p-wave velocity for water is much higher than for gas. However, the density and gamma ray values from the upper part of the water-saturated zone is quite similar to the layer above.

There seems to be thin, alternating clay and sand layers in the zone right below GWC. This layer ranges from 579 to 582 mbsl and named I in the well log (Figure 49). The varying density and gamma ray values indicates the presence of alternating sand and clay layers. At 580 mbsl there is a spike in both logs, while the values decreases at 581 mbsl. This could be a "transition zone" where changing depositional regime occur.

The second characteristic layer (II in Figure 49) occur from 582 to 588 mbsl. The density values remains constant at 2.27-2.30 through the complete layer. Sonic values are high in the upper part, up to 2300 m/s. During the lower part of II there is a linear decreasing velocity towards 1900 m/s. In Figure 49, the gamma ray alternate frequently during layer II. Minimum and maximum values are 75 and 98 gAPI, respectively. This means the sediments contain a lot of radioactive minerals, indicating relative high clay content. However, the grain composition seems to alternate between more sandy silt and silt with less sand content. This infers poor reservoir quality, high heterogeneity and a lot of potential "barriers" and compacted clay-rich sediment layers within layer II.

In the lowermost part of the reservoir a 5 m thick layer occur, from 588 to 593 mbsl, which is the zone delineated by layer III in Figure 49. The URU marks the base of this layer whereas

layer III is the lowermost subunit of the reservoir. The density values are constant at 2.15-2.20 while sonic velocity increases from 1840 to 2080 m/s. Gamma ray values are between 47 and 57 gAPI in upper 4 m before it increases dramatic up to 100 gAPI from 592 to 593 mbsl. Based on these readings, it seems to be a homogeneous layer (upper 4 m). The package got gamma values as low as the upper reservoir, while density values is a bit higher. This indicates a sand with similar reservoir properties as upper part of reservoir. The higher density values testifies that these sediments are water-saturated.

The synthetic seismic data correlates well with the p-cable seismic at the GWC. We see that the pink line correlates with a peak (blue color) in the seismic sections in Figure 49. The URU reflector at the base correlate with a non-reflective zone in the synthetic seismic, indicating low or now changes in the measured acoustic properties at the regional unconformity.

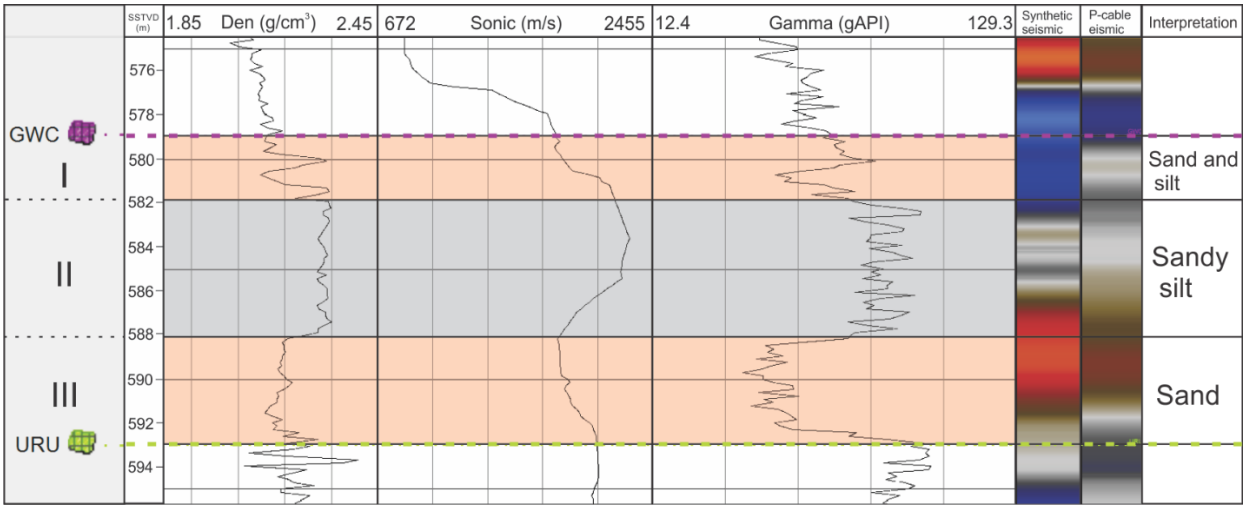

Figure 49: Density, sonic and gamma ray measurements within the water-filled part of reservoir from well 35/2-1. Correlated with synthetic seismic and p-cable seismic data. The depth is the subsea true vertical depth (SSTVD). Outer right column shows the lithological interpretation of the three layers (I, II and III). Values and type of log is indicated in the top row.

4.2.4.2 Intra-reservoir amplitude anomalies

Intra-reservoir seismic signature and configuration of the Peon reservoir is characterized by chaotic, discontinuous, low amplitude reflections with low degree of internal organization and pattern. This makes it difficult to map out extending horizons within the reservoir. The horizon interpreted as the gas-water contact (GWC) is the only prominent and extending intra-reservoir reflector interpreted with high degree of confidence. Despite the general pattern of chaotic

reflections and lack of internal organization, there occur several minor zones of high amplitudes within the reservoir. They are mapped out by seismic interpretation and use of seismic attributes to identify structures and patterns that could be useful for interpreting the depositional environment. These intra-reservoir reflections are observed at different stratigraphic level and will be considered in this section.

Elongated curved, channel-like features are visible in attribute maps and seismic sections. They hold a syncline or u-shape. These kind of reflectors are characteristic for the reservoir, and occur extensively in the area delimited by the outline of Peon. The occurrence of these systems are particularly present in the shallow stratigraphic level of the reservoir, and most common in the southern part. The channel-like reflectors reveal strong, positive amplitudes in general, but can also occur as weak reflectors. This feature is referred to as channels in time surface and attribute map visualizations (Figure 50, Figure 51 and Figure 54). The general direction for these features is SSE-NNW. There is some variability in direction, some more westward and some more northward directed. The Top Peon reflector truncates the reflectors at the base of the channels, indicating they have been cut or eroded in the top.

Some of the channel-like features are mapped out and interpreted, illustrated in Figure 50. The degree of confidence is variable. Channel 2 is the most prominent and reveals strongest amplitudes and the most continuous reflector. The maximum amplitude attribute map correlates very well with the interpretation of channel 2. Reflectors of channel 1 and 3 do not have the same reflection strength, but there occur some high amplitudes within the channels.

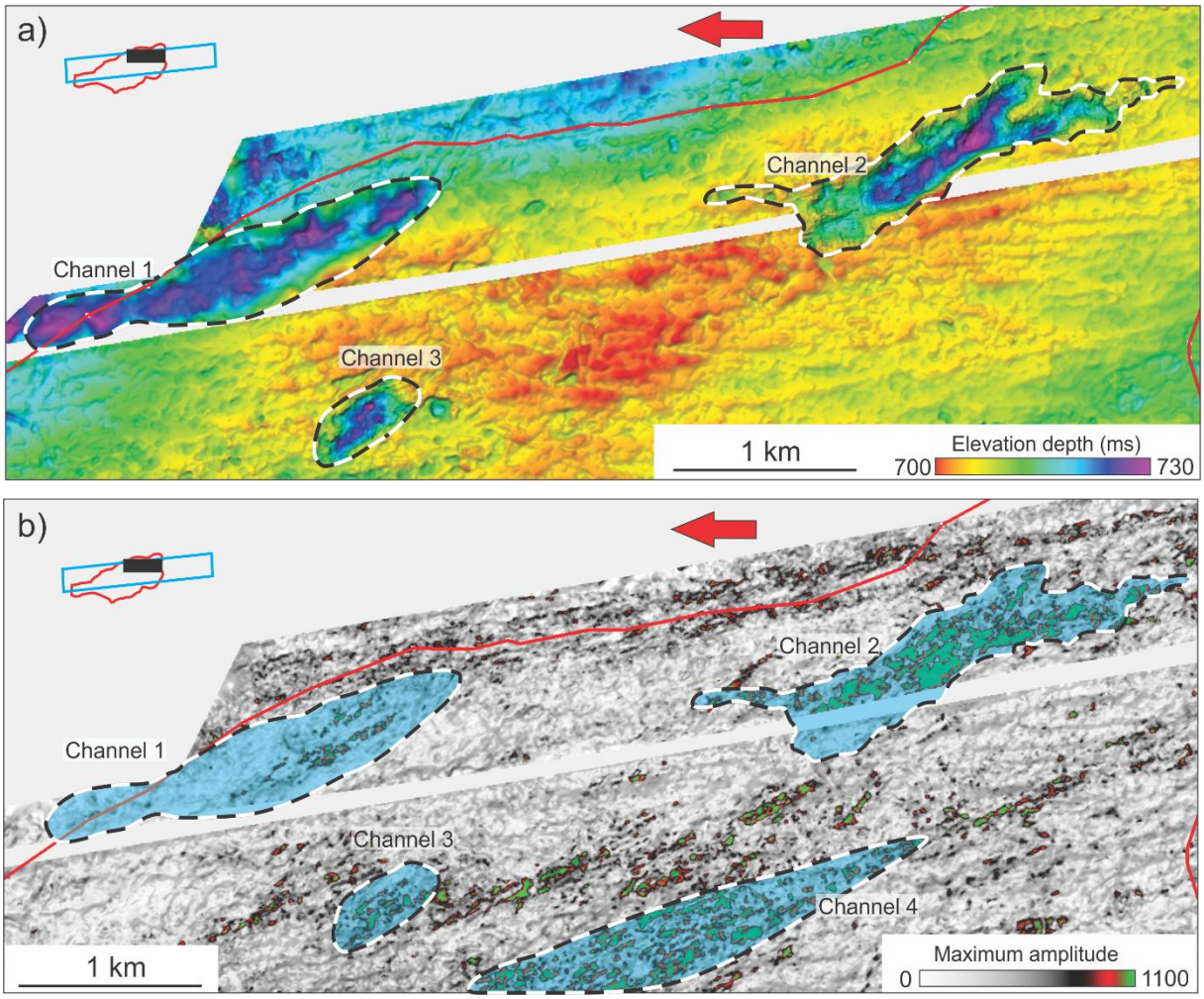

Figure 50: Visualization of interpreted channel-like structures. a) Time surface map interpreted channels and Top Peon in the surrounding areas. Channel 1-3 is interpreted and mapped out. b) Max amplitude map extracted from 8ms below Top Peon to 8 ms above GWC.

Channel 2 is located in the eastern part of the Peon reservoir (Figure 50). This channel-feature is interpreted on a continuous reflector at base. The feature is directed SSE-NNW, is about 2 km long, 400 m wide and up to 25 m deep. There are two smaller channels merging to a bigger channel from the south. It reveals a strong positive reflector, meaning an increasing acoustic impedance contrast. This may indicate presence of higher concentrations of gas within this channel-feature. This suggests more sandy deposits within the channels and probably more clay-rich sediments below, giving rise to the positive reflector at the base of the channels. However, the reflection strength at Top Peon remains the same. It would be expected stronger amplitudes on top those channel deposits if they contains higher concentrations of gas.

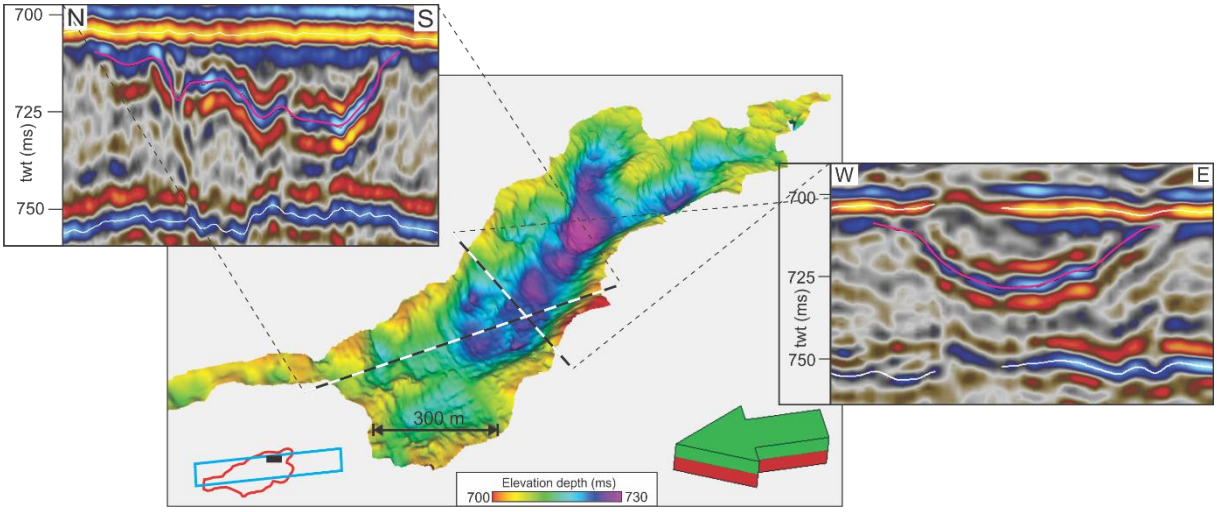

Figure 51: 3D view of interpreted channel 2 with seismic cross-profiles.

Channel 1 is about 2.5 km long and up to 500 m wide, while channel 3 is 700 long and 300 m wide. Both are up to 25 ms deep. Channel 3 is more like elliptical depression than a channel in shape (Figure 50).

The above-mentioned channels reveal relatively strong and continuous reflectors. A characteristic shape of the u-formed reflectors are observed. However, many of the areas with high amplitude anomalies do not have the same shape and extent. These HHAs appear with minor bright spots distributed; either closely related to each other or as single, separated bodies. They occur at different stratigraphic level, from Top Peon to the gas-water contact. In comparison, the erosional channel-feature occur more frequently in the upper part. Along or within the amplitude bodies/features, they tend to remain at the same stratigraphic level or slightly decline towards NNW. These amplitudes occur frequently in the Peon reservoir. The maximum amplitude map of the amplitudes within Peon (Figure 53a) provides us an indication of how they are laterally distributed. Several elongated features are stretching with a trending SSE-NNW direction. Especially in the southern areas, close to the outline, these elongated bodies are prominent in the attribute maps. Some of these high amplitudes reveals meandering shaped and stacked channel-like pattern.

North-western part of P-cable dataset reveals several smaller curvilinear channel-like features. These are visualized in Figure 52 by maximum amplitude map and a seismic cross-section. The high amplitudes occur as meandering channel-like features in the upper part of the amplitude map, while they are more randomly oriented in the lower part. The direction of the channels

(SE-NW) occur more towards west than the ones described earlier (SSE-NNW). These channels vary in width between 5 and 50 m and some of them are more than a kilometer long.

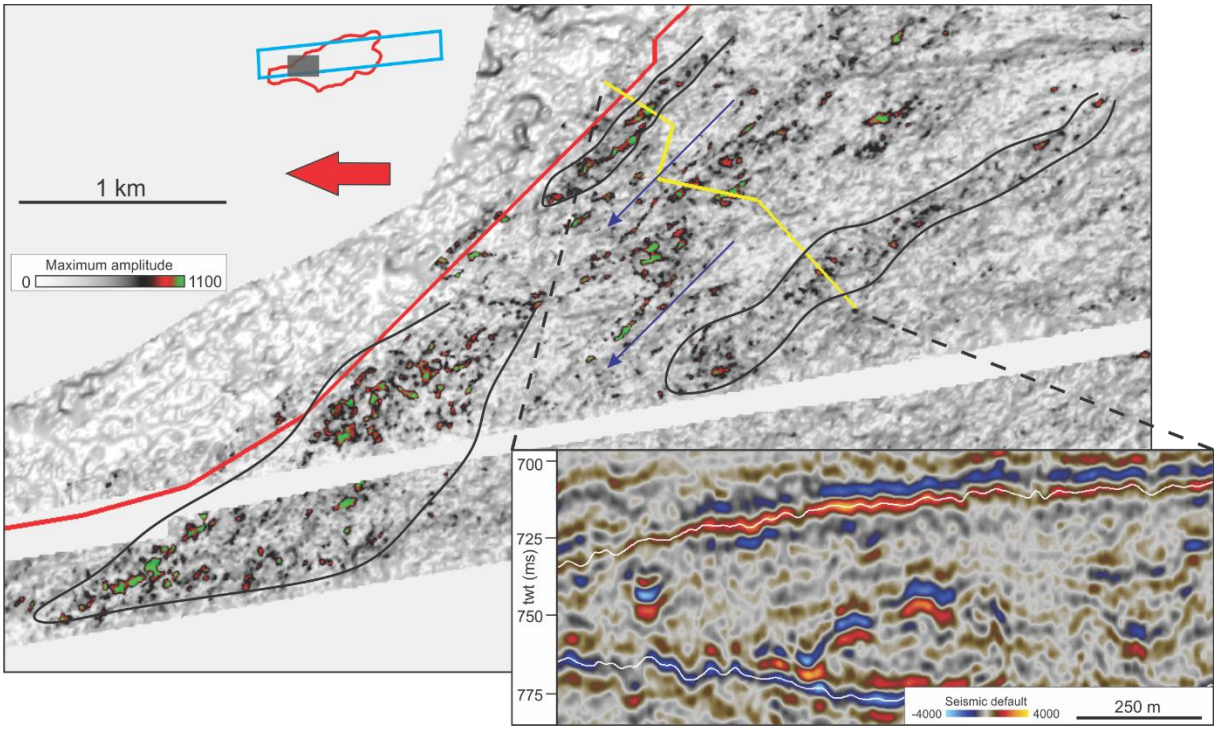

Figure 52: Maximum amplitude map extracted from p-cable dataset between 8ms below Top Peon and 8ms above GWC. Yellow line indicate position of arbitrary line in seismic view.

A south-north stretching curvilinear, massive, body of high amplitudes occur in the lower part of the reservoir. It builds out from south, and turns northwest closer to the northern border of the reservoir. Several curvilinear features are observed within a complex body of high amplitudes. These amplitudes are appointed and encircled by blue arrows and lines in Figure 53.

By correlating seismic x-line sections, lateral reservoir variations are observed, and how the internal structures and amplitudes occurs within the reservoir. Eight seismic cross-sections are displayed together with the maximum amplitude map in Figure 53a. Lateral extending high amplitudes coincides with channel-shaped reflectors and high amplitudes in the seismic displays are observed.

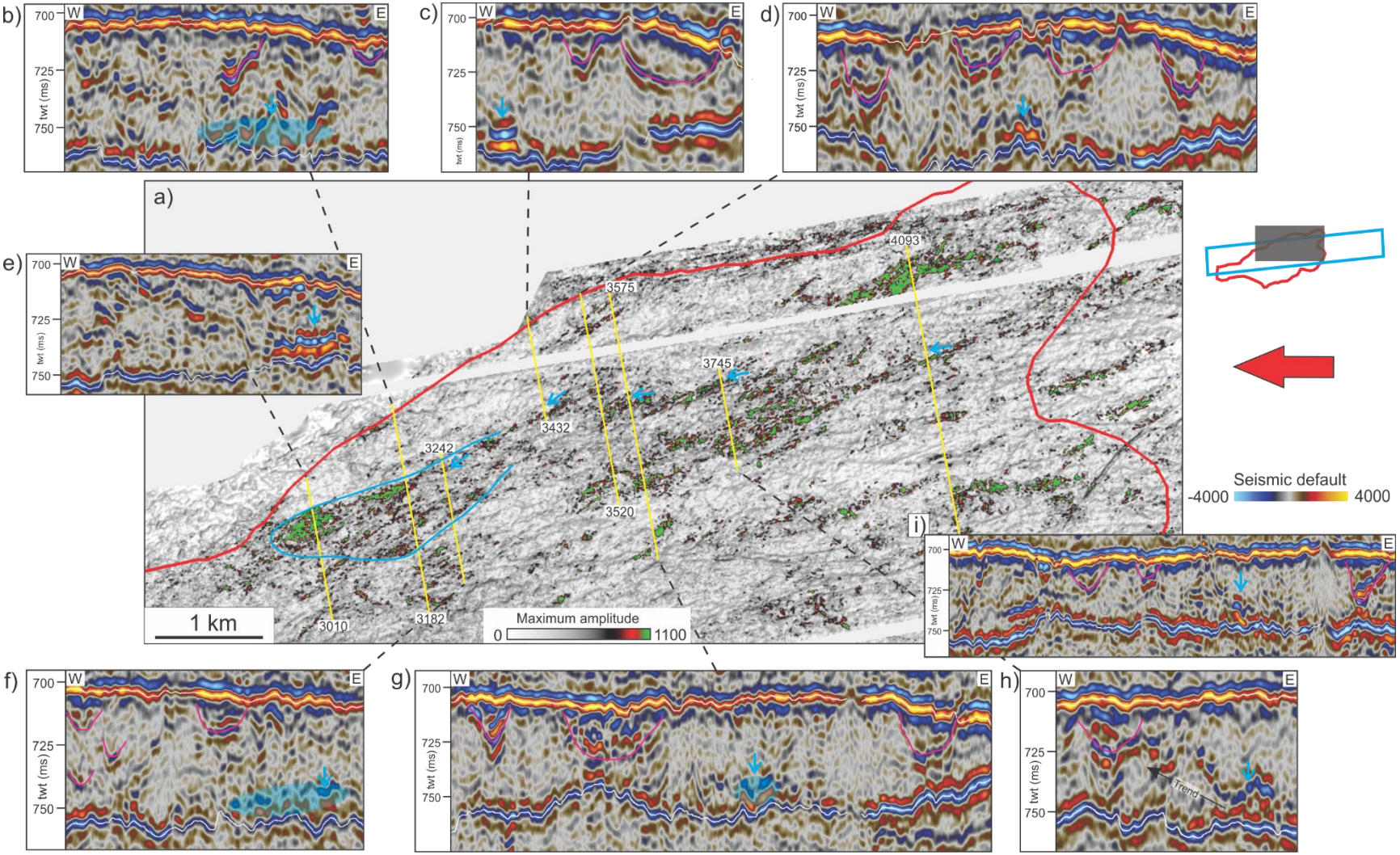

Figure 53: a) Maximum amplitude map extracted from p-cable dataset between 8ms below Top Peon and 8ms above GWC. Yellow lines indicate position of x-lines in seismic sections (b-i). Blue arrows point to high amplitudes close to the GWC. Pink lines in cross sections indicate channel-like features.

The described channels from the last section are mapped out and interpreted with high degree of confidence. Indication of the presence of other channel-features and high-amplitude bodies are shown in attribute maps and seismic cross sections. Figure 54 illustrates this by indicating the outline of elongated, high amplitude bodies. The general direction of them is SSE-NNW. This interpretation is done by correlating seismic inline and crosslines with the amplitude map. This indicate the distribution of HHA within the reservoir. The elongated bodies are up to 3 km long and generally 50-100 m wide.

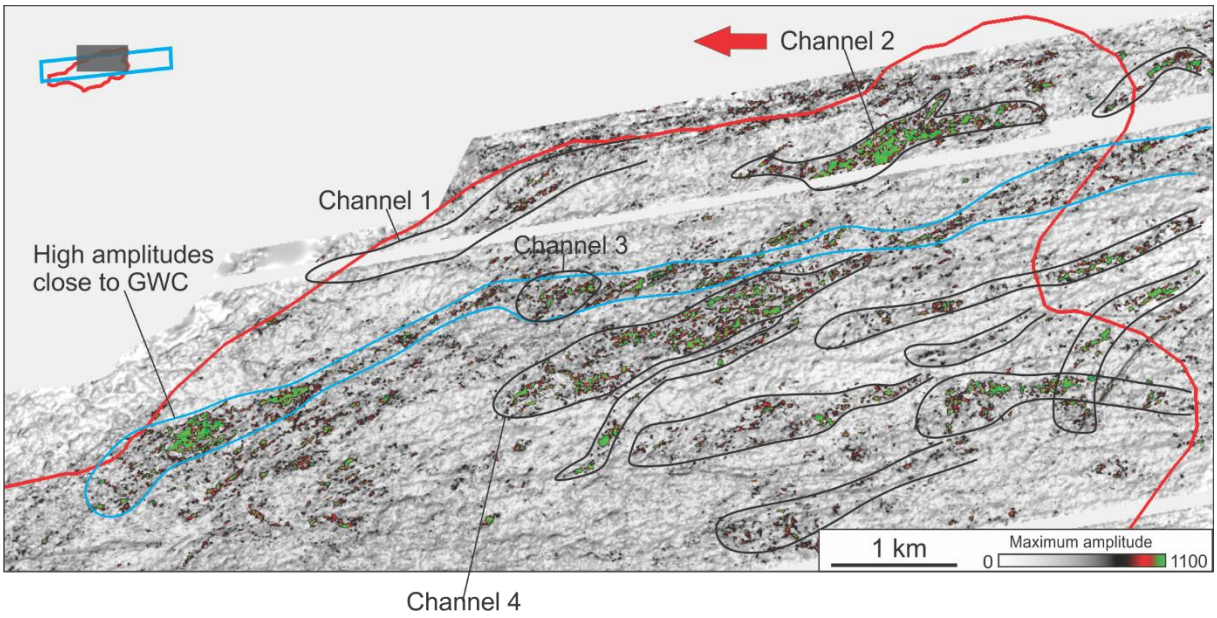

Figure 54: Maximum amplitude map map extracted from 8ms below Top Peon to 8 ms above GWC indications of channel-like features (black lobes). Blue area show extent of high amplitudes close to GWC.

4.3 Fluid flow structures

Several indications and seismic expressions associated with fluid flow and shallow gas are present in the Peon area. This includes deeper fluid migration into the reservoir, leakage from reservoir, shallower gas accumulation and fluid migration, as well as pockmarks at the seabed and older horizons. Acoustic pipes, high amplitude anomalies, wipeout zones, push-down effects, pockmark-like depressions, fault structures, chaotic reflections and disturbed stratified layers are among several seismic indications for this.

There has been observed and described circular depressional features at the Seabed horizon in both the p-cable and conventional 3D dataset. These are interpreted as pockmarks, which result from seepage of gas and pore fluids in soft sediments (Judd & Hovland, 2007). High concentrations of pockmarks is observed right south of the outline of Peon reservoir, as Figure

55 illustrate. 10 and 4 pockmarks is mapped out in the conventional and P-cable 3D dataset in that particular area, respectively.

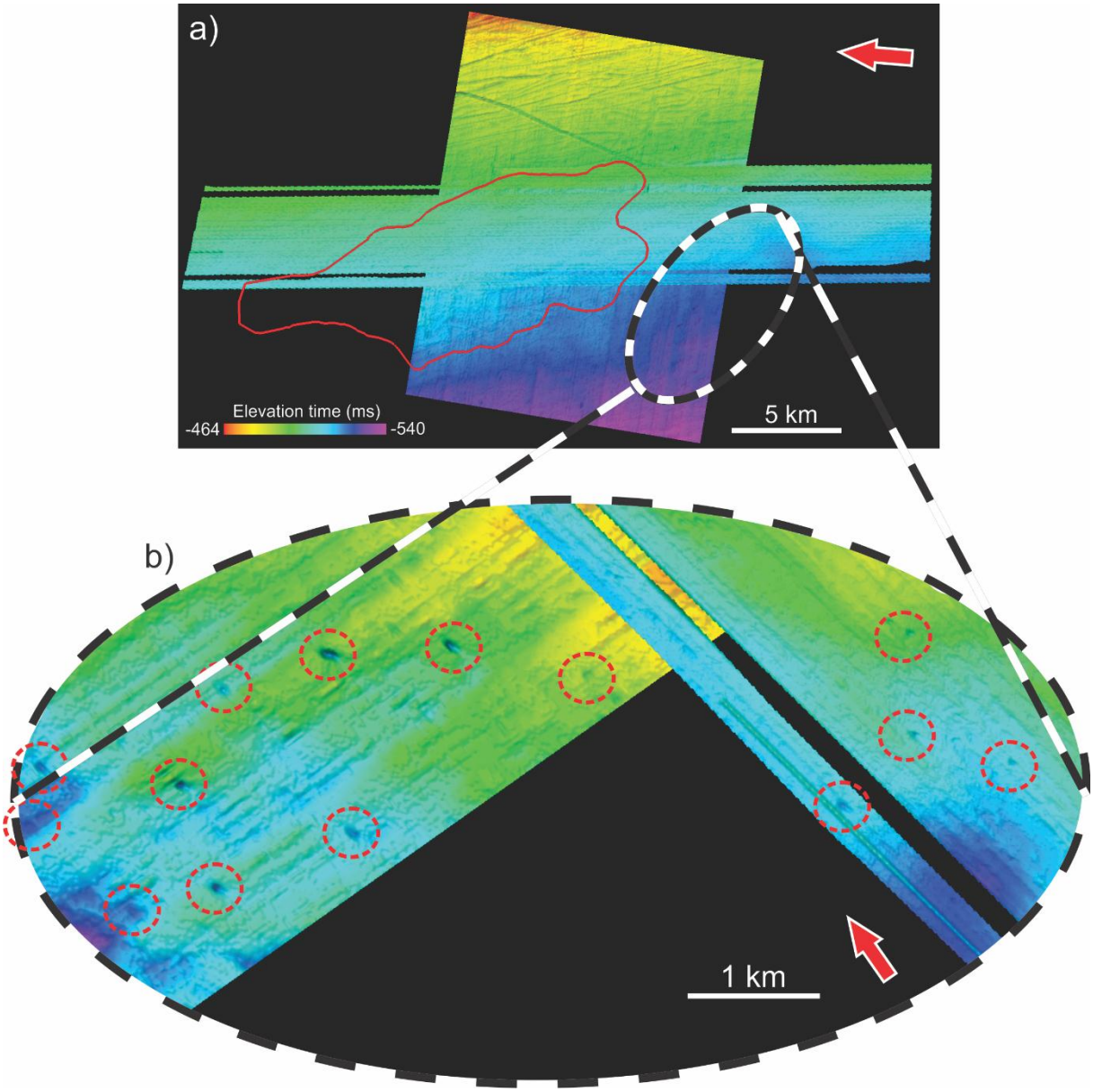

Figure 55: a) Combined view of interpreted Seabed horizon from P-cable and conventional 3D dataset. Outline of Peon reservoir indicated by red line. b) Area of interest zoomed. Red, dotted circles indicate position of pockmarks. Note different colorscale between the dataset to highlight the features.

4.3.1.1.1 High amplitude anomalies

High amplitude anomalies (HAA) are observed with large lateral extent in the layer in between reflector H3 and H4 (Unit 5). The seismic signature is chaotic and the reflectors have low degree of continuity. The HHAs are kind of displaced to each other and occur at a bit different stratigraphic levels. This chaotic pattern and "stealing" of acoustic energy makes it difficult to

interpret the horizons below the anomalies. The underlying reflectors occur as blurred and disturbed.

As the name of the anomalies infers, these reflections are composed of high amplitudes. The reflections are phase-reversed compared to seafloor reflector, indicating a negative acoustic impedance contrast. They are located in the stratigraphic column about 70-90 ms above the Top Peon. RMS amplitude attribute displays the distribution of the amplitudes in a good manner. The RMS map in Figure 56 is calculated on amplitude values between 13 and 31 ms below the H3 reflector. From the map, the HAAs are distributed in the northern and western part of the P-cable 3D data set (Figure 56). Black dotted lines delineate the amplitudes of interest. Stronger amplitude anomalies occur within the outline of Peon reservoir.

Gas decreases the sonic velocity dramatically. Also the density of the formation decreases. These negative reflections represent a big reduction in acoustic properties. Due to their very high, negative amplitudes, these HAA are interpreted as shallow gas accumulations. HAAs described and mapped in RMS amplitude map are the shallowest major observations of gas in the study area. These HAA are located directly above the Peon reservoir. We observe a dimming effect/wipeout zone below these HAA. Figure 43 and Figure 57 show that the Top Peon reflector reveals lower amplitudes in the areas vertically below the HHAs. Gas accumulations in layers above the reservoir may attenuate the seismic signal beneath these very shallow accumulations. This makes it reasonable to think this upper gas has migrated from the Peon reservoir. Shallow gas anomalies commonly overlie hydrocarbon discoveries indicating leakage of gas from the deeper formations (Vadakkepuliyambatta, et al., 2013).

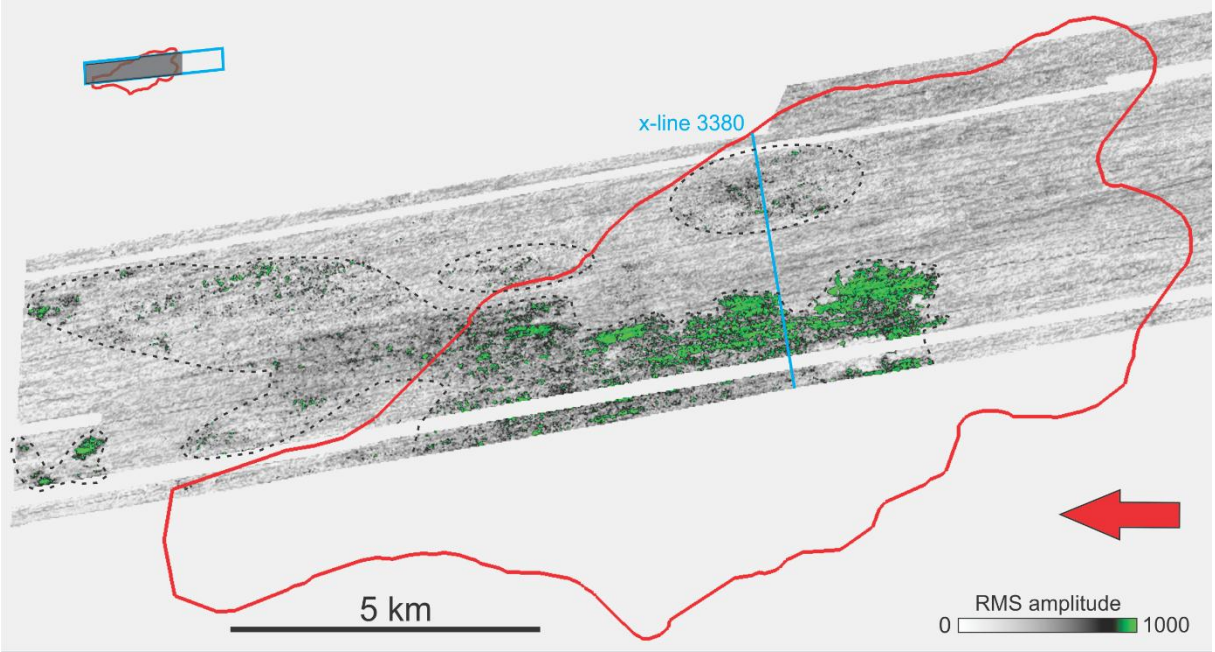

Figure 56: RMS amplitude map calculated on interval 13 to 31 ms below reflector H3. Blue line indicates position of x-line 3380 (displayed in Figure 57). Black dotted lines indicate areas of highest RMS values.

Discontinuous, chaotic reflections infer a disordered organization of the sediments. Minor faulting might have occurred in the stratigraphic column between the reservoir and H3. The accumulations illustrated in Figure 56 are the shallowest observations of gas in the area, which support a good sealing mechanism of the layers on top.

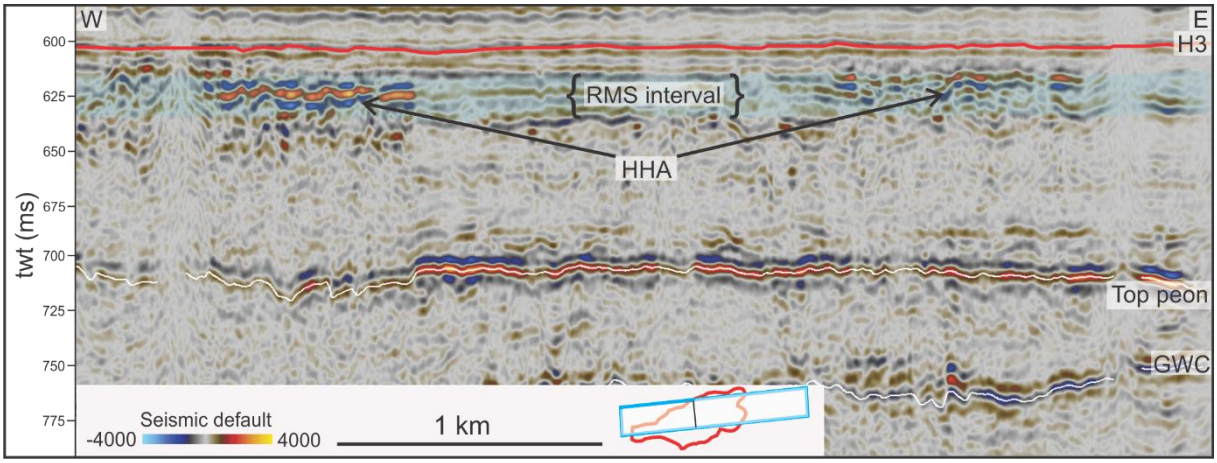

Figure 57: Seismic section of x-line 3380 indicating RMS interval for Figure 56. Horizon H3 is marked by red line. RMS amplitude window indicated by blue shaded zone and is 13-31 ms below H3.

5 Discussion

5.1 Depositional history

Lot of useful information can be extracted considering the interpreted and mapped out horizons in the overburden, as well as the units in between. Depressions and erosional features which occur on most of the horizons are interpreted as iceberg plough marks and testify the present of icebergs drafting in shallow water masses. They may erode the base on their way (Andreassen, et al., 2007), inferring these are erosional features. These are common features of glaciated continental margins (Ottesen et. al., 2012), and therefore over large areas off the coast of Norway.

The packages of sediments in the overburden is described by seismic signature and subdivided into units. Several units have the same seismic characterization, which could indicate similar depositional regime.

The laminated, parallel reflections in unit 1 may indicate a normal marine sedimentation regime in combination with distal glaciomarine deposition. The highly glacial-affected surface of H0 represent plough marks and imprints of glaciers. This testify that glaciers and icebergs have been present during the deglaciation. Sediment fall-out from suspension and from icebergs has likely occurred and ice-rafted debris is probably present in this unit, especially in the lower part.

Well 8903 is located approximately 126 km south of Peon (60º38.4'N, 3º43.4'E), and a bit south of the Troll field. Core data analysis from the well shows that the uppermost 16.9 meter of the stratigraphy consists of marine, partly glacial marine sediments and is dated to be sediments younger than 15.1 k.a.. Marine carbonate fossils analysis from well Troll 3.1 dates the upper 22.6 m to be younger than 14.7 k.a. (Sejrup, et al., 1994). The latter measurement is acquired 2 m above the underlying unit while the sample at 8903 is acquired only 10 cm above, which could explain the difference of 400 y. Both wells, as well as Peon, lies within the Norwegian channel. The parallel, laminated reflections observed in the seismic and the thickness of the layer corresponds with this well data. This upper layer seems to have a regional extent, and the seismic character described in the Peon area is present in the area close to 8903 (Fig 8 in (Sejrup, et al., 1994)). Due to these observations, unit 1 at Peon (upper 19 m at well location 35/2-1, Figure 41) could probably represent sediments deposited the last ca 15.1 k.a., after the Late Weichselian. (Sejrup, et al., 1994) stated that the Norwegian Channel was ice free

at ca 15 k.a. Transparent character in lower part of Unit 1 is observed, which may be indications of till, or a transition zone between till deposits and marine/distal glaciomarine deposits on top.

A possible readvance of glaciers occurred appr 18-15 k.a. in the North Sea Plateau and parts of the Norwegian Trench (Sejrup, et al., 1994). The Norwegian Trench was deglaciated at 15.1 k.a. (Sejrup & Aarseth, 1995). The glacial-affected H0 horizon (Figure 20) could represent advance and retreat of glacier in the period 18-15 k.a.. MSGLs are probably formed when the glacier advance and fast flowing ice sheets makes parallel imprints in the surface. During retreat and deglaciation, icebergs drifts around and erode into the surface. This result in more randomly oriented striations. This is reasonable when considering the relative age of two features; plough marks cutting across MSGLs.

The MSGLs observed east of Peon at the seabed (Figure 18) indicates that there has been low sedimentation rates after the last glacial advance, which occurred about 18 k.a.. However, there has been no observation of MSGLs within the outline of Peon, and therefore we may infer this distal glaciomarine/marine deposition could have occurred.

Both wells (8903 and Troll 3.1) indicate the presence of a till unit below layer described above. The seismic data at Peon reveals a transparent character, which is typical for a till deposit. This makes it reasonable to think of regional extending till deposit in the Norwegian Trench, and is represented by Unit 2 in the seismic section from Peon area (Figure 15). The seismic reflector H0 indicate decreasing acoustic properties when going in to Unit 2. This may also indicate that more fine-grained marine sediments overlies a mixture of sand and silt. Several evidence are found that the Ferder Glaciation occurred about 70 k.a and deposited tills, which extended laterally in the northern North Sea (Carr, 2004). Sub-glacially deformed till and infill channels have probably formed the upper Ferder Formation (Carr, 2004). Due to the seismic characteristics, well log data and considerations above, it is likely the Ferder Glaciation could have played a major role depositing the unit 2.

Unit 2 got a relatively constant thickness at around 20 ms, meaning a real thickness of about 15 meter (assuming p-wave velocity=1500m/s). The layer is measured to 16 m at well 35/2-1. There occur a major change in direction of dip at the H1 reflector. Where the Seabed, H0 and H1 surfaces got the same direction of the dip, i.e. towards WSW. All layers underneath H1 are

inclined different from the ones above. This could represent an erosional surface caused by an event which has eroded the surface and made this flat character. A time gap in the stratigraphic column can be present and it may have given rise to the strong seismic reflector H1 (Figure 15). The presence of mega-scale glacial lineations (Figure 23) testify that ice streams have been present before deposition of unit 2. This infers that tills likely have deposited during a glacial retreat or event. Plough marks are mapped out in the southern part of the dataset (Figure 23). The striations seems to contain lower relief northwards, and it may remind about a gradually wipe out. Ice streams may have eroded the surface, as well as the iceberg plough marks.

Unit 3 reveals a characteristic transparent seismic signature, even thicker and more transparent than unit 2 (Figure 15). The unit got gamma values between 60 and 75 gAPI, meaning a mixture of sand, silt and clay is reasonable. The transparent character gives rise to think of glacial till deposits. Similar characterization has previously been interpreted as a "till tongue" (TT) ((Ottesen et. al., 2012) (Rise, et al., 2005)). This supports a sedimentation regime dominated by glacial processes. King et al (1987, 1991) propose that several laterally stacked till tongues build out during the Saalian glaciation. This supports interpretation of unit 3 as Saalian deposits. The pinch out up-slope correspond with the description (Rise, et al., 2005) did of TT during Saalian glaciation. The thickness map of unit 3 (Figure 25) illustrate thinning against the direction of the ice sheets (SSE), according to Figure 58 and thickness map of unit 3 (Figure 25). This indicates that an active ice front was present during that time, since TT deposits are ice front proximal deposits. The curved depression-like features observed on the horizons, including the parallel striation feature on H2, are interpreted to be iceberg plough marks (Figure 26). These are good indications for the presence an active ice front, depositing the till. The presence of glacial eroded surface surrounding till units is typical (Sejrup, et al., 2004), as observed especially right below the TT (H2 reflector, Figure 26). The occurrence of possible erosional event represented by H1 may also have wiped out or cut through other glacially eroded surfaces on top of the TT.

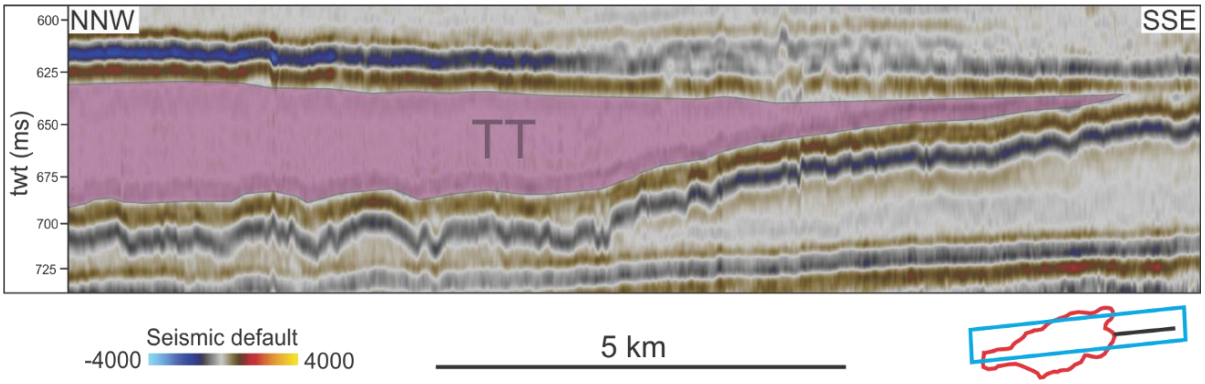

Figure 58: Seismic section of inline 2234 showing till tongue (TT) deposit pinching out towards SSE, south of the reservoir outline. The interpreted TT is indicated by pink shaded zone.

The NCIS fed the continental margin with sediments. The ice streams repeated and deposited sediments on top of each other, making up several packages of till deposits. This has probably occurred at Peon, as we observe these characteristic transparent layers on top of each other (unit 2, 3 and 4 in Figure 59), interbedded by glacially affected surfaces. These are revealed by time surface maps of H0 (Figure 20), H1 (Figure 23) and H2 (Figure 27). The Saalian glaciation occurred 0.2-0.125 M.a, and unit 3 could possible relate to that period. However, the possible unconformity at H2 could represent a time gap of more than 100 k.a. and these deposits could be older than Saalian deposits. Unit 4 reveals the same characteristics as the interpreted till units above and is hence interpreted as an older till deposit, most likely of Early Saalian or Late Elsterian age. A summary of this interpretation is visualized in Figure 59, which is a possible interpretation.

Considering the unit where the shallow gas anomalies occur, Unit 5, the well log data is of special interest. As observed from Figure 13 and Figure 56, there is relatively short lateral distance between the southern part of the HAAs and the well 35/2-1, 950 m to be precise. In the seismic picture (Figure 60), only minor evidence of leakage above the H3 reflector is evident. Some acoustic pipes are present. However, continuous reflectors and little signs of faulting, blanketing, acoustic pipes, bright spots and other seismic indications associated with fluid leakage are observed. This indicates that the migration has stopped at the stratigraphic level about 10 m below H3. Based on the gamma log (Figure 41), the uppermost of unit 5 layer is interpreted to consist of sediments rich in smaller clay and silt. It is the highest gamma ray reading done in the overburden (upper part of zoomed-in window in Figure 41). These sediments are therefore probably less permeable than other layers, and it could work as a good seal. Below this clay-rich layer the gamma log shows decreasing values and a more sand-rich

layer seems to be present (Figure 41). This layer is located in the same stratigraphic level as the HHA interpreted as shallow gas (seismic section in Figure 57). This could be an indication of a regional extent of the stratigraphy observed and inferred at well location 35/2-1. Gas may have migrated into a layer of shallow gas which is trapped by a more compacted and impermeable clay-layer. Obviously, the fine-grained layer in top of unit 3 works as barrier for upward migration in a large lateral extent. The HHAs is more or less at the same stratigraphic level. These two observations indicate that the stratigraphy in 35/2-1 could be present also in the area where the shallow gas occur (Figure 56). This sand layer may be deposited by glaciomarine processes, where an ice-proximal glacers feed a shallow basin with sediments. When the glacier retreats, a silent and low-energy regime dominates and fine-grained particles fell out of suspension building up this clay/silty-layer above. These two layers is stacked between till layers on top and below (Figure 59), which may indicate that they represent the interglacial part of the glaciation-cycles.

Unit 6 got two wedge-shape packages of transparent seismic signature in the top and base, marked by yellow shaded zones in Figure 59. These are similar to till units described and interpreted above (unit 2, 3 and 4). The package in between these have stronger amplitudes and are conform layered bedding planes (except for the areas disturbed by HHAs). This may represent an interglacial cycle where normal marine sedimentation dominated. It is difficult to age determine these deposits.

The absence of MSGLs on some of the horizons that contains plough marks is of special notice. The NCIS has brought enormous amounts of sediments to the North Sea Fan. Nygård et al (2007) calculated that up to 400 m and a volume of 6000 km^3 was brought to the fan during the last glaciation (Ottesen, et al., 2012). Ice stream pattern on the buried surfaces should be expected. Ottesen et. al. (2012) also indicate that the ice streams do appear less erosive, considering their transport capacity. This could be due to the extent of the glaciations. Peon is located in the outer part of the NC and close to the eastern border. However, these amounts of sediments strongly infer that glaciers covered the Peon area several times since the first advance of the Fennoscandian Ice Sheet. The presence of a dynamic, fast-flowing ice stream, where the ice was moving back and forth, may be the reason for the relatively few signs of mega-scale glacial lineations. Floating glaciers without directly being in contact with seabed may result in this.

5.2 The Peon Reservoir – how was it formed?

The ice sheets in the Norwegian Channel fed the Peon area with huge amounts of sediments. As already described, there are many seismic indications for deposits that are related to sub-glacial and sub-marine processes at Peon. Channel-like features occur in the upper and lower part of the gas-filled Peon and it occur south and further north within the elongated shaped sand body. We differ between the smaller, meandering channel-like feature and the major U-shaped feature. The meandering channel-system present along the north-western area is prominent and characteristic. The deposit reveals many depositional characteristics that indicate a glacial dominated depositional regime.

The deposition of the Peon sand seems to be a complex process. Obviously it is related to deglaciation of the Norwegian Channel, and it is described as a glaciomarine/glaciofluvial deposit ((Carstens, 2005), (Ottesen, et al., 2012)). The regional extending URU reflector makes the lower boundary for the Peon reservoir. Biostratigraphic analyses in well 35/2-1 revealed an age of about 1.8 M.a of sediments just below Peon. Knowing that ice streams formed the URU and that the start-up of Fennoscandian Ice Sheet occurred about 1.1 M.a., the URU represent a time gap of at least 0.7 M.a.. There is a major change in layering architecture, where older dipping stratas are separated from the overlying sub-horizontal layers. The Fedje Till is the oldest identified and dated till deposit on the NCS, and has been age determined to 1.1 M.a. ((Sejrup et al 2000), (Mangerud, 2004). There are indications that the Fedje Glaciation contributed to deposition of sediments over large areas in the northern North Sea (Eidvin, u.d.). Recordings from the central North Sea and the Vøring Plateau contain glacial evidence that correlate with glaciations of similar age (Eidvin, u.d.). The large extent of the glacial evidence testify a major expansion of ice sheets during that period, which was the first expansion of the Fennoscandian ice sheet. It is reasonable that the Peon could be deposited by the deglaciation of this ice expansion at 1.0-1.1 M.a BP. The URU represent several hundred years of deposition that eroded when the glaciers advanced within the NCIS. However, since the glacial evidence from the cores are the oldest signs of glaciation, it is hard to argument that the Peon sand is older than 1.1 M.a.. Ottesen et. al. (2012) infer that the extensive ice sheets formed the URU during the Elsterian Glaciation. Elsterian Ice Sheet took place between 400 and 200 k.a. (Rise, et al., 2006). If this is valid, the URU represent a time gap of more than 1.4 M.a.. Hence, deposits from the Naust A and Naust U are more or less absent in the geological record at Peon.

This suggests the deposition of Peon sand occurred in the period 200-400 k.a. Anyway, the Elsterian glaciation fed the NCS and the NC with huge amounts of sediments ((Rise, et al., 2005), (Ottesen, et al., 2012)), and such a massive Peon sand coincide with these observations.

Figure 59 visualize a possible interpretation of the stratigraphic column from seabed to URU. Since we have no measurements or datings that can age determine the Peon sand, we base the interpretation on the study of Ottesen et. al. (2012). This infers an age of maximum 400 k.a, which was the start-up of the Elsterian Glaciation. Thus, unit 1-4 relate to Naust T, while sediments from unit 5-7, as well as the reservoir, relate to sequence S. Unit 4 could possibly be a Naust S.

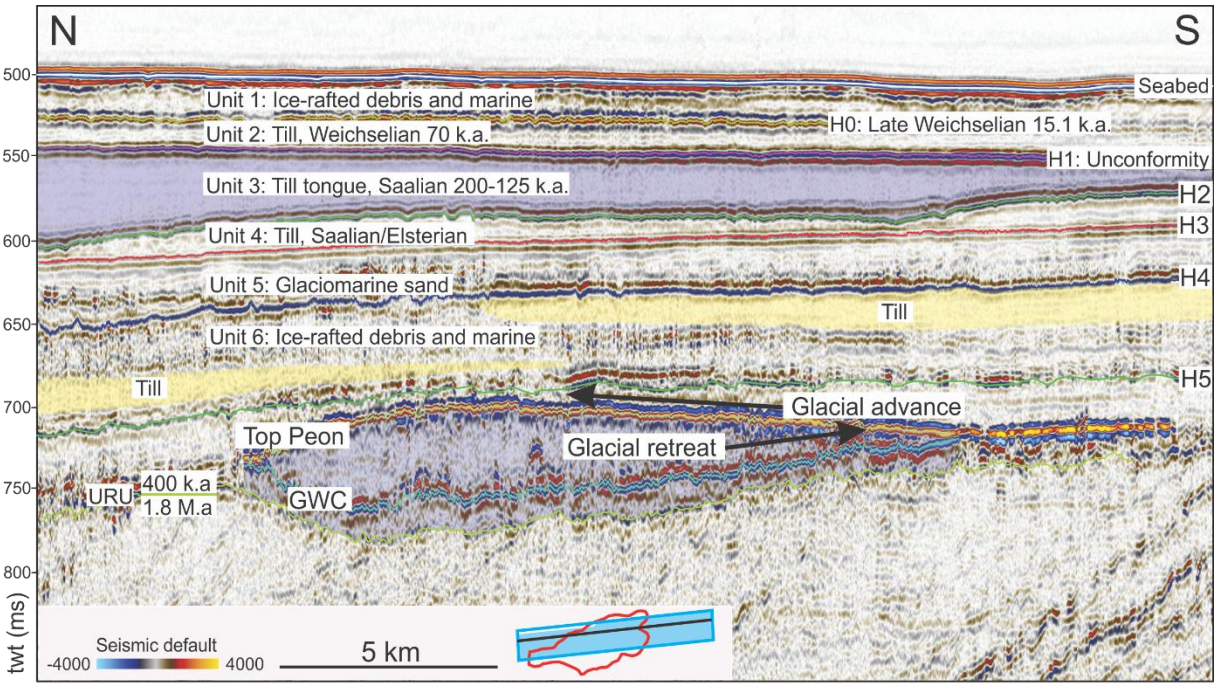

Figure 59: Interpreted stratigraphy of the overburden and Peon reservoir. Unit 1 consist of ice-rafted debris and marine deposits from the last 15.1 k.a. Upper regional unconformity (URU) separates dipping sediments below from upper sub-horizontal bedded sedimentary layers on top. The unconformity represents probably a time gap of 1.4 M.a. The Peon reservoir has probably deposited when glaciers have retreated southwards within the Norwegian Channel. A readvance has likely remobilized the reservoir. Seismic display is from inline2570 of p-cable dataset.

The deposition of Peon seems to be related to glaciation advance and retreat. The first glaciation brought out sediments and eroded the base, contributed to the origination of URU. During a retreating sequence, the glacier has stopped at the Peon where sand deposition occurred in large scale. The size of the Peon sand is very large. A major event like a glaciation retreat is likely to be the depositional agent. Subglacial channels, melt-out tills, glaciofluvial channels and more distal, glacial-marine deposition has probably taken place.

Two main layers occur in the in the water-filled reservoir; a sand-layer at the base and an overlying clay-rich layer. This may represent one cycle of glaciation, where the sand was deposited during a retreat. Then a period of normal marine and silent conditions may have occurred, depositing fine-grained material on top. According to the seismic data, this silty and clay-rich layer seems to be extending throughout the whole reservoir.

The gas-filled part of the lensoid-shaped reservoir consist of thickness greater than 30 m and a lateral extent up 20 km in N-S and 8 km in W-E direction. The formula for an ellipsoid provides a total volume of 2.51 km^3 with sediment within the gas-filled reservoir. These calculations are based on an ellipsoidical-shaped reservoir. However, this is an indication of the enormous amounts of sands. This testify the presence of a major depositional mechanism.

In the lower and middle stratigraphy of the gas-filled Peon, there are zones described as minor channels in different areas of the dataset. They are distributed as we can see on attribute maps in Figure 52 and Figure 54. These can be acoustic impedance changes by sub-glacial meltwater channels acting below and in front of a glacier. Both erosional and depositional processes within the channels would occur, and are considered as glaciofluvial.

In the upper stratigraphy of Peon we have observed and described large channel-like features and named four of them as channel 1, 2, 3 and 4, as seen in Figure 50. These are most likely formed by eroding events and later filled in by sediments. They are such large features, stretching more than 2 km, indicating a major agent. It may be due to glacial erosion when the ice retreats, and thereby scar into the sandy and till deposits. Sand is very soft compared to silt and clay. Hence, eroding events would set bigger imprints to sands. The channels have probably filled by sand of ice-proximal processes. In some of the channels, there occur minor high amplitude channel-like deposits that are similar to those in the northern area discussed above. This could testify deposition by sub-glacial rivers. Probably glaciomarine deposition have occurred as well.

At Top Peon, the strong reflector truncates the major channels (seismic profiles in Figure 51). This indicates that the channels have been exposed to another glacial event. Probably a new glacial advance has occurred, where ice streams have truncated and reworked the deposited

sand. This event could fill in channels and irregularities. Plough marks and scars are present on the surface of Top Peon (Figure 44). This indicates the presence of glaciers occurred when these features where formed.

Considering the shape and thickness (Figure 46) of the Peon sand reservoir, with the ice stream (NCIS) direction from the southeast in mind. It has been building out towards northwest and ice streams has probably contributed to this lense-shaped body of the reservoir. There are thicker deposits in the northwest due to the direction of the stream. Could have been scoured and moved by glaciers, and therefore the very thin reservoir reveals high amplitude anomalies in the southeastern part (Figure 42a). The sandy deposit was less affected by ice streams in the northwestern part, and could therefore build up thicker accumulations of sand. Sand could have rolled over and been remobilized, which means that originally deposited sand in the southeastern part were affected by glaciers and later deposited in the northwestern part (indicated by arrow in Figure 59). This coincide with the truncation of the channel-like erosional feature observed close to the Top Peon.

5.2.1 GWC

The "wavy", dipping fluid contact (according to the time surface map of GWC in Figure 45) infers a heterogeneous reservoir. Within a homogeneous reservoir, the buoyancy forces gas to flow on top of water, making up a horizontal contact. This could be due to the way the sedimentation and deposition of the reservoir occurred, and glacial processes reworking the sediment making up internal compartments. Changing properties, like porosity and permeability, may occur throughout the reservoir. Perhaps finer particles have been mixing into the Peon sand, and result in these irregular GWC. This internal lithology variability and irregularities could act as barriers and trapping mechanisms. However, the GWC tends to incline NNW, which is the same as the general direction for the plough marks and glacial lineations observed on younger horizons and the direction of the NCIS. This indicates lithological changes and depositional regime play a major role for the extent, configuration and dip of the GWC. Correlating well data and seismic data testifies this. There is an abrupt increase in gamma ray values at the interpreted GWC reflector (579 mbsl), from 45-60 to 80-90. Also the sonic velocity increases from 850 to 2200 m/s. This package is stretching down to 587 mbsl. The well data indicates presence of clay-rich sediments occurring below the GWC, and hence the quality of the reservoir decreases dramatic. A good sand with high porosity and permeability

lies on top of finer sediments with poorer pore space and drainage capacity. This could indicate that the complete gas-filled part of the reservoir is closed and trapped at both the top and the base. As seen on the time map for the GWC (Figure 45), it dips towards NNW. Considering the clay layer in the upper part of water-saturated zone as a barrier for lateral and downwards migration of the gas, the Peon gas may be completely trapped by clay. In the N-S profile in Figure 42 the GWC has a syncline shape. The conventional 3D data infers a syncline shape in the W-E direction as well (Figure 47). If the reservoir was not completely sealed, the gas would spilled out at the flanks and the GWC would tend to be horizontally due to buoyancy forces. Hence, the GWC should appear as a horizontal instead of a syncline reflector.

The likelihood of a completely sealed reservoir should be very low. There should be endless possibilities for the gas to migrate in all directions trying to escape due to the law of buoyancy forces. An other thing is how the gas could migrate in to the reservoir and accumulate there if the reservoir was completely trapped. However, the seismic indications for an enclosed reservoir are good. Towards SSE, the Top Peon reflector becomes very bright. South of the Peon outline the reflector is even brighter than within the outline. The GWC and Top Peon coincides or merges together, entrapping the Peon sand. The high-resolution p-cable dataset reveals only minor indications of fluid leakage at the southern boundary, at the point where Top Peon and GWC merges together.

The available datasets only covers the eastern flank of the northern part of the reservoir. This boundary is described as a steeper and more abrupt boundary, where the GWC and Top Peon merges during a short horizontal distance, illustrated by the thickness map of the reservoir (Figure 46). The Peon sand terminates in this lensoid-shaped, outer part of the reservoir.

It is necessary to collect more data from the eastern part of the reservoir to conclude on the dipping nature of the fluid contact. If the reservoir is closed in all directions, it is likely that the GWC depends and lies on a lithological change. Interpretation of well data infers this silty layer right below the GWC: The GWC can laterally be followed in the seismic throughout the complete reservoir. These are clear indications that the silty layer is present regionally. The few signs of gas migration into the younger units supports this. The depositional mechanism at Peon is unique, with a sand entrapped by shale layers on top and bottom. This regional unconformity at the base gives a good fundament that this could occur, and the location of the reservoir with

the base at the URU was probably not a coincident. The deposition of a large sand body on top of the URU could have been a key factor for the presence of this large and shallow gas accumulation.

Another scenario to consider is the misinterpretation of the GWC. The occurrence of a such dipping fluid contact as the time-surface map of the GWC reveals, is characteristic and deviates from the ordinary nature of fluid contacts. There is a question if the strong reflector could be due to other acoustic property changes. Perhaps this could be a lithological boundary with water present above as well. However, there is now signs of a fluid contact in the seismic data above the interpreted GWC. The differences in acoustic properties between gas and water should appear in seismic data with such a high seismic resolution.

As mentioned, gas has low p-wave velocities compared to water-filled sediments. This makes the seismic signals travel slower in gas-filled sediments, and the seismic signals delays. Pushdowns below shallow gas anomalies could therefore occur. Let us consider the gas-filled Peon reservoir and the anticlinal shape of Top Peon reflector (Figure 42). The seismic signals would delay more in thicker gas accumulations. The question is if this velocity effect may give rise to the dipping nature and kind of syncline shape of the GWC. An anticlinal shaped body filled with gas, will theoretically make up a syncline shaped reflector at the base. This is valid before the seismic data is processes, and should be corrected in the processed seismic data. However, this is an issue to consider when we got this shape of the Top Peon and the gas-water contact.

5.3 Fluid leakage

The disturbed seismic signals and chaotic signature described as HAAs in the western and middle areas extent vertically from the reservoir, crosscutting the horizon H4 and goes into unit 5. It has more or less the same extent as the shallow gas, visualized in Figure 56. This supports a theory of vertical migration of gas escaping from the reservoir. In addition, the fact that the HAA occur stronger within the reservoir outline than the HAA in north (shown in Figure 43), as well as the blanketing and disturbed seismic signals below, indicates that the reservoir is the source of the shallow gas in unit 5. Figure 60 visualize this fluid migration process in a seismic section view. Fluid migration has likely occurred at the green arrows. There are seismic indications for a pockmark at the seabed and related vertical fluid migration. We see a

depression on the seabed and acoustic pipe characteristics below. The pockmark is appointed in Figure 60.

The high-amplitude anomalies in unit 5 described in previous sections are interpreted as shallow gas. This gas has probably accumulated in sand-rich sediment below a clay-rich seal. These are clear indications that the reservoir does not contain a trapping mechanism that seals the reservoir completely. Fluid leakage has probably occurred from the top of the reservoir structure, as indicated in Figure 60. However, the reservoir is filled with gas to the GWC. This infers that the infill and supply of gas into the reservoir has been greater than the leakage above. The shale-layer on top of the shallow gas in unit 5 seems to have good sealing properties. However, there occur acoustic pipes in seismic sections above H3, but have limited extent and few signs of HHA accumulations relates to them, as seen from the visualization below (Figure 60). The time surface map of the seabed (Figure 55) indicated several pockmarks with location south of Peon. These are indications for vertical fluid flow in that area. Together with the acoustic pipe structures, they infer that gas migration has occurred in the upper stratigraphy. Nevertheless, fluid migration is not extensive in this part and the glacigenic units above the HHAs in unit 5 seems to be relative impermeable and act as a barrier for gas migration.

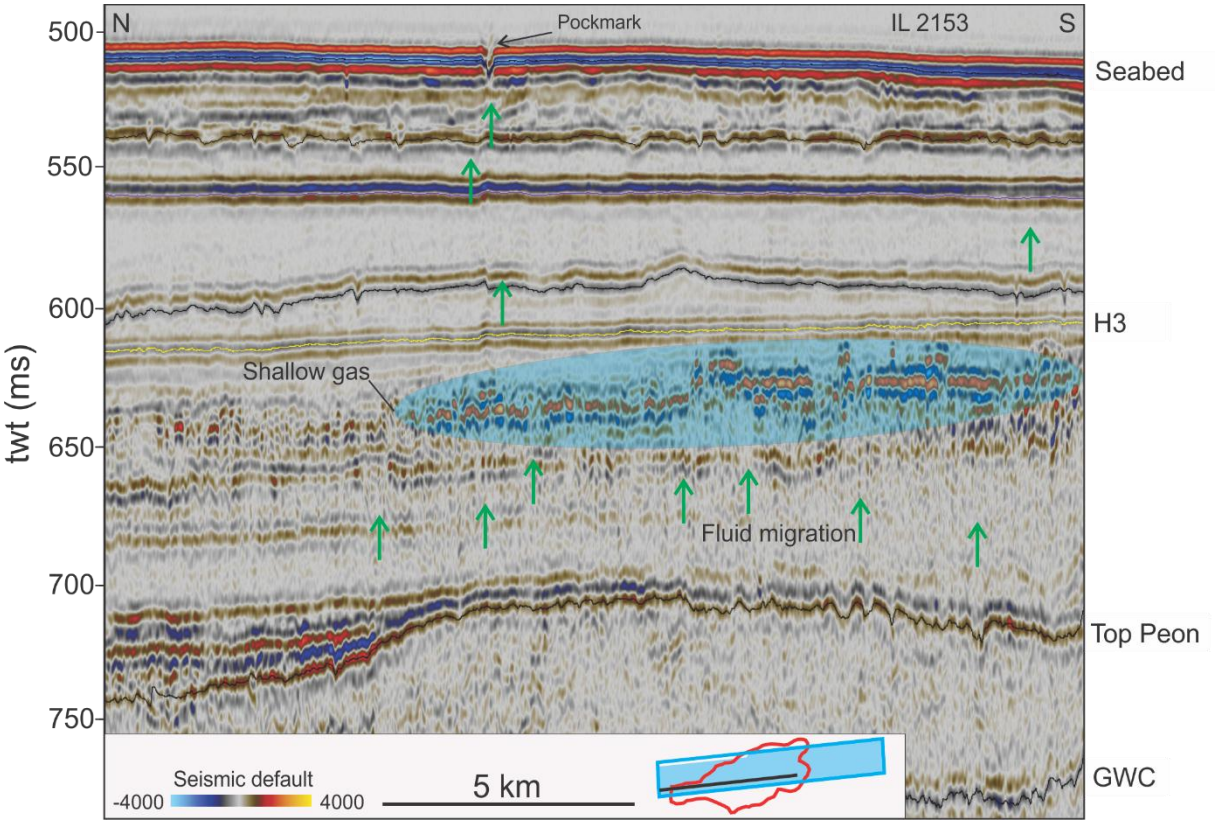

Figure 60: Vertical fluid migration from reservoir into shallow gas accumulation right below H3 reflector. Green arrows indicate fluid migration. In addition, minor migration above H3 and up to the seafloor may have occurred, where a pockmark is formed. Extent of large shallow gas accumulation indicated by blue shaded zone. Seismic section is from inline 2153 in p-cable dataset.

6 Conclusions

In this thesis we have touched upon the geology of the northern North Sea, and looked further into the upper stratigraphy of the Peon area. Attribute analysis of shallow horizons reveals clear indications of glacigenic processes. Sediments are deposited during glaciomarine environments and are reworked and affected by ice stream processes. However, some of the horizons are unaffected by ice streams. Several till units are present in the geological record. The described and interpreted surfaces and units reveals several indications for this. The direction of transport of sediments and ice stream direction coincides with the direction of interpreted plough marks and foot-prints of fast flowing ice streams.

The depositional system at Peon has likely been glaciomarine and glaciofluvial. Features described in section 4.2.4.2 reveal shape, acoustic properties, extent, direction and frequent occurrence that can relate them to glaciofluvial/glaciomarine depositional environment. It seems likely that glaciers have advanced and retreated at the Peon area. The sandy reservoir is most probably deposited during a glacial retreat or several sequences of advances and retreats. Glaciers that stop during a retreat could deposit huge amounts in front of the glaciers. The Peon reservoir has a lensoid structure, pinching out towards SSE. In addition, we have described truncated channels in the upper reservoir. This makes us believe that ice streams working from SSE to NNW have remobilized the sediments and formed this lensoid-shaped structure. The Top Peon horizon shows elongated features, indicating active ice streams during and after deposition of the reservoir.

The gas-water contact is correlated with well data, and is interpreted as the strong, dipping reflector, right above the URU. More detailed studies of the GWC have to be carried out to conclude on the dipping nature.

Fluid leakage structures and shallow gas accumulations within the Peon area has been identified. Shallow gas accumulations with a large lateral extent occur in the stratigraphic column above Peon, located about 80 meter above the reservoir. This gas has most likely leaked out through the sealing mechanism above Peon and accumulated in a lateral extending sand in unit 5. This is indicative of a not completely working seal, which may be due to the shallow reservoir and little compaction of the overburden. The stratigraphy above the shallow gas anomalies reveals minor signs of fluid leakage within the outline of Peon.

7 Bibliography

Andreassen, K. (2007). *Imprints of former ice streams, imaged and interpreted using industry three-dimensional seismic data from the south-western Barents Sea.*

Andreassen, K. (2009). *Marine Geophysics, Lectures Notes for GEO-3123, University of Tromsø.*

Andreassen, K., Nilssen, E., & Ødegaard, C. (2007). Analysis of shallow gas and fluid migration within the Plio-Pleistocene sedimentary succession of the SW Barents Sea continental margin using 3D seismic data.

Brown, A. (1996). *Seismic attributes and their classification.*

Carr, S. (2004). The North Sea basin. In J. Ehlers, & P. Gibbard, *Quarternary Glaciations - Extent and Chronology* (pp. 261-270).

Carstens, H. (2005). *"Fra problem - til mulighet.*

Cartwright, J., & Huuse, M. (2005). 3D seismic technology: the geological "Hubble". *Basin Research*, pp. 1-20.

Cartwright, J., Huuse, M., & Aplin, A. (2007). Seal bypass system.

Castagna, J. P., Sun, S., & Siegfried, R. W. (2003). Instantaneous spectral analysis: Detection of low-frequency . pp. 120-127.

Chopra, S., & Marfurt, K. (2005). Seismic attributes - A historical perspective. *Geophysics*, pp. 3-28.

Dalland, A., Worsley, D., & Ofstad, K. (1988). A lithostratigraphic scheme for the Mesozoic and Cenozoic succession offshore mid-and northern Norway. *Nor. Pet. Direct. Bull. 8.*

Davis, A. (1992). *Continental Shelf Research: "Shallow gas: an overview".*

Dowdeswell, J., Ottesen, D., & Rise, D. (2005). *Flow switching and large-scale deposition by ice streams draining former ice sheets.*

Eidsnes, H., & Sonnonberg, S. (2013). *Structural and Stratigraphic Factors Influencing Hydrocarbon Accumulations in the Bakken Petroleum System in the Elm Coulee Field, Williston Basin, Montana.*

Eidvin, T. (n.d.). *Biostratigraphic investigation of well 35/2-1.*

Floodgate, J., & Judd, A. (1992). The origins of shallow gas. *Continental Shelf Research*, pp. 1145-1156.

Heggland, R. (1998). Gas seepage as an indicator of deeper prospective reservoirs. A study based on exploration 3D seismic data.

Henrich, R., & Baumann, K.-H. (1994). *Age determinations for ODP Sites in the Norwegian-Greenland Sea.*

Hjelstuen, B., Sejrup, H., Haflidason, H., Nygård, A., Ceramicola, S., & Bryn, P. (2005). Late Cenozoic glacial history and evolution of the Storegga Slide area.

Hovland, M., Gardner, J., & Judd, A. (2002). The significance of pockmarks to understanding fluid flowprocesses and geohazards.

http://www.open.edu/openlearn/science-maths-technology/science/environmental-science/earths-physical-resources-petroleum/content-section-2.2.1. (n.d.).

Internal report, S. (n.d.). *Peon discovery - http://bergen.spe.no/publish_files/Erichsen.pdf.*

Isaksen, D., & Tonstad, K. (1989). A revised Cretaceous and Tertiary lithostratigraphic nomenclature for the Norwegian North Sea.

Jansen, E., Fronval, T., Rack, F., & Channe, J. (2000). Pliocene-Pleistocene ice rafting history and cyclicity in the Nordic Seas during the last 3.5 Myr.

Jordt, H., Thyberg, B. I., & Nøttvedt, A. (2000). Cenozoic evolution of the central and northern North Sea with focus on differential vertical movements of the basin floor and surrounding clastic source areas. *Geological Society, London, Special Publications*, 219-243.

Judd, A., & Hovland, M. (2007). *Seabed Fluid Flow*.

Judd, A., & Hovland, M. (2007). Seabed Fluid Flow: The Impact on Geology, Biology and the Marine Environment.

King, L., Rokoengen, K., Fader, G., & Gunleiksrud, T. (1991). Till-tongue stratigraphy. *Geological Society of America Bulletin*, pp. 637-659.

Laberg, J. S., & Vorren, T. (1996). The Middle and Late Pleistocene evolution of the Bear Island Trough Mouth Fan. 1-22.

Ligtenberg, J. (2005). Detection of fluid migration pathways in seismic data:impl icati o ns for fau lt sea l ana lysis.

Løseth, H., Gading, M., & Wensaas, L. (2008). Hydrocarbon leakage interpreted on seismic data. *Marine and Petroleum Geology*, pp. 1304-1319.

Løseth, H., Gading, M., & Wensaas, L. (2009). Hydrocarbon leakage interpreted on. *Marine and Petroleum Geology 26*, pp. 1304-1319.

Mangerud, J. (2004). Ice sheet limits in Norway and on the Norwegian continental shelf. In J. Ehlers, & P. Gibbard, *Quarternary Glaciations - Extent and Chronology* (pp. 271-294).

Nauriyal, A., Sarkar, A., & Kamat, V. (2010). Identification of discontinuities by attribute analysis and planning of wells for basement exploitation - A case study in Mumbai High Field.

Nygård, A., Sejrup, H., Haflidason, H., & Bryn, P. (2005). The glacial North Sea Fan, southern Norwegian Margin: architecture and evolution from the upper continental slope to the deep-sea basin. *Marine and Petroleum Geology*, pp. 71-84.

Ottesen, D. (2006). Ice-sheet dynamics and glacial development of the Norwegian continental margin during the last 3 million years.

Ottesen, D., Dowdeswell, J., Rise, L., & Bugge, T. (2012). Large-scale development of the mid-Norwegian shelf over the last three million years and potential for hydrocarbon reservoirs in glacial sediments. *Geological Society, London, Special Publications*, pp. 53-73.

Ottesen, D., Rise, L., Sletten Andersen, E., Bugge, T., & Eidvin, T. (2009). Geological evolution of the Norwegian continental shelf between 61ºN and 68ºN during the last 3 million years. 251-265.

Planke, S., Eriksen, F., berndt, C., Mienert, J., & Masson, D. (2009). Spotlight on Technology: P-cable High Resolution Seismic. *Oceanography*, p. 85.

PSA. (2007). *Shallow gas events 1984 – 2006 in the Norwegian Sector.*

Rise, L., Olesen, O., Rokoengen, K., Ottesen, D., & Riis, F. (2004). Mid-Pleistocene ice drainage pattern in the Norwegian Channel imaged by 3D seismic. *Quarternary Science Reviews 23*, pp. 2323-2335.

Rise, L., Ottesen, D., Berg, K., & Lundin, E. (2005). Large-scale development of the mid-Norwegian margin during the last 3 million years. *Marine and Petroleum Geology*, pp. 33-44.

Rise, L., Ottesen, D., Longva, O., Solheim, A., Andersen, E., & Ayers, S. (2006). The Sklinnadjupet slide and its relation to the Elsterian glaciation on the mid-Norwegian margin. *Marine and Petroleum Geology*, pp. 569-583.

Rokoengen, K., & Rønningsland, T. M. (1982). *Regionale bakgrunnsdata for prosjekt Grunn Gass mellom 60N og 62N.*

Schlumberger. (2010). *Schlumberger Oilfield Glossary.*

Sejrup, H. P., & Aarseth, I. (1995). Quarternary of the Norwegian Channel: glaciation history and paleoceanography. *Norwegian Journal of Geology*, 65-87.

Sejrup, H. P., & Larsen, E. (2003). Configuration, history and impact of the Norwegian Channel Ice Stream. *Boreas*, pp. 18-36.

Sejrup, H., Haflidason, H., Aarseth, I., King, E., Forsberg, C., Long, D., & Rokoengen, K. (1994). Late Weichselian glaciation history of the northern North Sea.

Sejrup, H., Haflidason, H., Hjelstuen, B. O., Nygård, A., Bryn, P., & Lien, R. (2004). Pleistocene development of the SE Nordic Seas margin.

Selley, R. C. (1998). *Elements of Petroleum Geology.*

Taner, M., Koehler, F., & Sheriff, R. (1979). Complex seismic trace analysis. 1041-1063.

Taner, T. (2001). Seismic attributes.

Vadakkepuliyambatta, S., Buenz, S., Mienert, J., & Chand, S. (2013). Distribution of subsurface fluid-flow systems in the SW Barents Sea. *Marine and Petroleum Geology*, pp. 208-221.

Vadakkepuliyambatta, S., Planke, S., & Buenz, S. (2014). *Fluid leakage pathways and shallow gas accumulation in the Peon field, northern North Sea, from hig resolution P-Cable 3D seismic data.*

Veeken, P. (2007). Seismic Stratigraphy, basin analysis and reservoir characterisation. In *Handbookin Seismic Exploration* (pp. 111-141; 229-234; 254-263; 268-279).

Veeken, P., & Moerkerken, B. V. (2013). Seismic Stratigraphic Techniques. 2-109.

Vevik, K. (2011). *A gas-hydrate related BSR on the W-Svalbard margin: distribution, geological control and formation mechanisms.*